SAPIENZA
UNIVERSITÀ DI ROMA

DOTTORATO DI RICERCA IN BIOCHIMICA
CICLO XXVI (A.A. 2010-2013)

# Biochemical characterization of glutamate decarboxylase from *Brucella microti* and *Escherichia coli*

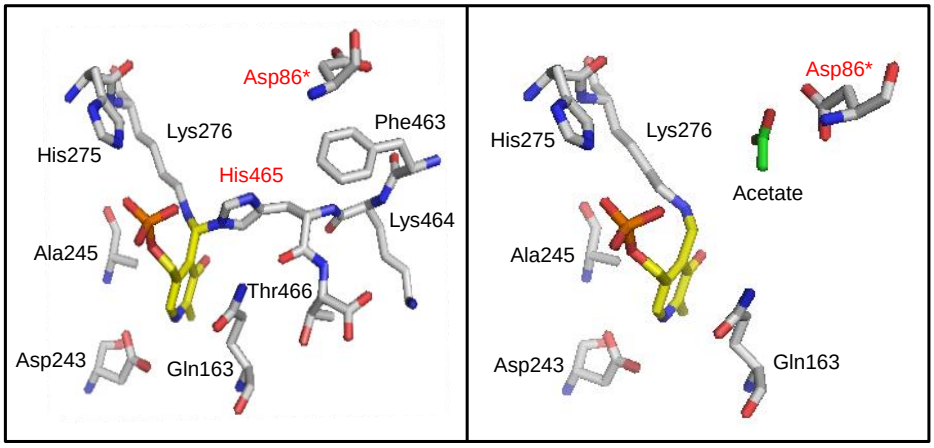


Docente guida
Prof. Roberto Contestabile

Coordinatore
Prof. Francesco Malatesta

Tutor
Prof.ssa Daniela De Biase

Dottoranda
Gaia Grassini

Dicembre 2013

SAPIENZA
UNIVERSITÀ DI ROMA

DOTTORATO DI RICERCA IN BIOCHIMICA
CICLO XXVI (A.A. 2010-2013)

# Biochemical characterization of glutamate decarboxylase from *Brucella microti* and *Escherichia coli*

**Dottoranda**
**Gaia Grassini**

**Docente guida**
**Prof. Roberto Contestabile**

**Coordinatore**
**Prof. Francesco Malatesta**

**Tutor**
**Prof.ssa Daniela De Biase**

**Dicembre 2013**

# INDEX

## Abbreviations used

| | |
|---|---|
| **GIT** | gastrointestinal tract |
| **SCFAs** | short chain fatty acids |
| **AR** | acid resistance |
| **PLP** | pyridoxal 5'-phosphate |
| **GDAR** | glutamate-dependent AR |
| **ADAR** | arginine-dependent AR |
| **Gad** | glutamate decarboxylase |
| **GABA** | γ-aminobutyrate |
| **AFI** | acid fitness island |
| **PMP** | pyridoxamine 5'-phosphate |
| **LAB** | Lactic Acid Bacteria |
| **CaM** | calmodulin |
| **CaMBD** | $Ca^{2+}$/calmodulin Binding Domain |
| **AID** | autoinhibitory domains |
| **ORF** | open reading frame |
| **DTT** | dithiothreitol |
| **SDS** | sodium dodecyl sulphate |
| **SDS-PAGE** | SDS-polyacrylamide gel electrophoresis |
| **DEAE** | diethylethanolamine |
| **HEPPS** | 3-[4-(2-Hydroxyethyl)-1-piperazinyl]propanesulfonic acid |
| ***Bm*GadB** | *Brucella microti* GadB |
| ***Ec*GadB** | *Escherichia coli* GadB |
| **DDC** | L-DOPA decarboxylase |

# *Introduction*

## 1.1 Glutamate decarboxylase-dependent acid resistance in orally-acquired bacteria

### 1.1.1 Acid resistance in orally-acquired bacteria

Acid stress is one of the most hostile conditions for the bacterial cell. Generally, even small changes in the intracellular pH ($pH_i$) have drastic effects on cell growth and this is why most bacteria are able to maintain a fairly constant internal pH when grown in a wide range of media at different external pH ($pH_o$) (Slonczewski *et al.*, 2009, Krulwich *et al.*, 2011). The $pH_i$ of *Escherichia coli* for example changes only from 7.2 to 7.8 over a $pH_o$ range of 5.5 to 9 (Slonczewski *et al.*, 1981). The outcome is that the $pH_i$ is always kept higher respect to an acidic $pH_o$ and lower with respect to an alkaline $pH_o$. Thus fluctuations in $pH_i$ are clearly undesirable, as confirmed by the fact that bacteria are limited, for example, in the range of acidic pH values at which they are able to grow and show a transcriptional and translational response to a drop in pH. In fact, most of the biological molecules carry out their functions only in a limited range of pH.

This assumptions are particularly important for neutrophilic orally-acquired bacteria which, in order to colonize the mammalian host gastrointestinal tract (GIT), must survive a > 2-hour exposure to the extremely acid secretions (pH < 2.5) of the stomach, the major bactericidal barrier of the GIT (Giannella *et al.*, 1972). Additional acid stress occurs in the distal gut, where the short chain fatty acids (SCFAs) such as acetic, propionic, butyric and lactic acid are produced by the resident microbiota via anaerobic fermentation (Flint *et al.*, 2008). In fact, SCFAs are able to cross

the cell membrane in the undissociated form and then, once in the cytoplasm, dissociate, thereby causing internal pH acidification.

Therefore the ability to perceive and cope with acid stress is crucial for successful colonization of the GIT and to survive in other acidic environments (i.e. fermented food).

In enteric pathogens, acid resistance (AR) is considered a virulence trait. In fact the infectious dose (ID) of different enteric pathogens is directly proportional to their relative ability to withstand acid. Acid-sensitive pathogens, like *Vibrio cholerae* ($ID_{50} = 1x10^9$), overcome the stomach barrier only by a massive entry, which allows few cells to survive and reach the gut. On the contrary, acid-resistant enterobacteria such as *E. coli* and *Shigella flexneri* ($ID_{50} = 1x10^2$) possess a combination of various molecular mechanisms which collectively work by counteracting the entry of protons, mostly by consuming and pumping out them in order to prevent damage of macromolecules.

Bacterial acid survival systems are typically classified either as ATR (acid tolerance response) or as AR (acid resistance). The two systems differ in that the ATR (log- or stationary-phase) requires pre-exposure of the bacteria to a mildly acidic pH before the acid challenge at $pH \geq 3.0$, whereas AR typically protects from an extreme acid stress ($pH \leq 2.5$) stationary-phase cells which were not pre-adapted (Foster, 2001, Merrell & Camilli, 2002).

In *E. coli* the acid stress response (reviewed by (Kanjee & Houry, 2013)), consists of (i) *passive mechanisms*, owing to the buffering capacity of amino acids, proteins, polyamines, polyphosphate, and inorganic phosphate present in the cytoplasm; (ii) *physiological adaptations*, such as membrane modifications (i.e. content of fatty acids and outer membrane porins to reduce proton influx) and acid pH-triggered activity of periplasmic chaperones; (iii)

*metabolic responses*, such as those occurring during aerobic growth under mild acid stress, that support proton efflux *via* the components of the electron transport chain; (iv) *proton-consuming and ammonia-producing reactions* that rely on the activation of acid-inducible amino acid-dependent decarboxylases and deaminases (Kanjee & Houry, 2013, Lu *et al.*, 2013). In the latter case five acid resistance (AR) systems have been characterized, and each has two components: a cytoplasmic pyridoxal 5'-phosphate (PLP)-dependent decarboxylase or a deaminase (in one case), that catalyses the reaction on the relevant amino acid, and an inner membrane antiporter which exchanges the incoming substrate for the exported product of the reaction (Foster, 2004, Lu *et al.*, 2013).

In addition to the amino acid-dependent AR systems which are typically, though not exclusively, induced under fermentative conditions, *E. coli* possesses also an oxidative (glucose-repressed) AR system, named AR1 (Lin *et al.*, 1995, Lin *et al.*, 1996). Very little is known about the major players of this latter system, whereas many data, including transcriptional, regulatory and structural data, are available for the amino acid-dependent systems, some of which are depicted in Fig. 1.1 (Foster, 2004, Zhao & Houry, 2010, De Biase & Pennacchietti, 2012, Kanjee & Houry, 2013).

In particular, the glutamate(Glu)-dependent and the arginine(Arg)-dependent AR systems, named GDAR and ADAR respectively, require the addition of glutamate or arginine during the challenge at pH 2.5. These two systems provide the most robust protection from extreme acid stress (Lin *et al.*, 1995, Lin *et al.*, 1996, Castanie-Cornet *et al.*, 1999, De Biase *et al.*, 1999).

The GDAR system consists of the two homologous inducible glutamate decarboxylases GadA and GadB, and the antiporter GadC, for glutamate/γ-aminobutyrate (GABA) antiport (Castanie-Cornet *et al.*, 1999, De Biase *et*

*al.*, 1999, Richard & Foster, 2004, Ma *et al.*, 2012). The corresponding genes (i.e. *gadA*, *gadB* and *gadC*) are expressed upon entry into stationary phase in rich medium (independently of pH), and further induced upon hypo- and hyperosmotic stress, or by log-phase growth in minimal medium containing glucose at a pH of 5.5 (De Biase *et al.*, 1999, Castanie-Cornet & Foster, 2001, Ma *et al.*, 2003). The ADAR system consists of the inducible arginine decarboxylase AdiA and the arginine/agmatine antiporter AdiC (Castanie-Cornet *et al.*, 1999, Gong *et al.*, 2003), whose expression is maximal in rich medium at acidic pH, under anaerobic conditions and in the presence of arginine (Lin *et al.*, 1995).

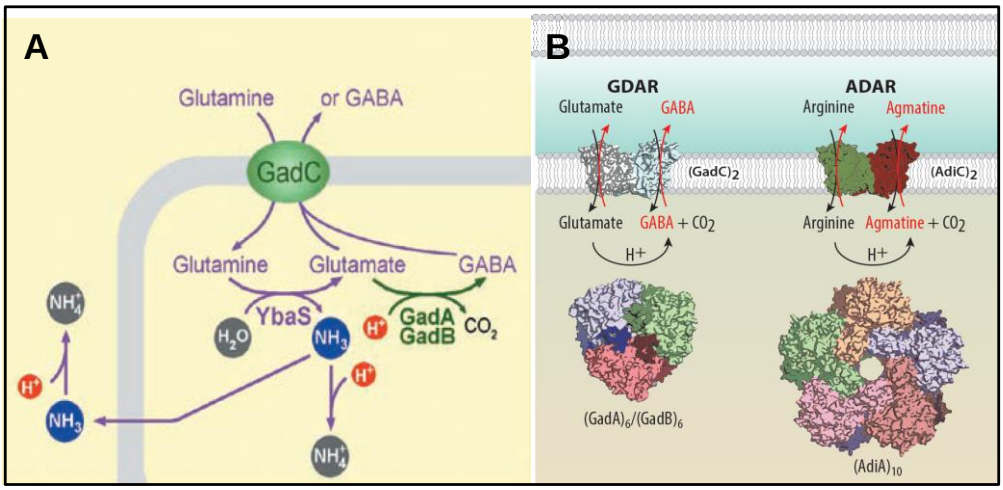


**Figure 1.1.** *AR systems in* E. coli. **(A)** The Glutamine(Gln)-dependent system. GadC is an amino acid antiporter with specificity for Gln, Glu and GABA. Upon uptake, Gln is converted to Glu by the acid-activated glutaminase YbaS, with concomitant release of gaseous ammonia. Free ammonia neutralizes the excess of protons, thereby elevating intracellular pH. Glu can be either directly exported by GadC or further decarboxylated by GadA/B to generate GABA. **(B)** Schematic diagram illustrating the structural components (decarboxylase and antiporter) of the GDAR and ADAR systems for which the crystallographic structures are available. (Adapted from (Kanjee & Houry, 2013, Lu *et al.*, 2013)).

The lysine- and ornithine-dependent systems provide a much more limited protection to extreme acid stress because the corresponding decarboxylases

possess a pH optimum of activity which is between 5.5-6.0 and therefore cannot provide protection when the intracellular pH drops to <5 as a consequence of an external pH of <2.5 (Kanjee & Houry, 2013).

### 1.1.2 The GDAR system: function and regulation

GDAR is by no doubt the major AR system in several food-borne pathogens and orally-acquired bacteria such as *E. coli*, *Shigella flexneri*, *Lactococcus lactis* and *Listeria monocytogenes* (Lin *et al.*, 1995, Lin *et al.*, 1996, Sanders *et al.*, 1998, Cotter *et al.*, 2001, Bhagwat & Bhagwat, 2004).

According to the proposed model for the GDAR system of *E. coli* (De Biase & Pennacchietti, 2012), when the extracellular proton concentration sharply increases to harmful levels (i.e. pH ≤ 2.5), as during transit through the host stomach, the inner membrane cannot avoid the passive entry of protons (and probably undissociated HCl), the intracellular pH drops and the import of $Glu^0$ *via* GadC is triggered (Fig. 1.2) (Richard & Foster, 2004, Ma *et al.*, 2012, Ma *et al.*, 2013). Once inside, Glu remains protonated on the γ-carboxylate to allow binding to and decarboxylation by GadA and GadB , which are maximally active in the pH range 4–5 (Shukuya & Schwert, 1960, Fonda, 1972, Pennacchietti *et al.*, 2009). The α-carboxyl group, leaving as $CO_2$, is thus replaced by a cytoplasmic proton, yielding $GABA^{+1}$, which is exported via the functionally associated antiporter GadC in exchange for a new Glu molecule. The export of $GABA^{+1}$ contributes to the net export of positive charges (0.9 $H^+$/exchange cycle), further relieving from intracellular acidification (Tsai *et al.*, 2013).

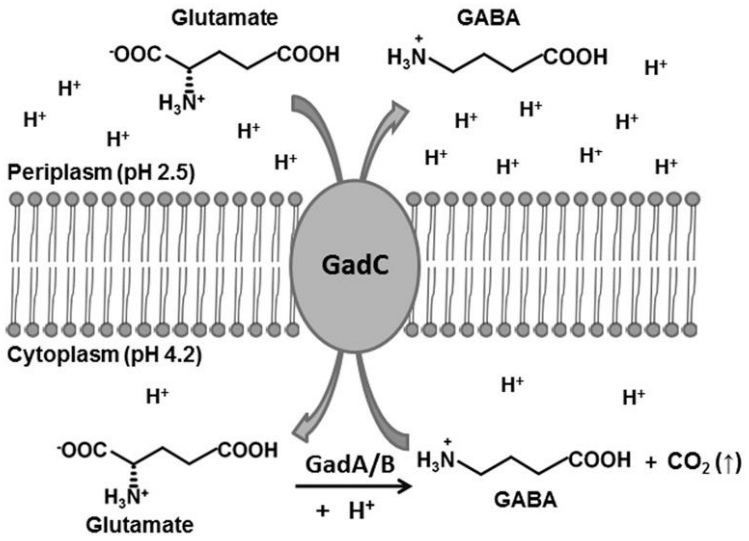


**Figure 1.2.** *Glutamate-based acid resistance system*. Schematic representation of the mechanisms (antiport + decarboxylation) required for its activity (De Biase & Pennacchietti, 2012).

In vivo studies on *E. coli* cells also showed that GDAR not only contributes to pH homeostasis but, by transiently accumulating GABA in the cell, it counteracts illicit entry of protons by inversion of the membrane potential ($\Delta\Psi$), a strategy similar to that adopted by extreme acidophiles (Foster, 2004). Indeed, in *E. coli* grown at pH 7, in aerobic conditions, the $\Delta\Psi$ is -90 mV and -50 mV in exponential phase in the stationary phase. When cells of *E. coli* are transferred to pH 2.5, in the presence of glutamate, their cytoplasm is acidified to a pH value equal to 4.5 and the $\Delta\Psi$ becomes positive (+30 mV) slowing down proton entry. Chloride channels performing the $H^+_{out}/Cl^-_{in}$ antiporter have also been proposed to play an important role in AR system, by counteracting the excessive hyperpolarization of the membrane (Accardi & Miller, 2004, Foster, 2004).

*E. coli* GadA and GadB are coded by the corresponding genes at 3665 kb and 1570 kb respectively (Fig. 1.3). The *gadC* gene is immediately

downstream of *gadB* with which it can be cotranscribed (De Biase *et al.*, 1999), whereas the distantly located *gadA* gene belongs to the acid fitness island (AFI), a 14 kb genome region, repressed by HNS (the histone like nucleoid-structuring protein) and controlled by RpoS (the stationary phase σ factor of the RNA polymerase) (Hommais *et al.*, 2004, Weber *et al.*, 2005). *gadA* can be either independently transcribed or co-transcribed with the downstream *gadX* gene (De Biase *et al.*, 1999, Tramonti *et al.*, 2002).

AFI comprises 14 genes in the following operon arrangement: *slp-yhiF*, *hdeAB-yhiD*, *gadE-mtdEF*, *gadXW* and *gadAX* (Fig 1.3) (Tramonti *et al.*, 2002, Tucker *et al.*, 2003). Notably the AFI contains many genes coding for transcriptional regulators, which include YhiF, GadE, GadX, GadW, ArrS and GadY: the first two belong to the LuxR family, the second two belong to the AraC-family, whereas the last two are small RNAs, which affect the stability of the *gadE* and *gadX* transcripts respectively (Tramonti *et al.*, 2002, Ma *et al.*, 2003, Tucker *et al.*, 2003, Opdyke *et al.*, 2004, Tramonti *et al.*, 2006, Tramonti *et al.*, 2008, Aiso *et al.*, 2011). GadE, GadX, GadW and GadY were all shown to positively affect the expression of the *gadBC* operon (Tramonti *et al.*, 2002, Hommais *et al.*, 2004, Tramonti *et al.*, 2006). Besides *gadA* and the genes coding for the regulators, all the AFI genes contribute at various levels to AR: *hdeA* and *hdeB* code for pH-regulated acid stress periplasmic chaperones, which facilitate the refolding of acid-denaturated proteins in this cellular compartment (Hong *et al.*, 2005, Kern *et al.*, 2007); *slp*, *yhiD* and *hdeD* code for membrane proteins participating in the protection from acidic metabolites such as lactate, succinate and formate (Mates *et al.*, 2007); the *mdtE* and *mdtF* genes code for multidrug exporters whose expression is induced in stationary phase and is GadX-dependent (Kobayashi *et al.*, 2006, Nishino *et al.*, 2008).

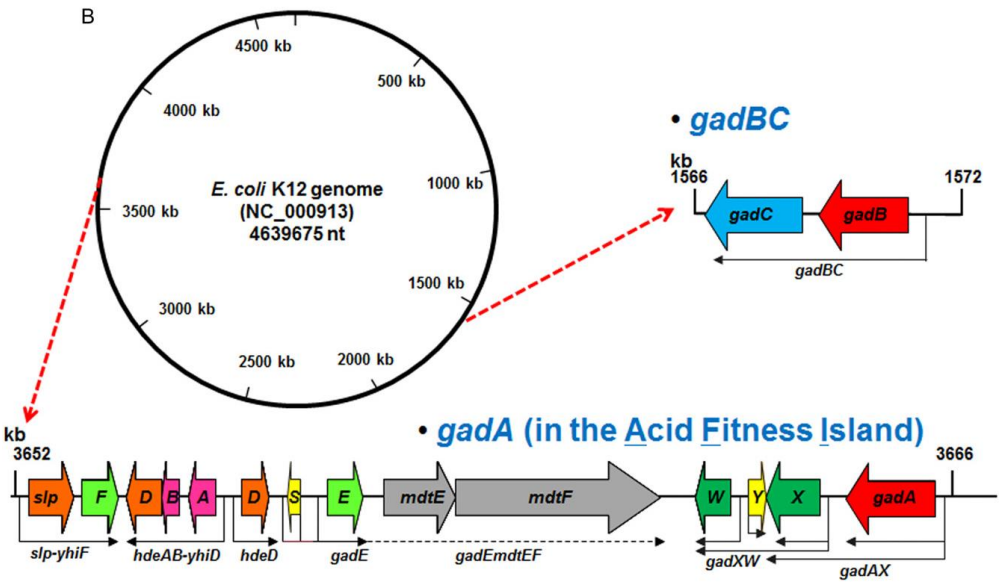


**Figure 1.3.** *Genomic organization of the GDAR and AFI genes*. Representation of the *E. coli* genome map with the location of the loci encoding GadA/B (red), GadC (blue), additional membrane proteins (orange), multidrug exporters (gray), acid stress periplasmic chaperons (magenta), LuxR-like transcriptional regulators (light green), AraC-like transcriptional regulators (green) and a small regulatory RNAs (yellow). The bent arrows show the transcripts' start and length of the operons (De Biase & Pennacchietti, 2012).

The activation of *gadBC* and the AFI genes occurs under many stress conditions, including entry into the stationary phase (i.e. nutrient limitation), acidic pH, high and low osmolarity, anoxia (De Biase *et al.*, 1999, Weber *et al.*, 2005, Hayes *et al.*, 2006) and requires the direct or indirect control of the response regulator of the two-component systems EvgAS, RcsBC, PhoPQ, EnvZ/OmpR and TorRS (Bordi *et al.*, 2003, Castanie-Cornet *et al.*, 2007, Itou *et al.*, 2009, Burton *et al.*, 2010, Stincone *et al.*, 2011).

The expression of *gadE*, coding for the essential regulator GadE (Ma *et al.*, 2003) is under the control of three activation circuits which respond to different growth conditions: the EvgAS-YdeO circuit is operative in the

exponential phase of growth in minimal medium EG at pH 5.5 (Masuda & Church, 2002, Ma *et al.*, 2004, Itou *et al.*, 2009); the TrmE-dependent circuit is operative in stationary phase in unbuffered LB medium containing glucose (Gong *et al.*, 2004); the GadX/GadW-dependent circuit (Tramonti *et al.*, 2002, Tramonti *et al.*, 2006, Tramonti *et al.*, 2008) is required for *gadE* activation upon entry into the stationary phase in buffered LB medium (Sayed *et al.*, 2007). The latter circuit is the most complex and best characterized at the molecular level. Besides GadX and GadW, it involves the global transcriptional regulators H-NS and CRP, which act as repressors, and RpoS, which instead positively affects *gadA* and *gadBC* transcription (De Biase *et al.*, 1999, Castanie-Cornet & Foster, 2001, Hommais *et al.*, 2001, Tramonti *et al.*, 2002, Giangrossi *et al.*, 2005, Weber *et al.*, 2005).

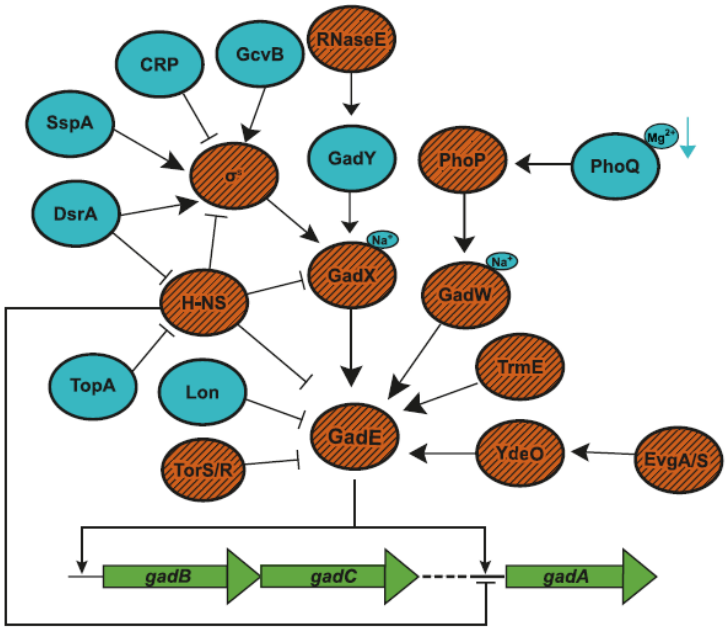


**Figure 1.4.** *Regulators cascade controlling the activation of GDAR system*. In this scheme is emphasized the role of GadE as a central activator of the *gad* genes (Zhao & Houry, 2010).

Atypical is the role played by RcsB (not shown in Fig. 1.4) belonging to the sensor-regulator system RcsCB. In fact, the basal activity of this regulator is required for the expression of *gadA* and *gadBC* genes in the presence of GadE, whereas its activation, through the sensor RcsC, leads to a decrease of AR in the stationary phase (Castanie-Cornet *et al.*, 2007, Castanie-Cornet *et al.*, 2010).

The intricate regulative network that allows in *E. coli* a fine tuning of *gadA* and *gadBC* expression in response to various environmental stimuli clearly indicates that the activity of the GDAR system must be timely controlled and also that its role might go beyond that of protecting from the extreme acid stress.

### 1.1.3 The GDAR system: structural components

In *E. coli* the two major structural components of the GDAR, GadB and GadC, display an acidic pH optimum (Pennacchietti *et al.*, 2009, Ma *et al.*, 2012). The combination of crystallographic and site-directed mutagenesis studies has allowed to investigate on the molecular mechanisms underlying GadB and GadC activation, which share indeed amazing similarities. In fact both proteins undergo auto-inhibition at pH > 5.5 thanks to the occurrence in the C-terminal region of amino acid residues that organize into structures that plug either the active site (in GadB) or the substrate entry channel (in GadC). Notably, in both proteins histidine residues play an active role as gate-keepers.

### 1.1.3.1 GadC

GadC is a representative member of the amino-acid-polyamine-organocation (APC) superfamily of membrane transporters, which also includes AdiC of the ADAR system.

GadC is composed by 12 trasmembrane helices (TMs) which are arranged into two inverted repeats, contributed by TM1-TM5 and TM6-TM10, and of TM1 and TM6 each containing two short α-helices connected by a discontinuous stretch in the middle (Ma *et al.*, 2012). The recently published structure of GadC was solved at pH 8.0 and shows the features of the inactive conformation (inward-open) of this protein (Ma *et al.*, 2012). In fact i*n vivo* and *in vitro* (i.e. proteoliposome-based) studies have shown that substrate transport by GadC is strictly pH-dependent, with robust activity at pH 5.5 or below and no detectable activity at pH ≥ 6.5. In sharp contrast, AdiC still allows moderate transport activity up to pH 8.0 (Fang *et al.*, 2007).

The path where the putative substrate-binding residues are located provides a negatively charged environment. The C-terminal portion of the protein comprises residues 477-511 which make the C-plug, structurally arranged so to completely block the path to the putative substrate-binding site (Fig 1.5; (Ma *et al.*, 2012)). The deletion of the C-plug, in which several His and Arg residues contribute to the stability of the C-plug itself and to its interaction with other residues in the protein (making multiple hydrogen bonds), shifts the pH-dependent substrate transport towards higher pH values. As in the case of GadB (cfr. 1.1.3.2), the p*Ks* of His residues in the C-plug could play a major role in controlling its displacement following intracellular acidification. The closed conformation of GadC is attained not only by the C-plug in the cytoplasm but also by the L7 loop at the periplasmic side (Fig.

1.5). The substrate transport path is sandwiched axially between C-plug and L7 loop and surrounded by TM1-2-6-8-10. Thus, the displacement of both, the C-plug and the L7 loop, is a prerequisite for the transport activity of GadC.

The structure of GadC, together with the availability of the structure of *E. coli* AdiC in the free (outward-open) and Arg-bound form (Fang *et al.*, 2009, Gao *et al.*, 2009, Kowalczyk *et al.*, 2011), provides insights into the mechanism of substrate transport and helped to identify six gating residues in GadC (Ma *et al.*, 2012) (Fig. 1.5). In fact, the six variants in which residues Tyr96, Tyr214, Glu18, Trp308, Tyr378 or Tyr382, all located near the putative transport path, were substituted into Ala, all show a significant decrease in substrate transport. Under the assumption of conserved transport mechanism between AdiC and GadC, the structural alignment ($AdiC_{out}$/$GadC_{in}$) allowed to identify an almost static core domain and a gate domain (TM1-2-6-7) that seems to rotate clockwise by 35°, resulting in an inward-open conformation. The proposed transport mechanisms consists in a rocking-bundle movement in which individual TMs largely retain their conformations.

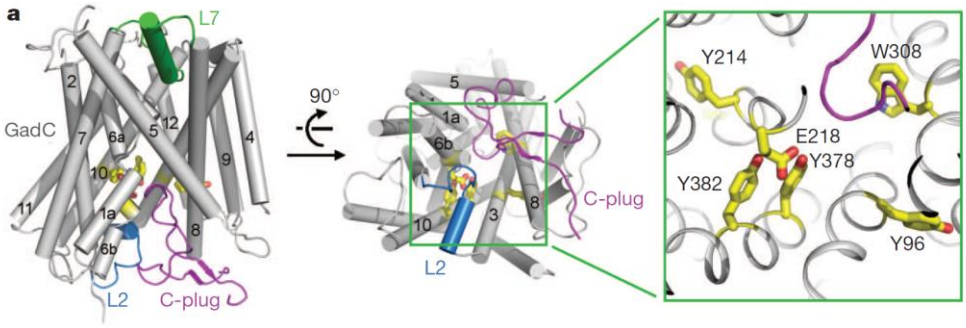


**Figure 1.5.** *GadC structure and transport path.* The six key residues considered essential in the transport path are shown in a close-up view in the right panel (from (Ma *et al.*, 2012)).

Noteworthy GadC is highly selective in substrate transport. In addition to Glu, GadC also efficiently transports three additional amino acids: Gln and, to a smaller extent, Met and Leu (Ma *et al.*, 2012). GadC selectively transports $Glu^0$ and $GABA^+$, indicating that the protonation state of a given substrate is crucial for transport and that side chain deprotonation of Glu and GABA at neutral pH impedes Glu/GABA exchange (Ma *et al.*, 2013).

Tsai et al. proposed that at a pH of 2.5 GadC (as well as AdiC (Tsai & Miller, 2013)) uses a charge-based mechanism to recognize its substrates, suggesting that the outward-open conformation, hostile to the +1 valence ($GABA^+$ and $Glu^+$), might import both $Glu^0$ and the less abundant $Glu^{-1}$ (Tsai *et al.*, 2013). The inward-open conformation, which needs to reject $GABA^0$ and discharge $Glu^0$ or $Glu^-$, also adhere to this electrostatic picture. Moreover, in contrast to the current model (Foster, 2004), they proposed that GadC acting as a virtual proton-pump should polarize the membrane in the negative direction (Tsai *et al.*, 2013).

### 1.1.3.2 GadB

The crystal structure of *E. coli* GadB was reported in 2003 (Capitani *et al.*, 2003). This was the first structure of a prokaryotic glutamate decarboxylase to be released, followed by those of *E. coli* GadA in complex with glutarate, a substrate analogue (Dutyshev *et al.*, 2005), human Gad65 and Gad67 (Fenalti *et al.*, 2007) and plant Gad1 (Gut *et al.*, 2009).

The crystallographic structure of wild type GadB was solved at both acidic pH (4.6) and neutral pH (7.6) and has provided insights on the molecular basis of its intracellular activation (Capitani *et al.*, 2003). GadB is a homoexamer of 320 kDa that can be described as a trimer of dimers, the basic

catalytic unit in most PLP-dependent enzymes. The structure is arranged on two layers with each dimer contributing to both layer. The comparison of the structure of GadB obtained at the two values of pH provided evidence that the overall structure of the hexamer remains unaffected by the shift in pH change (Fig. 1.6). However, three major structural reorganization occur in the N- and C-terminal regions of each subunit and in a β-hairpin, which includes residues 300-313, thus leading to the conversion of GadB from the inactive into the active form and *vice versa*.

In the neutral pH-structure (Fig. 1.6, on the left), residues 3-15 in the N-terminal region are disordered. Nevertheless, *via* the narrow central channel, each N-terminal domain (residues 1-57) acts like a hook and contributes to stabilize the hexamer, i.e. it departs perpendicularly from the subunit surface and reaches the opposite layer where it make contacts both with the counterpart in the functional dimer and with a subunit belonging to a neighboring dimer. In the structure at pH 4.6 (Fig. 1.6, on the right), residues 3-15 of each subunit assume an α-helix conformation, which close the central channel and give rise to two triple helical bundles, parallel to the threefold axis and protruding on each (top and bottom) side of the hexamer. This occurs only at acidic pH since the side chains of acidic residues in the N-terminal regions become protonated, thus abolishing negative charges repulsion. Functional studies on the GadBΔ1-14 deletion mutant, allowed to demonstrate that the formation of the triple helical bundles is required for the recruitment of the enzyme to the plasma membrane, where the protons are more abundant and its decarboxylase activity functionally match to that of the antiporter GadC (Capitani *et al.*, 2003).

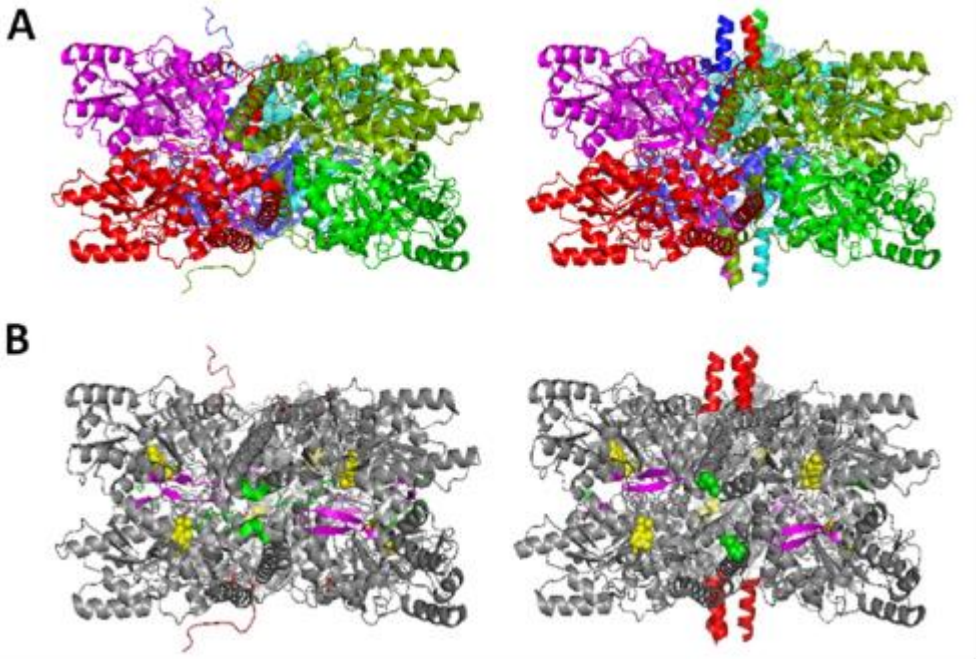


**Figure 1.6.** *Side views of the E. coli GadB hexamer at neutral (left) and acidic (right) pH.* **(A)** The two-layered GadB hexamer is shown in colors. Each dimer contributes to both layers. **(B)** Major conformational changes in GadB. The hexamer is in gray, but the 1–14 N-terminal region (red), the 452–466 C-terminal tail (green) and the 300–313 β-hairpin (magenta). PLP is shown in filled space (yellow) (De Biase & Pennacchietti, 2012).

Furthermore, the N-terminal regions contribute to the cooperativity of the system providing protonable residue side chains and surmount the halides binding sites. Of particular physiological relevance is the finding that chloride ions act as positive allosteric modulators (O'Leary & Brummund, 1974) by strongly stabilizing the triple helical bundles (Gut *et al.*, 2006). Indeed, in the variant GadBΔ1-14 cooperativity in the absorbance change (indicative of the conversion between the active and inactive forms) is greatly reduced ($n \approx 2$) and is insensitive to the presence of chloride ions.

At neutral pH, the C-terminal residues 452-466 are well ordered and protrude into the active site of each monomer with residues His465 and Thr466 that

preclude the access to the binding site to Glu (Fig. 1.7). At acidic pH however the C-terminal tail is not visible in the active site and has not been possible to assign to this protein portion any electron density, probably as a consequence of increased conformational flexibility (Fig. 1.6; (Capitani *et al.*, 2003)). The area of access to the active site, left free after the displacement of the C-terminal tail from the active site, is accompanied by an increased accessibility of the active site, partially occupied by the β-hairpin region belonging from the neighboring subunit of the functional dimer.

Biochemical (cfr. 1.2.1) and crystallographic studies provided evidence for the existence, at neutral pH, of a ternary complex, i.e. substituted aldamine, arising from reaction of the distal nitrogen of imidazole ring of His465 with the PLP-Lys276, which constitutes the catalytically inactive species (Fig. 1.7). Aldamine formation represents an elegant auto-inhibition mechanism, which ensures the enzyme to independently control its catalytic activity in a pH-dependent manner (Gut *et al.*, 2006). The functional analysis of GadBH465A and GadBΔHT mutants, in which the residue His465 is replaced or deleted, respectively, demonstrated that in the absence of this residue the active site becomes accessible to the substrate and the enzymatic activity persists at pH values at which the wild-type enzyme is typically inactive (Pennacchietti *et al.*, 2009). His465 is highly conserved in prokaryotic Gads and contributes to the cooperativity of the system (Pennacchietti *et al.*, 2009).

Experiments of cellular partition have pointed out that opening/closing of the active site of GadB does not affect the folding/unfolding of N-terminal triple-helix bundles, required for membrane recruitment (Pennacchietti *et al.*, 2009). Conversely, the unfolding of the α-helices affects the rate at which the C-terminal ends regain access into the active site (Gut *et al.*, 2006).

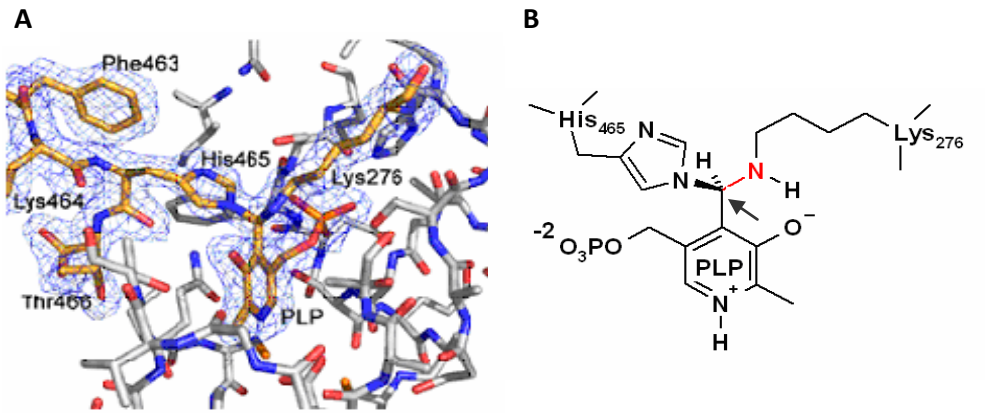


**Figure 1.7.** *GadB active site at neutral pH*. **(A)** Electron density map of substituted aldamine and residues involved in locking the active site (Phe463 to Thr 466). **(B)** Chemical structure of substituted aldamine. The arrow indicates the C4' carbon of the coenzyme which becomes $sp^3$ hybridized and asymmetric (Gut *et al.*, 2006).

## 1.2 Glutamate decarboxylase

### 1.2.1 Glutamate decarboxylases

Glutamate decarboxylase (Gad; EC 4.1.1.15) is an essential enzyme present in eukaryotes and prokaryotes, in which it plays different physiological roles (Ueno, 2000). It catalyzes the irreversible α-decarboxylation of L-glutamate to GABA (γ-aminobutyrate or 4-aminobutyrate).

Gad is a pyridoxal 5'-phosphate (PLP)-dependent enzyme. Members of this superfamily catalyze a range of important reactions, including α-decarboxylation, transamination, racemization and aldol cleavage (Jansonius, 1998), and many of these enzymes catalyze more than one reaction.

Unlike the aminotransferases, that constitute a family of homologous proteins, the PLP-dependent amino acid decarboxylases seem to be evolved along multiple lineages (Sandmeier *et al.*, 1994). The explanation for this

difference may be sought in the type of catalyzed reaction: transaminases react reversibly with two substrates, with a ping-pong mechanism, and generate changes not only in the covalent bond between Cα and the substrate, but also in the bond involving the C4' of the coenzyme. Thus, the complexity of the reaction could have prevented the evolution of aminotransferase according to multiple pathways. Instead the α-decarboxylation of an amino acid is a simpler process: it consists in an irreversible reaction which occurs on the Cα of the sole substrate used in the reaction, for which in the course of evolution were introduced amino acid substitutions to favor specificity towards different substrates.

Regarding the mechanism of action of PLP-dependent decarboxylases (Fig. 1.8), the transaldimination reaction leads to the formation of external aldimine so that the α-carboxylic group is oriented perpendicularly to the PLP pyridine ring. To this follows the release of $CO_2$ and, therefore, the formation of the quinonoid intermediate stabilized by the coenzyme. The protonation on Cα of the former substrate generates the enzyme-product complex, which is hydrolyzed with release of the corresponding amine. The PLP then reconstitutes the Schiff base with the lysine residue at the active site of the enzyme (internal aldimine).

For many decarboxylases, it was observed that the quinonoid intermediate can undergo an alternative fate (Sukhareva, 1986): in fact the protonation on C4', rather than on the Cα, and subsequent hydrolysis leads to the formation of the corresponding aldehyde and pyridoxamine 5'-phosphate (PMP), resulting in enzyme inactivation (Fig. 1.8b). This type of side reaction is known as abortive decarboxylation-transamination. The ability of PLP-

dependent enzymes to perform multiple reactions is clearly the result of an evolutionary reminiscence.

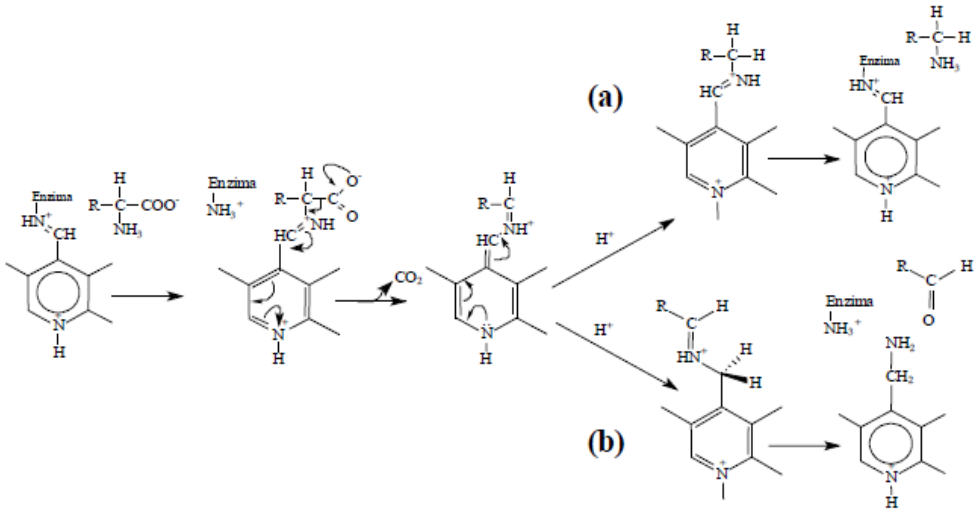


**Figure 1.8.** *Glutamate decarboxylase reaction mechanism.*

Based on multiple sequence alignment, the PLP-dependent decarboxylase have been divided into four distinct groups (Sandmeier *et al.*, 1994). Glutamate decarboxylases belong to the group II, which includes the decarboxylases acting on glutamate, histidine, tyrosine and aromatic-L-amino-acid.

Gad is widespread among living organisms, with low sequence identity (12%) between the vertebrate (human GAD65) and bacterial (*E. coli* GadB) proteins. Conversely, plant (*Arabidopsis thaliana* Gad1) and bacterial enzymes (*E. coli* GadB) are more similar in terms of sequence identity (39%) as well as oligomeric assembly.

### 1.2.2 Biochemical insights into *Escherichia coli* GadB

The kinetic properties of *E. coli* Gad reveal that it is highly specific for L-Glu glutamate and pH-dependence of the activity, with a maximum activity at pH 4.5 (Fonda, 1972). In particular, the enzyme is catalytically active at pH < 5.5, while at pH > 5.5 is inactive.

The two glutamate decarboxylase isoforms of *E. coli*, GadA and GadB, are 466 amino acids-long and differ in only 5 amino acid positions, four of which are located in the N-terminal region, while the last different residue is at position 153. The substitutions (GadA into GadB) are the following: Gln3Lys, Leu6Val, Phe9Leu, Ala22Ser and Asn153Asp. The separate overexpression and characterization of the two isoforms (De Biase *et al.*, 1996) indicated that the biochemical and kinetic properties of the two isoenzymes are identical, and also gave new impetus to structural studies for which purity and homogeneity of the starting material is a necessary precondition (Capitani *et al.*, 2003). The GadB isoform is expressed in recombinant form at higher levels compared to GadA and for this reason was chosen for both structural and biochemical studies.

The absorption spectrum of GadB varies as a function of pH (Fig. 1.9): at pH 4.5 the enzyme is catalytically active, has a yellow color and the coenzyme exhibits maximum absorption at 420 nm, while at pH 6 the enzyme is catalytically inactive, colorless and the chromophore displays maximum absorption at 340 nm.

The pH-dependent spectroscopic events have been investigated in detail (O'Leary & Brummund, 1974, Tramonti *et al.*, 2002): the transition from the inactive form (max. abs. 340 nm) to the active (max. abs. 420 nm) of GadB is a highly cooperative process as it involves the acquisition of 4-6 protons.

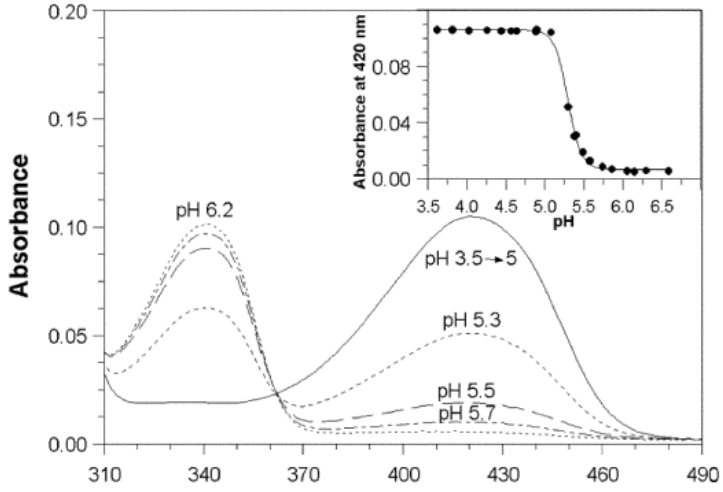


**Figure 1.9**. *Absorption spectra of wild type GadB as a function of pH*. In the region 300 nm - 500 nm, the transition between the 420nm-absorbig species and the 340 nm-absorbing species is observed. The spectrum at pH 5.3 is the one closest to the *pK* of the spectroscopic transition. The inset shows the titration curve obtained by plotting the values of absorbance at 420 nm as a function of pH (Tramonti *et al.*, 2002).

Following the pH increase, however, the loss of as many protons generates the inactive species of the enzyme. Analysis by rapid kinetics of this interconversion have shown that the equilibrium is affected by halides (O'Leary & Brummund, 1974). In particular, their presence favors 340 $\rightarrow$ 420 nm conversion, while significantly slows the conversion 420 $\rightarrow$ 340 nm. The enzyme activity therefore depends on these anions in solution according to the following scale of strength: $I^- > Br^- > Cl^-$. Among these, chloride is the physiologically more relevant halide because it is abundant in gastric secretions and thus directly involved in the intracellular activation of GadB, as demonstrated by crystallographic data (Gut *et al.*, 2006).

The spectroscopic change as a function of pH has been attributed, similarly to other PLP-dependent enzymes, to a different chemical state of the coenzyme

that in the active site is linked to the ε-amino group of Lys276 (internal aldimine) (Fig. 1.10, left). In fact, while in a hydrated active site the internal aldimine is predominantly represented in the ketoenamine form, which absorbs at 420 nm, in a less hydrated active site the enolimine form, which absorbs at 340 nm, will be the most likely species. However, previews studies and, more recently, crystallographic and site-specific mutagenesis studies (Gut *et al.*, 2006, Pennacchietti *et al.*, 2009) led to the conclusion that the species with maximum absorption at 340 nm corresponds to the substituted aldamine as hypothesized (cfr 1.1.3.2). This arises from the reaction between the nitrogen of the imidazole ring of the residue His465 and Lys276-PLP Schiff base, resulting in a change of the hybridization state of the C4' of the cofactor from $sp^2$ to $sp^3$ (Fig.1.7; Fig.1.10).

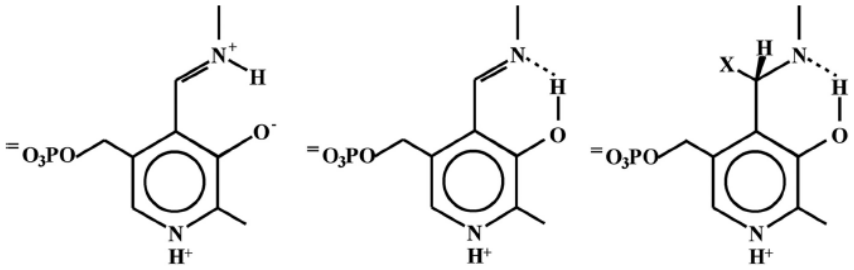

**Figure 1.10.** *Chemical structure of ketoenamine (on the left), enolimine (center) and substituted aldamine (right)* (Pennacchietti *et al.*, 2009).

In the last decade, crystallographic and biochemical studies allowed to identify the nature and the functional outcomes of the pH-dependent conformational changes (Capitani *et al.*, 2003, Gut *et al.*, 2006). On the other hand, the structural role of PLP concerning folding, oligomeric assembly and stability of the enzyme has not yet been fully investigated. The few available knowledge dates back to some decades ago, when *E. coli* GadB was first characterized in terms of biochemical and biophysical properties (for a

review (Sukhareva, 1986)). In the *holo*-form GadB is a hexamer, in which each subunit binds one PLP molecule (Shukuya & Schwert, 1960, Strausbauch & Fischer, 1970, To, 1971). The hexamer dissociates into inactive dimers when the enzyme is very diluted or when it is present in the apoenzymatic form and the pH of the solution is > 6 (Tikhonenko *et al.*, 1968) (Fig. 1. 11). This dissociation is reversed by the addition of PLP to apodimers: 3 equivalents of PLP are sufficient to reconstitute the hexamer, but the enzyme activity is fully restored only when 6 equivalents of coenzyme are added.

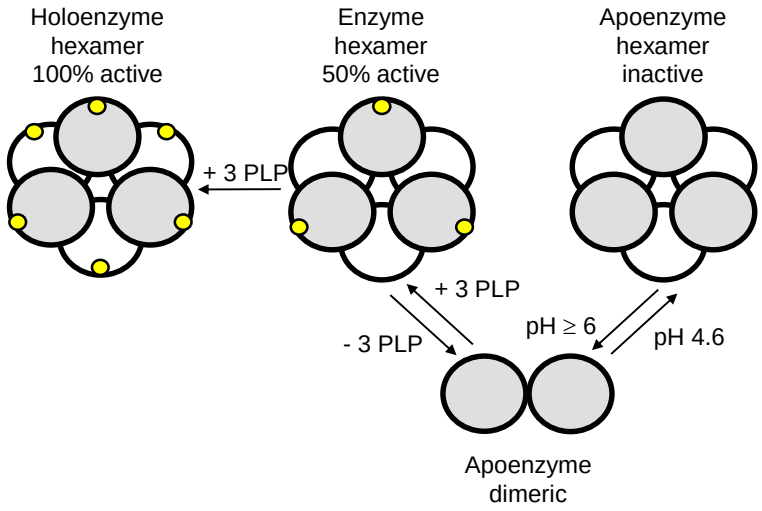


**Figure 1.11**. *Interconversion between the hexameric and dimeric form of Gad*.

The structure of the active site of GadB ((Capitani *et al.*, 2003); Fig. 1.7) has similarities with other fold-type I enzymes that belong to the structural family of aspartate aminotransferase. The residues Lys276, His275, Asp243 and Ala245 are the ones who primarily participate in securing and properly orienting the coenzyme in the active site. Indeed, the ε-amino group of

Lys276 forms the Schiff base with the C4' of the PLP (Tramonti *et al.*, 2002), the imidazole group of His275 interacts with the phosphate of the PLP (Tramonti *et al.*, 1998), the carboxyl group of the Asp243 residue forms a salt bridge with the nitrogen N1 of the PLP pyridine ring and the methyl group of the residue Ala245 provides a hydrophobic contact with the pyridine ring (Capitani *et al.*, 2003). However, some amino acid residues in the active site establish unusual interactions that have no counterparts in other decarboxylases belonging to the same structural family. For example, the pyridine ring of the cofactor establishes a hydrophobic interaction with the carbons in the side chain of Gln163. In other PLP-dependent enzymes this interaction typically involves π contacts with the aromatic side chains of phenylalanine, tryptophan, tyrosine and histidine residues. Moreover, in the GadB active site there are three cysteine residues, Cys64, Cys130 and Cys165, the last two of which appear to be involved in the formation of a disulfide bridge (Capitani *et al.*, 2003). The role of these residues has not been elucidated yet.

An element of absolute novelty is represented by the occurrence at neutral pH of the last two residues at the C-terminal tail, i.e. His465 and Thr466, in the active site. As mentioned before, these two residues occupy approximately the position of the natural substrate, Glu. The residue Asp86 is one of the few residues of the active site that is provided by the other subunit of the functional dimer and is essential for the stabilization of γ-carboxyl group of glutamate at acidic pH values, i.e. when at least one of the two carboxyl groups is protonated. The residue Phe63 plays an important role in GadB as it precludes residue Arg422 to interact with the α-carboxylic group of glutamate, which must be removed. It is noteworthy that in transaminases the residue that occupies the position of Arg422 in GadB is free to establish an

interaction with the α-carboxyl group of the substrate, and this is indispensable for correct catalysis.

### 1.2.3 Bacterial Gads

*E. coli* GadB is definitely the most extensively characterised bacterial Gad (cfr 1.1.3.2 and 1.2.2). In fact only few reports dealing with the biochemical properties of other bacterial Gads have been published (Table 1.1). Among these, Gad from *Clostridium perfrigens*, a major cause of food poisoning in developed countries, was purified by homogeneity and partially characterized (Cozzani *et al.*, 1970). It exhibits spectroscopic and kinetic properties, as well as the oligomeric assembly, resembling those of the *E. coli* enzyme.

More recently, the increased interest in high GABA-producing strains of LAB (Lactic Acid Bacteria) for biotechnological applications (cfr. 1.3.1), led to the purification and functional analysis of Gads from *Lactococcus lactis* (Nomura *et al.*, 1999), *Lactobacillus paracasei* (Hiraga *et al.*, 2008) and partial characterization of *Lactobacillus brevis* (Komatsuzaki *et al.*, 2008).

Notably, highly heat stable Gads from the hyperthermophilic archaea *Pyrococcus horikoshii* (Kim *et al.*, 2009) and *Pyrococcus furiosus* (Lee *et al.*, 2013) were purified as recombinant proteins and characterized for potential industrial applications. Compared to *E. coli* enzyme, the Gads from *Pyrococcus* species showed different biochemical features, such as an unusual monomeric assembly, a pH optimum in the neutral-alkaline range and broader substrate specificity (*P. furiosus*).

**Table 1.1.** *Prokaryotic Gads.*

| Species | Subunit MW | No. of subunits | Max. Abs. (nm) | pH optimum | $K_m$ (mM) | Sp. Act. µmol/ min/mg | Ref. |
|---|---|---|---|---|---|---|---|
| *Escherichia coli* | 50 | 6 | 340-420 | 3,8-4,6 | 2,32 | 240-235 | * |
| *Clostridium perfrigens* | 48-50 | 6 | 333-410 | 4,7 | - | 238[§] | (Cozzani et al., 1970) |
| *Listeria monocytogenes* | - | - | - | - | 16 | 39 | (Shah et al., 1981) |
| *Lactobacillus brevis IFO12005* | 54 | 2-4 | - | 4,2-4.6 | 1-9,3 | - | (Ueno *et al.*, 1997, Hiraga *et al.*, 2008) |
| *Lactococcus lactis* | 54 | - | - | 4,7 | 0,51 | 53,2 | (Nomura et al., 1999) |
| *Lactobacillus paracasei* | 57 | 2 | - | 5 | 5 | 7,5 | (Komatsuzaki et al., 2008) |
| *Pyrococcus horikoshii* | 42-45 | 1 | - | 8 | 3,9 | - | (Kim et al., 2009) |
| *Pyrococcus furiosus* | 41 | 1 | 340-420 | 6 | 2,22 | - | (Lee et al., 2013) |
| *Neurospora crassa* | 33 | 1 | - | 5 | 2,2 | 2,8 | (Hao & Schmit, 1993) |
| *Aspergillus oryzae* | 48 | 6 | - | - | 13,3 | 48,2 | (Tsuchiya et al., 2003) |

*(Shukuya & Schwert, 1960, De Biase *et al.*, 1996, Capitani *et al.*, 2003, Pennacchietti *et al.*, 2009)
[§] µl $CO_2$/min/mg

A ClustalW alignment generated with 20 bacterial Gads, mostly from Gram-positive and Gram-negative enteric bacteria, showed that 84 residues (18% of the *E. coli* GadB sequence) are strictly conserved (De Biase & Pennacchietti, 2012). Several of these residues are known to occupy critical positions in *E. coli* GadB, i.e. in or near the active site or at sites where the conformational changes occur. In addition to the 8 residues which are shared with group II decarboxylases (mainly involved in anchoring PLP and in structural roles), the concurrent presence of the residues listed in bold in Table 1.2 (numbering refers to *E. coli* GadB) may be regarded as the signature for bacterial Gad (De Biase & Pennacchietti, 2012). The latter residues play different roles and are: Asp86* (*from the neighboring subunit in the functional dimer), with its side-chain tilted towards the active site in the open conformation, interacts with the γ-carboxylate of the substrate

glutamate; Glu89* in the low-pH structure is not far away from Asp86*, from which in the neutral-pH structure it points in opposite direction (Capitani *et al.*, 2003); Gln163 with its side-chain alkyl portion acts as stacking residue for the PLP ring; Thr62 side chain hydroxyl and Phe63 amide nitrogen provide additional hydrogen bonds to the γ-carboxylate of the substrate; Phe63 with its side-chain ring plays also an important role in preventing the binding of the α-carboxylate of glutamate to Arg422; His275, preceding the PLP-binding residue Lys276, is critical for keeping the cofactor in place by making an hydrogen bond with an oxygen of the PLP phosphate group via its side-chain τ nitrogen (Tramonti *et al.*, 1998, Capitani *et al.*, 2003); Tyr305* and Leu306*, at the tip of the β-hairpin 300–313, interact with residues 461–463 at the C-terminus in the inactive form; Tyr305* in addition may be involved in protonating the substrate during the decarboxylation reaction, just as reported for Tyr332 in 3,4-dihydroxyl-L-phenylalanin (L-DOPA) decarboxylase (Bertoldi *et al.*, 2002); His465 is responsible for GadB auto-inhibition via formation of the substituted aldamine (cfr. 1.1.2.2; (Gut *et al.*, 2006, Pennacchietti *et al.*, 2009)).

Notably, the residue corresponding to *E. coli* GadB His465 is not present in the GadB homologue from *Lactobacillus brevis* ATCC367. The absence of this residue may be explained by the different structural organization of this enzyme. Hiraga *et al*. (Hiraga *et al.*, 2008) showed that Gad from *L. brevis* IFO12005 is dimeric in the inactive form and tetrameric in the active. Treatment of Gad with high concentrations of ammonium sulphate and subsequent dilution with sodium glutamate were essential for tetramerization and activation. Gad from *L. paracasei* was also reported to be dimeric (Komatsuzaki *et al.*, 2008).

**Table 1.2.** *Amino acid residues composing the bacterial Gad signature.*

| Residue[a] | Role |
|---|---|
| **Thr62** (side chain OH) | Binding of substrate γ-carboxylate |
| **Phe63** (amide N) | Binding of substrate γ-carboxylate |
| **Phe63** (side chain) | Prevents Arg422 binding to substrate α-carboxylate |
| **Asp86*** (β-carboxylate) | Binding of substrate γ-carboxylate |
| **Glu89*** (side chain) | Significant change in orientation upon pH-shift |
| Gly120[b] | Structural role |
| **Ser126** (amide N) | Hydrogen bond with PLP phosphate oxygen |
| **Ser127** (side chain OH) | Hydrogen bond with PLP phosphate oxygen |
| **Gln163** (alkyl chain) | PLP stacking |
| Gly210 | Probable structural role |
| Thr212 (side chain OH) | Interacting with PLP OH (intramolecular proton transfer?) |
| His241 (side chain π N) | Hydrogen bond with Ser269 |
| Asp243 (β-carboxylate) | Interacting with the pyridine N of PLP |
| Ala245 (side chain) | Hydrophobic contact with the pyridine ring of PLP |
| Ser269 (side chain OH) | Hydrogen bond with His241 |
| **His275** (side chain τ N) | Hydrogen bond with PLP phosphate oxygen |
| Lys276 (e-amino group) | Forming the Schiff-base with the C4' of PLP |
| **Tyr305*** (side chain OH) | Interacts with residues 461–463 of the C-terminus (reprotonation?) |
| **Leu306*** | Interacts with residues 461–463 of the C-terminus |
| **Gly307*** | In the β-turn of β-hairpin 300–313 |
| **His465** (side chain τ N) | Covalent bond with PLP-Lys276 Schiff base |

**a**. Numbering refers to *E. coli* GadB.
**b**. Residues in plain text are the residues strictly conserved in the decarboxylases of the PFAM PF00281.
The asterisk '*' indicates residues contributed by the neighbouring subunit in the functional dimer.
(Adapted from (De Biase & Pennacchietti, 2012))

Although the GDAR system was shown to play a pivotal role in the acid resistance of several orally-acquired bacteria, the corresponding Gads have not been characterized at the molecular level. For example Gad from the food-borne pathogen *L. monocytogenes* was only partially purified (Shah *et al.*, 1981). A potentially functional *gadBC* operon is present in the genome of several bacterial species. For instance in *Brucella microti*, a recently described, fast-growing *Brucella* species, the *gadB* and *gadC* genes are intact (Audic *et al.*, 2009). The role of GDAR system in *B. microti* was recently investigated (Occhialini *et al.*, 2012). GadB from *B. microti*, which shares 73% sequence identity with *E. coli* GadB, was purified as recombinant protein and extensively characterized in this thesis work.

### 1.2.4 Eukaryotic Gads

In the four last decades, several studies have been carried out to elucidate the physiological role and the functional properties of Gad in Eukaryotes (Tab 1.3), i.e. vertebrates and plants.

**Table 1.3.** *Eukaryotic Gads.*

| Species | Subunit MW | No. of subunits | Max. Abs. (nm) | pH optimum | $K_m$ (mM) | Sp. Act. µmol/ min/mg | Ref. |
|---|---|---|---|---|---|---|---|
| Mouse | 44 | 2 | - | 7 | 0,7 | 2 | (Wu *et al.*, 1973) |
| Human | 67 | 2 | 332-422 | 6,8 | 1,3 | 1 | (Blindermann et al., 1978, Chen et al., 1998) |
| Porcine α-β-γ | 60 | 2 | - | 6,2-6,5 | 0,17-0,45-1,25 | 0,48-1,2-2,3 | (Spink *et al.*, 1985) |
| Chicken | 62, 59 | 2 | - | - | - | 2,6 | (Gottlieb *et al.*, 1986) |
| Rat | 40-80-44 | 2 | - | 7,3 | 1,6 | 2,4 | (Denner *et al.*, 1987) |
| Feline | 59 | 2 | 338-420 | 6.6 | 1,37 | 3,25 | (Chu & Metzler, 1994) |
| Human GAD65 | 65,4 | 2 | 332-422 | - | 1,41 | - | (Chen *et al.*, 1998, Battaglioli *et al.*, 2003, Fenalti *et al.*, 2007) |
| Human GAD67 | 66,6 | 2 | - | - | 0,33 | - | (Battaglioli *et al.*, 2003, Fenalti *et al.*, 2007) |
| Monkey | 61 | - | - | 7 | - | 0,0011 | (Inoue *et al.*, 2008) |
| Squash | - | - | - | 5,8 | 8,3 | 25,8 | (Matsumoto *et al.*, 1986) |
| Soybean | - | - | - | 5,8 | 9 | 1,1 | (Snedden *et al.*, 1995) |
| Petunia | 58 | - | - | 5-6 | 8,2 | 30 | (Snedden *et al.*, 1996) |
| *Arabidopsis thaliana* Gad1 | 57,1 | 6 | 338-425 | 6 | - | 33,6 | (Zik et al., 1998, Gut et al., 2009) |
| *Arabidopsis thaliana* Gad2 | 56,1 | - | - | - | - | 20,1 | (Zik et al., 1998) |
| Locust | 51 | 2 | - | 7,2 | 5 | 1,10 | (Stapleton *et al.*, 1989) |
| *Saccaromyces cerevisiae* | 66 | - | - | 5 | - | - | (Coleman *et al.*, 2001) |

Recently, the structures of the two isoforms of human Gad (GAD65 and GAD67) and of the *Arabidopsis thaliana* Gad1 isoform were disclosed

(Fenalti *et al.*, 2007, Gut *et al.*, 2009), providing structural evidences of the diversified functional properties of Gads in living organisms.

Although prokaryotic and eukaryotic Gads all possess the PLP fold typical of the largest of the PLP-dependent enzyme families (Momany *et al.*, 1995), each Gad is unique in terms of distinctive structural features, such as mobile loops (human), a calmodulin binding domain (plant) or regions undergoing pH-dependent conformational changes (*E. coli*), relevant for activity in the corresponding organism (De Biase & Pennacchietti, 2012).

In mammals, Gad exists as two isoforms, named GAD67 and GAD65, encoded by different, independently regulated genes. Human Gads maintains the physiological supply of GABA, the most abundant inhibitory neurotransmitter of the CNS and control fundamental processes such as neurogenesis (Fagiolini *et al.*, 2004, Ge *et al.*, 2006), movement and tissue development (Nakatsu *et al.*, 1993, Asada *et al.*, 1997, Kash *et al.*, 1997). Altered GABA-mediated signaling is likely to play a role in a number of pathological conditions including Parkinson's disease, epilepsy, schizophrenia, autism, anxiety and bipolar disorder (Treiman, 2001, Akbarian & Huang, 2006, Thompson *et al.*, 2009, Lanoue *et al.*, 2010). Moreover GABA and Gad are present in several non-neuronal tissues including the pancreatic β-cells, from which GABA is released to regulate glucagon secretion by α-cells (Rorsman *et al.*, 1989), the adrenal medulla and the gastrointestinal tract (Tillakaratne *et al.*, 1995).

The two isoforms can undergo different post-translational modifications (Christgau *et al.*, 1992), have different intracellular distributions (Esclapez *et al.*, 1994) and are found in soluble and membrane-bound states (Dirkx *et al.*, 1995). GAD67 is constitutively active and is responsible for basal GABA production, while GAD65 is transiently activated in response to an additional

demand for extra GABA in neurotransmission (Asada *et al.*, 1996, Soghomonian & Martin, 1998), for example in response to stress (Kash *et al.*, 1997, Kash *et al.*, 1999). GAD65 exists predominantly in an inactive apo-form that can be rapidly activated via PLP supply.

Initial studies on preparations of the porcine enzyme revealed that Gad can undergo an abortive decarboxylative-transamination that produces succinic semialdehyde and pyridoxamine-5'-phosphate, which readily dissociates from the enzyme, leaving it as inactive apoenzyme (Porter *et al.*, 1985). Studies on human recombinant Gad showed that GAD65 is at least 15 times more efficient than GAD67 at catalyzing this side reaction, which leads to rapid loss of enzyme activity (Battaglioli *et al.*, 2003). It has been suggested that this represents a key mechanism for the control of GABA production.

Both isoforms of human Gad are dimeric, with the two active sites formed at the dimer interface. Structural and mutational data reveals that each active site is substantially covered by an extended loop (residues 432–442, termed the 'catalytic loop') contributed *in trans* by the other monomer (Fig. 1.12) (Fenalti *et al.*, 2007).

In GAD67 the catalytic loop is well ordered and provides the conserved residue Tyr434 in the correct orientation to allow protonation at the Cα position (Fig 1.12 b,c). The dynamic conformation of the catalytic loop is crucial in the inactivation of GAD65 (Fenalti *et al.*, 2007). In fact, in GAD67 the continuous presence of Tyr434 in the correct orientation favors protonation of the Cα atom and uninterrupted GABA production, whereas in GAD65 it is mobile and its flexibility causes the transient displacement of the catalytic tyrosine from the active site thereby rendering it more exposed and allowing protonation at C4'. This in turn leads to SSA production, release of PMP and enzyme autoinactivation.

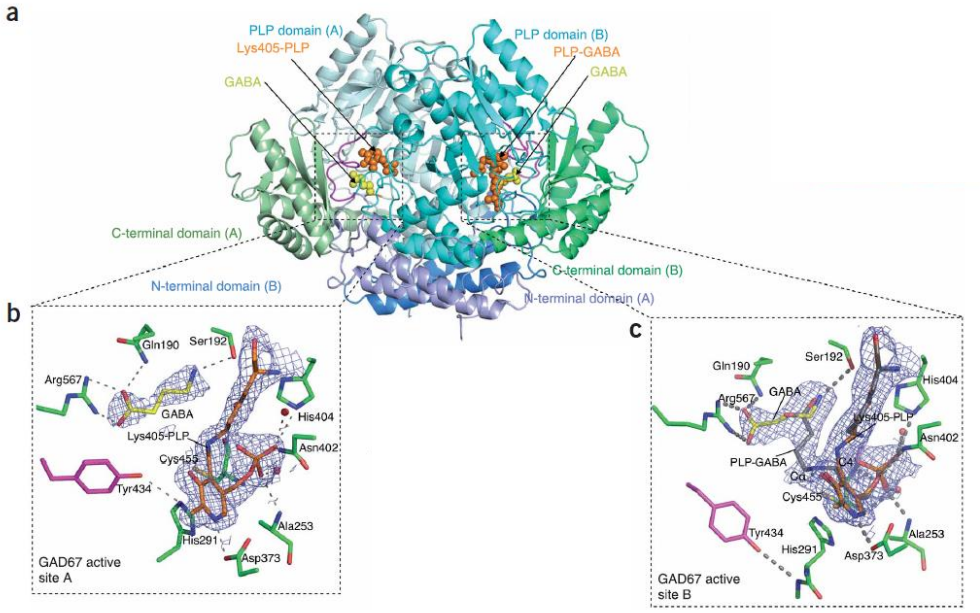


**Figure 1.12**. *Dimeric structure of human GAD67*. **(a)** The N-terminal (blue), PLP-binding (cyan) and C-terminal (green) domains are labelled. Monomer A is colored slightly lighter than monomer B. In the active sites: Lys405-PLP Schiff base and PLP-GABA (orange spheres) and bound GABA (yellow spheres). The catalytic loop forms a flap over the active site of an adjacent monomer *in trans* and is colored magenta in each monomer. **(b, c)** Active sites of GAD67, showing a close-up of Lys-PLP (shown as orange sticks), PLP-GABA (dark grey) and non-covalently bound GABA (yellow) moieties. In the active site of monomer A, the side chain hydroxyl group of Tyr434 (magenta) forms a hydrogen bond to the Nε2 of His291, and would be 2.8 Å from the protonation site (Cα) of a PLP-GABA moiety (grey, in active site B). In the active site of monomer B, Tyr434 is flipped to an alternative conformation where it interacts with the backbone nitrogen of Tyr292 (adapted from (Fenalti *et al.*, 2007)).

A recent study revealed that the C-terminal domain also plays a critical role in the autoinhibition process via stabilizing the catalytic loop (Langendorf *et al.*, 2013). GAD65, but not GAD67, is autoantigenic, with autoantibodies characteristically detectable in type 1 diabetes, autoimmune polyendocrine syndrome (APS), and more rarely in neurological disorders, i.e. Stiff-Person

syndrome (Solimena *et al.*, 1988, Solimena *et al.*, 1990), Batten's disease (Ramirez-Montealegre *et al.*, 2005), cerebellar ataxia (Honnorat *et al.*, 2001) and epilepsy (Peltola *et al.*, 2000). The high-resolution crystal structures of both isoforms in combination with the epitope-mapping reveal key differences that correlate with known epitope regions in the antigenic isoform GAD65 (Arafat *et al.*, 2009, Fenalti & Buckle, 2010). Specifically, the above mentioned flexibility in GAD65 at the C-terminal domain and catalytic loop, a property that is required for enzymatic function, may be the cause of the increased B-cell antigenicity.

In plant, Gad is involved in development (Baum *et al.*, 1996) and stress response (Bouche *et al.*, 2004). Recent findings suggest that GABA also has a role as a signaling molecule in plants (Bouche & Fromm, 2004)**.**

Plant Gad exhibits two independent level of regulation: one is pH-dependent, providing an acidic activity maximum (pH 6), and the other is $Ca^{2+}$-dependent and mediated by $Ca^{2+}$/calmodulin (CaM) binding, which is most efficient at pH 7.5. Thanks to this two-level regulation, Gad can flexibly respond to different kind of cellular stress occurring at different pH: at physiological pH, $Ca^{2+}$/CaM-mediated Gad activation is required to respond to abiotic stress, whereas the acidic pH-dependent level of regulation might be involved in tissue wounding by larval footsteps and herbivores, which causes cytoplasm acidification as consequence of the release of vacuolar and apoplastic protons (Bown *et al.*, 2006).

In the model plant *Arabidopsis thaliana*, five Gad isoforms exist. Among them two, i.e. Gad1 and Gad2, have been biochemically characterized (Zik *et al.*, 1998). The X-ray crystallographic structure of the root-specific isoform Gad1 (Fig. 1.13) is similar to that of *E. coli* GadB, with which it shares the

same fold and oligomeric assembly (Gut *et al.*, 2009). Moreover, the active site and the cofactor binding mode are well conserved.

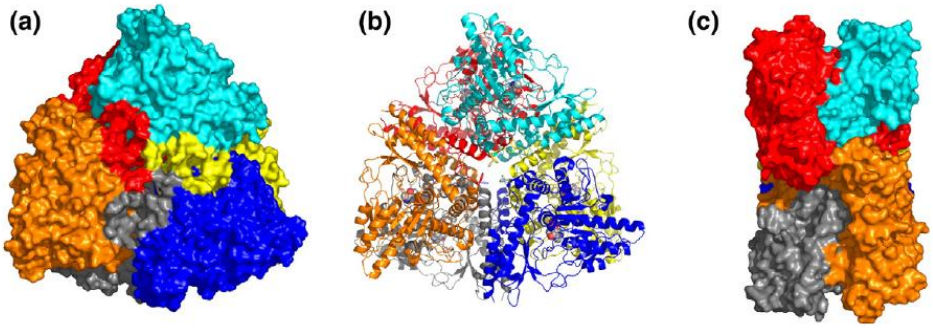


**Figure 1.13.** *Crystal structure of* A. thaliana *Gad1*. **(a and c)** Surface representations of the Gad1 homohexamer. View along the 3-fold (a) and the 2-fold (c) non-crystallographic symmetry axes of the protein. **(b)** Cartoon representation of Gad1. The six subunits are depicted in different colors. (Gut *et al.*, 2009).

Conversely, the key functional modules at the N-terminal and C-terminal regions of Gad1 differ significantly, reflecting adaptations to different function and regulation.

Similarly to *E. coli* GadB N-terminal domain has an important role in the formation and stabilization of the dimer and hexamer, while the triple helical bundles and the halide binding sites, typical of *E. coli* GadB, are not conserved. The C-terminal domain consists of a linker of approx. 20 residues followed by the well characterized and conserved CaMBD (CaM Binding Domain), which regulates enzyme activity in a CaM-dependent manner. According to a low-resolution structure by small-angle X-ray scattering (SAXS), CaM actives Gad1 in a unique way (Fig. 1.14): one CaM1 molecule attaches to two Gad1-CaMBDs of the neighboring subunits in a homoexameric enzyme, activating two adjacent active sites by relief of the corresponding autoinhibitory domains (AIDs) (Gut *et al.*, 2009).

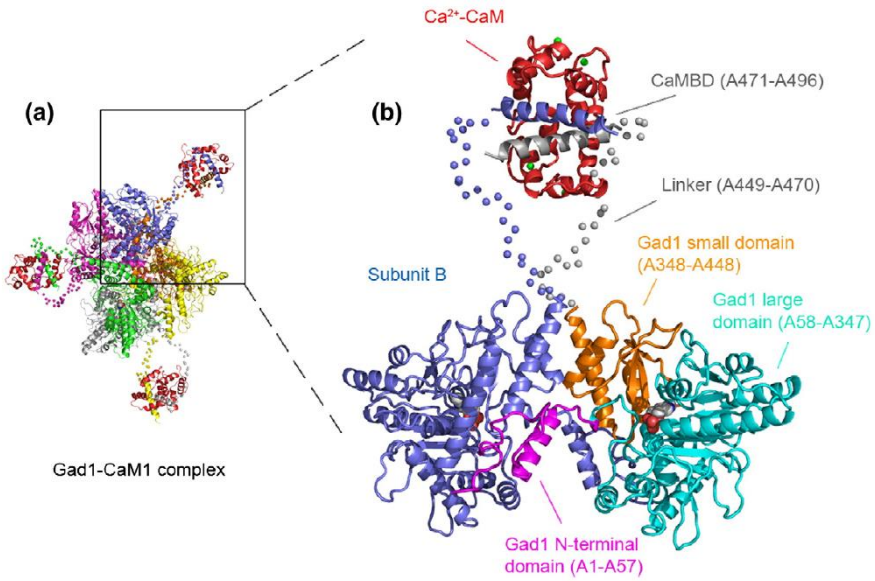


**Figure 1.14.** *Domain organization of Gad1 and CaM-binding mode*. (a) Cartoon representation of the Gad1–CaM1 complex from the SAXS model. Each Gad1 subunit is in a different colour, and the CaM molecules are in red. (b) Gad1 subunits are depicted as a cartoon with the linker atoms as spheres. Subunit B is in blue, subunit A is colour-coded by domain: N-terminal domain, magenta; large domain, cyan; small domain, orange; C-terminal linker, grey spheres; CaMBD, grey. CaM (red) is depicted as a cartoon with bound $Ca2^{+}$ as green spheres. The cofactors of two adjacent active sites appear in space-fill mode. (Gut *et al.*, 2009)

According to the model proposed for the regulation of Gad1 activity (Gut *et al.*, 2009) the AID of Gad1 folds into the active site in a pH-dependent fashion, and the ionization state of K496-K497 influences the tautomerization equilibrium of PLP and enzyme activation. The affinity of AID for the active site is stronger at pH above 6.9, resulting in the prevalence of the 338 nm-absorbing enolimine tautomer and consequent autoinhibition. A pH below 6.9 destabilizes the folded-CaMBD and results in the unfolding of this domain with a shift to the 415-nm-absorbing ketoenamine form of PLP. In the Gad1-CaM1 complex: CaM1 wrapped around two CaMBDs, keeps two AIDs away from the respective active sites and the cofactor is in its

ketoenamine form over the entire pH range. Notably, CaM1 enhances the activity of Gad1 more effectively at neutral-to-high pH, where C-termini are folded over the active sites.

## 1.3 Biotechnological aspects

### 1.3.1 GABA production by GDAR system in health and disease

In mammals GABA exherts well-known physiological functions such as neurotransmission, induction of hypotension, and diuretic and tranquilizer effects (Wong *et al.*, 2003). GABA is also employed for treatment of sleeplessness, depression, and autonomic disorders (Okada *et al.*, 2000), chronic alcohol-related symptoms (Oh *et al.*, 2003) and stimulation of immune cells (Oh & Oh, 2003). In addition, GABA was reported to be a strong secretagogue of insulin (Adeghate & Ponery, 2002), to promote the healing process of cutaneous wounds (Han *et al.*, 2007) and to enhance survival of dermal fibroblasts exposed to oxidative stress (Ito *et al.*, 2007). Owing to these physiological functions, several GABA-enriched fermented food, such as yogurt, cheese, green tea, rice germ (Abe *et al.*, 1995, Oh *et al.*, 2003, Hayakawa *et al.*, 2004, Zhang *et al.*, 2006, Park & Oh, 2007) are considered commercially promising functional foods (Gobbetti *et al.*, 2010).
Functional foods were first described by M. Roberfroid as "food similar in appearance to conventional food that is intended to be consumed as part of the normal diet, but has been modified to sub-serve physiological roles beyond the provision of simple nutrient requirements" (Roberfroid, 1999). The health benefits of fermented functional foods are expressed either directly through the interactions of ingested live microorganisms with the host (probiotic effect) or indirectly as the result of the ingestion of microbial

metabolites synthesized during fermentation (biogenic effect) (Stanton *et al.*, 2005).

Some food substrates (e.g. whey milk and grape must) could be enriched in GABA by fermentation with high GABA-producing LAB strains (Nomura *et al.*, 1998, Siragusa *et al.*, 2007). For example in a recent work it was shown that grape must fermented with *L. plantarum* DSM 19463 yields Gad-derived GABA at mM levels (Di Cagno *et al.*, 2010). The resulting freeze-dried preparation together with GABA, contained niacin, minerals, and polyphenols due to the use of grape must. Although the primary use of this preparation is as a functional food supplement, it can also find application in dermatology. In fact, following application to Skin Ethic Reconstructed Human Epidermis, it induces the expression of human genes involved in skin protection, i.e. β-defensin-2, hyaluronan synthase and filaggrin (Di Cagno *et al.*, 2010). This intriguing finding might open the way to new strategies for antimicrobial therapy in cosmetics.

### 1.3.2 The application of glutamate decarboxylase in the manufacturing of biobased industrial chemicals

Glutamic acid is a non-essential amino acid and is the most abundant amino acid in many plant proteins. Agricultural surplus and waste stream from biofuel production are now being considered as a low cost sources of glutamate for biotechnological conversion into GABA, and production of bio-based chemicals (Lammens *et al.*, 2012). Examples of protein-containing materials are bioethanol byproduct streams such as DDGS (dried distiller's grains with solubles, from maize and wheat) or vinasse (from sugarcane or sugar beets), but also plant leaves, natural oil or biodiesel byproducts, and

slaughterhouse waste. In the future algae could also provide an additional source for biodiesel and also Glu.

Currently the proteins from plant leaves usually exit from biorefinery either in the form of fertilizers or in the form of animal feed. The protein-rich fraction of plants can be further split into more- and less-nutritious fractions, for example by hydrolyzing the proteins and separating the essential (nutritious) from the non-essential (less nutritious) amino acids. Non-essential amino acids (e.g. glutamic acid, aspartic acid), with no significant value for food or feed could be very suitable raw materials for preparing (highly) functionalized chemicals, traditionally prepared by the petrochemical industry.

Nitrogen containing molecules production usually involves reactions of molecules, such as propylene with ammonia, in very energy-intensive process (Veatch *et al.*, 1960). Amino acids already contain nitrogen and can represent the starting material to by-pass the use of ammonia for the synthesis of nitrogen containing bulk chemicals (Scott *et al.*, 2007). In this way it is possible to find new ways to decrease our dependency on fossil fuels.

The structure of glutamic acid resembles many industrial intermediates, so a variety of chemicals could be made from it using a relatively limited number of steps. Examples of nitrogen-containing molecules that can in theory be produced from glutamic acid are the lactams N-methylpyrrolidone and N-vinylpyrrolidone (Fig. 1.15). They are cyclic compounds containing four carbons, of which one is oxidized and involved in an amide bond with a nitrogen in the ring. N-methylpyrrolidone (NMP) is an industrial solvent that is used in the manufacture of plastics and as an ingredient in paint removers. N-vinylpyrrolidone (NVP) finds applications in the manufacturing of poly(vinylpyrrolidone) and copolymers, for example together with vinyl

acetate and methyl acrylate. Further it is used as solvent in the production of inks and paints, as an additive in the cosmetics industry, and in the pharmaceutical industry for the production of a disinfectant.

On the pathway from glutamic acid to a range of molecules, decarboxylation of glutamic acid to GABA, enzymatically performed by Gad, is an important reaction. GABA in fact can be an intermediate from which various other chemicals can be synthesized, such as pyrrolidones. This can be done by combining the enzymatic decarboxylation performed by Gad with the one-pot cyclization of GABA to 2-pyrrolidone and methylation to form NMP (Lammens *et al.*, 2010). By not fully converting 2-pyrrolidone into NMP, part of it could also be used for the simultaneous production of NVP. Another interesting material synthesized by ring-opening polymerization of 2-pyrrolidone is Nylon 4 (Park *et al.*, 2013), a four-carbon polyamide suitable for application as an engineering plastic due to its superior thermal and mechanical properties (Cho *et al.*, 2011). Contrary to other nylon polymers, nylon 4 is heat-resistant, biodegradable, biocompatible and compostable (Tokiwa *et al.*, 2009).

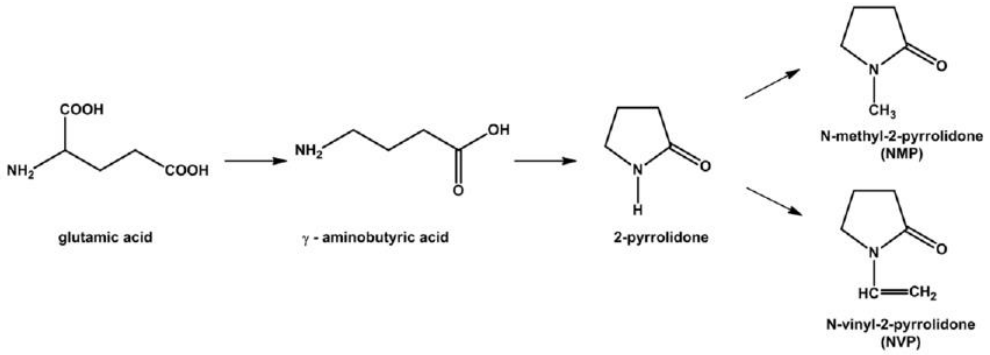


**Figure 1.15**. *The pathway from glutamic acid to pyrrolidone-based chemicals* (Adapted from (Lammens *et al.*, 2011)).

Bio-based synthesis of GABA can be achieved either by whole cell reaction employing natural and recombinant microorganism or by purified Gad. Many prokaryotic Gad have recently been overexpressed in different bacteria such as *E. coli* (Le Vo *et al.*, 2011), *L. brevis* (Park & Oh, 2007, Se-Hee Kim, 2007), *B. subtilis* (Park & Oh, 2006) and *B. longum* (Park *et al.*, 2005). However, using whole cells has disadvantages such as the decomposition of the product by GABA transaminase or the possible decrease in activity due to lack of nutrients for the cells. The use of purified Gad seems to be economically more feasible because of the simplified downstream purification of GABA from less complex reaction conditions. Recent reports have described Gad immobilization for re-use, like GadB immobilized on calcium alginate beads in bioreactor (Lammens *et al.*, 2009), Gad immobilized as fusion protein to a cellulose-binding domain (Park *et al.*, 2012) and Gad immobilized to metal affinity gel (Lee *et al.*, 2013). Moreover, engineered *E. coli* GadB, such as a C-terminal truncated mutant (Yu *et al.*, 2012), His465 mutants (Pennacchietti *et al.*, 2009) and Glu89/His465 mutants (Ho *et al.*, 2013) were designed with the aim of improving the enzymatic properties of Gad and the reaction conditions for potential industrial applications.

## 1.4 Aims

The scientific relevance of studying glutamate decarboxylase resides in its diversified physiological role and functional properties in living organisms.
In humans alterations of GABA-signaling and autoantibodies anti-Gad have been related to neurological disorders (Treiman, 2001, Lanoue *et al.*, 2010) and autoimmune diseases (Lernmark, 1996) respectively.

Bacterial glutamate decarboxylases are interesting both for their physiological role in GDAR system (De Biase & Pennacchietti, 2012) and for the understanding of structure-function relationships in decarboxylases. Furthermore, exploring the catalytic mechanism, the molecular basis for enzyme activation/inactivation, and the role of PLP in the folding and oligomeric state of this enzyme is of relevance as it may have implications in both biomedical and biotechnology fields. In the latter case, glutamate decarboxylase reaction can find applications in the production of GABA-enriched functional food (Di Cagno *et al.*, 2010) and manufacturing of bio-based industrial chemicals using GABA as an intermediate for the synthesis of biopolymers (Lammens *et al.*, 2009).

Glutamate decarboxylase (GadB) from *E. coli* has been extensively studied in our laboratory for many years. This thesis work has been undertaken with the aim of better understanding the functional role of specific amino acid residues involved in substrate binding and control of the enzyme activity in *E. coli* GadB. In addition, in order to gain further insights into the structural features of GadB *apo* form and the role of PLP in protein folding, a preliminary structural study on dimeric *apo*GadB was carried out.

To date, except for *E. coli* GadB, there are no reports on an in-depth functional, biochemical and spectroscopic characterization of bacterial Gad. Therefore, one of the goals of my work was to investigate whether the pH-dependent molecular mechanisms controlling *E. coli* GadB activation are also conserved in other bacterial Gads, such as GadB from *B. microti*, in which the role of GDAR system was recently investigated (Occhialini *et al.*, 2012). Thus, GadB from *B. microti* was expressed and purified as recombinant protein in a laboratory strain of *E. coli*, and extensively characterized at the biochemical level.

# *Materials and Methods*

## 2.1 Growth media, bacterial strains and plasmids

Bacteria were grown in the following media, which were sterilized in autoclave for 20 minutes at 120°C before use: LB, pH 7.4; SOB, pH 7.5; SOC (SOB supplemented with 0.2% glucose and 10 mM $MgCl_2$); 2XL, pH 7.5; SB, brought to pH 7.5 with 50 mM potassium phosphate buffer, pH 7.5 (Sambrook *et al.*, 1989); LB agar (LB containing 15 g/l Bacto Agar). Antibiotics were added to the growth media at the following concentrations: ampicillin (100 µg/ml), kanamycin (25 µg/ml), and chloramphenicol (34 µg/ml). Bacto-tryptone, yeast extract and Bacto-agar are from Difco (BD & Co., France).

The wild type *E. coli* K12 and B strains and plasmids used in this work are listed in Table 2.1.

**Table 2.1.** *E. coli strains and plasmids used in this study.*

| **Bacterial strains** | **Genotype** | **Source** |
|---|---|---|
| MG1655 | F-, $\lambda^-$, *rph-1* | GSC7740 |
| MG1655Δ*gadA*Δ*gadB* | MG1655 knockout mutant, in which *gadA* and *gadB* genes are deleted | (Occhialini *et al.*, 2012) |
| MG1655Δ*gadA*Δ*gadBC* | MG1655 knockout mutant, in which *gadA*, *gadB* and *gadC* genes are deleted | D. De Biase (unpublished) |
| CC118 | $F^-$, *araD139*, Δ(*ara*, *leu*)7697, Δ*lac*X74, *phoA*Δ20, *galE*, *galK*, *thi*,*rpsE*, *rpoB*, $argE_{am}$, *recAl* | (Manoil & Beckwith, 1985) |
| StrataClone SoloPack | $F^-$, $r^-$, *endA*$^-$, *recA*$^-$, *tonA*$^-$, *cre*, *lacZ*Δ*M15*, $Sm^R$ | Stratagene |
| BL21(DE3) | F-, *omp*T, *hsd*$S_B$ ($r_B^-m_B^-$), *dcm*, *gal*, *lon*, λ(DE3) | (Studier *et al.*, 1990) |
| DH5α-$T1^R$ | F-, *rec*A1, *end*A1, *hsd*R17($r^-_k$,$m^+_k$), *sup*E44, *thi*-1, *gyr*A96, *rel*A1, *deo*R, *phoA*, Δ*(lacZYA-argF)* U169[ϕ80 *lac*ZΔM15], *ton*A | Invitrogen |

| | | |
|---|---|---|
| JM109 | F'[*tra*D36, *pro*A$^{+}$, *pro*B$^{+}$, *lac*I$^{q}$, *lac*ZΔ(M15)], *rec*A1, *end*A1, *gyr*A96(Nal$^{R}$), *thi*, *hsd*R17($r^{-}_{k}$,$m^{+}_{k}$), *sup*E44, *rel*A1, Δ(*lac-proAB*), *mcr*A | (Ausubel *et al.*, 1987) |
| **Plasmids** | | |
| pBBR1MCS | Expression plasmid (4707 bp): *lac*, T3 and T7 promoters, CAT/Cam$^{R}$. | (Kovach *et al.*, 1994) |
| pBBR-*gadBC_Bm* | pBBR1MCS containing a 3523-bp genome fragment from *B. microti* CCM4915, inserted between *Pst*I and *Xba*I restriction sites. | (Occhialini *et al.*, 2012) |
| pBBR-*gadBC_Ec* | pBBR1MCS containing the *gadB-gadC* genomic region of *E. coli*. | (Occhialini *et al.*, 2012) |
| pSC-A | Cloning plasmid (4.3 kb): pUC ori, f1 *ori*, P*lac*, lacZ, *neo* (Kan$^{R}$), *bla* (Amp$^{R}$), *loxP*, PCR product insertion site. | Stratagene |
| pSC-A_*Bm-gadB* | pSCA containing a PCR product of 1395 bp, from pBBR-*gadBC_Bm* and corresponding to the *gadB* ORF from *Brucella microti*. | This study |
| pET3a | Expression plasmid (4640 bp): pBR322 origin, T7 promoter, *bla* (Amp$^{R}$) | Novagen |
| pET3a_*Bm-gadB* | pET3a containing a fragment of 1395 bp (*gadB* ORF from *Brucella microti*) inserted between *Nde*I and *Bam*HI restriction sites. | This study |
| pQE60 | Expression plasmid (3429 bp): ColE1 *ori*, $P_{T5}$-*lacO* RBSII, *bla* (Amp$^{R}$) | Qiagen |
| pQ*gadB* | pQE60 containing a fragment of 1411 bp (1398 bp *gadB* ORF and 13 bp downstream) inserted between *Nco*I and *Hin*dIII restriction sites. | (De Biase *et al.*, 1996) |
| pQ*gadB*H465A | pQ*gadB* in which the fragment *gadB Eco*RV-*Hind*III (639 bp) is replaced by a 639-bp fragment, containing the mutation H465A, obtained by PCR and digested with *Eco*RV-*Hind*III. | (Pennacchietti *et al.*, 2009) |
| pQ*gadB*D86N | pQ*gadB* in which the Asp86 has been mutated to Asn using the Gene Tailor system (Invitrogen) which inserts the mutation by amplification of the entire plasmid. | (Pennacchietti *et al*., submitted to FEBS) |
| pQ*gadB*D86N-H465A | pQ*gadB* in which the fragment *gadB*H465A *Nco*I-*Eco*RV (771 bp) is replaced by a 771-bp fragment, containing the mutation D86N, obtained by digestion with *Nco*I-*Eco*RV from pQ*gadB*D86N. | (Pennacchietti *et al*., submitted to FEBS) |
| pREP4 | Accessory plasmid (3740 bp): p15A *ori*, *lacI*, *neo* (Kan$^{R}$) | Qiagen |

- **pBBR1MCS** (Fig. 2.1) is a relatively small (4.7 kb) broad-host-range plasmid, derived from pBBR1CM (Antoine & Locht, 1992), which confers chloramphenicol resistance, has a multiple cloning site (Kovach *et al.*, 1994) and is stably maintained as an extrachromosomal element in both *E. coli*, *Bordetella bronchiseptica* and *Brucella* species (Elzer *et al.*, 1995).

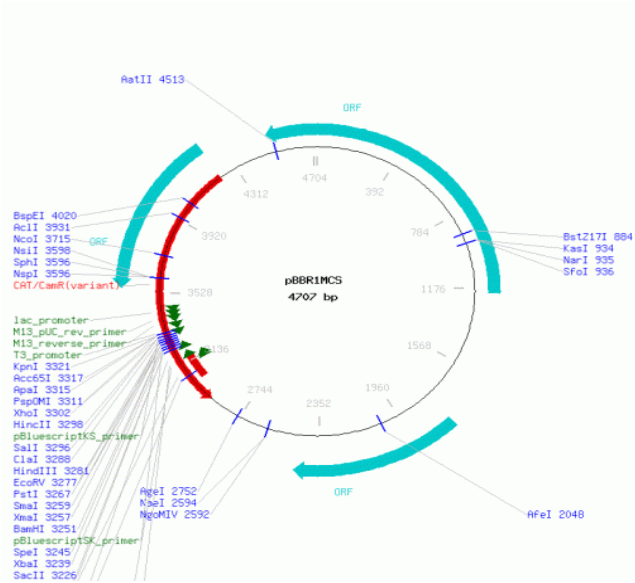


**Figure 2.1.** *Circular map of plasmid pBBR1MCS.* Unique-cutting restriction sites are shown in blue together with the position at which they cut.

- **pSC-A** is a plasmid of 4.3 kb provided with the StrataClone PCR Cloning K for high-efficiency ligation and cloning in *E. coli* StrataClone SoloPack cells. The plasmid pSC-A is supplied with two DNA arms, each charged with topoisomerase I (from *Vaccinia* virus) on one end and containing a *lox*P recognition sequence on the other end (Fig. 2.2). The topoisomerase-charged ends have a modified uridine (U*) overhang. Taq-amplified PCR products, which contain 3´-adenosine overhangs, are efficiently ligated to these vector arms in a 5-minute ligation reaction, through A-U* base-pairing followed by topoisomerase I-mediated strand ligation. The resulting linear molecule is

transformed into competent cells engineered for the expression of Cre recombinase from bacteriophage P1. Cre-mediated recombination between the vector *lox*P sites creates a circular DNA molecule (Fig 2.2) that is proficient for replication in cells growing on media containing ampicillin and/or kanamycin.

The pSC-A plasmid has two origins of replication, contains genes for ampicillin (*bla*) and the kanamycin (*neo*) resistance, and allows the blue/white selection of clones, since the insertion of the PCR fragment interrupts a *lacZα* cassette.

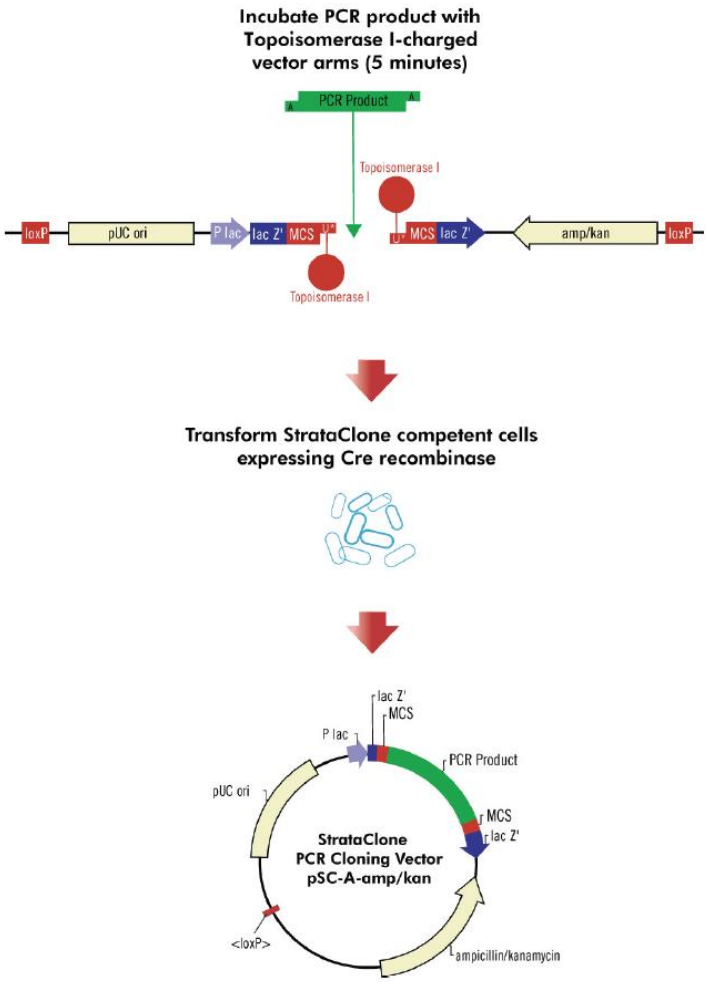


**Figure 2.2**. *pSC-A and Strataclone PCR cloning kit strategy.*(Stratagene).

- **pET-3a** (Fig. 2.3). The pET System is a powerful system for the cloning and expression of recombinant proteins in *E. coli*. Target genes are cloned in pET plasmids under control of strong bacteriophage T7 transcription and (optionally) translation signals; expression is induced by providing a source of T7 RNA polymerase in the host cell, that selectively transcribes target genes. Target genes are initially cloned using hosts that do not contain the T7 RNA polymerase gene, thus eliminating plasmid instability due to the

production of proteins potentially toxic to the host cell. Once established in a non-expression host (e.g. *E. coli* DH5α), plasmids are then transferred into the expression hosts containing a chromosomal copy of the T7 RNA polymerase gene under lacUV5 control (e.g. *E. coli* BL21(DE3)), and gene expression is induced by the addition of isopropyl-β-D-thiogalactoside (IPTG), an analogue of lactose.

- **pQE60** (Fig. 2.3) belongs to the pDS family and derived from pDS556/RBSII plasmid. It consists of 3429 bp and contains phage T5 promoter and two *lac* operators. The regulation of the promoter/operator is very efficient: the transcription is blocked in the presence of *lac* repressor (lacI), while it is rapidly induced by the addition of IPTG, which inactivates the repressor and makes the promoter accessible. The plasmid has a polylinker immediately downstream of a synthetic ribosome binding and carries the ampicillin resistance *bla* gene. Furthermore, it possesses a sequence coding for six histidine residues (His tag), which precedes the translation termination codons. This accessory protein portion can be used to purify the expressed protein, by affinity chromatography on a nickel column, which was not the case for GadB and its variants characterised in this work.

- **pREP4** is a 3740 bp plasmid, which contains the *lacI* gene encoding the *lac* repressor. The presence of this accessory plasmid in the cell carrying pQE60 or its derivatives provides high levels of repressor, thus increasing the efficiency in repressing the *lac* operator of pQE60. This plasmid contains also the kanamycin resistance gene (*neo*) and an origin of replication (p15A) different from that of pQE60, which allows their co-existence in the host.

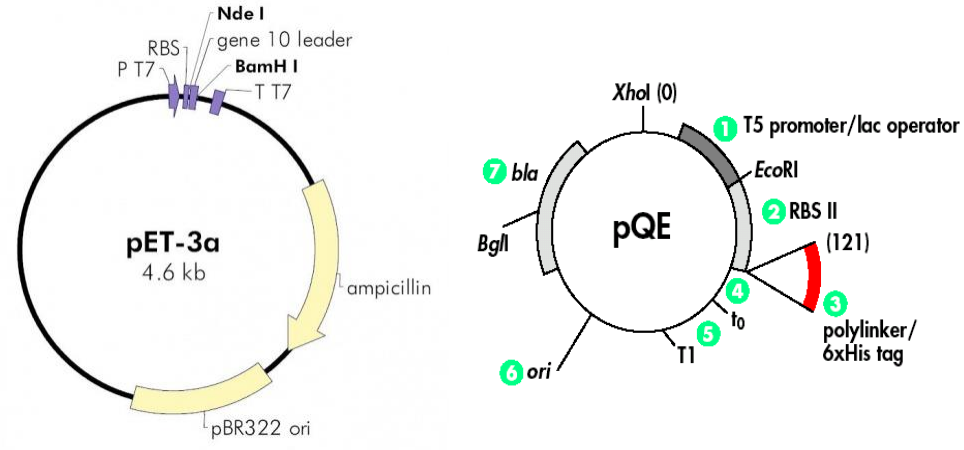


**Figure 2.3.** *Maps of pET-3a and pQE60 plasmids.*

## 2.2 N-terminal sequence determination of *Bm*GadB

The low-copy-number plasmid pBBR-*gadBC_Bm* (Tab. 2.1), carrying a 3.52 kb genome fragment encompassing the whole *B. microti gadBC* operon under its indigenous promoter, was used to transform the *E. coli* strain CC118 (cfr. 2.3.2).

Preliminary analysis on the expression and functionality of *Bm*GadB was performed. Briefly, a 50-ml culture was grown overnight (i.e. 18 hours) in LB broth at 37°C. Bacterial cells were collected by centrifugation at 3500 rpm, resuspended in 1 ml of an aqueous solution containing 1 mM PLP/1 mM DTT and disrupted by sonication. The cleared supernatant was subjected to western blotting (cfr. 2.6.6) and Gad activity assay (cfr. 2.6.3). As control, the *E. coli* strain CC118 carrying the empty plasmid pBBR1MCS was analysed in parallel.

A 11 µg aliquot of partially purified *Bm*GadB (corresponding to approx. 5 µg of pure *Bm*GadB) was subjected to SDS-PAGE followed by blotting onto

polyvinylidine difluoride (PVDF) membrane (cfr. 2.6.6). The area of the PVDF membrane corresponding to *Bm*GadB was excised and subjected to N-terminal sequencing (Proteome Factory AG, Berlin, Germany).

## 2.3 Recombinant DNA techniques

### 2.3.1 Purification of plasmid DNA, digestion with restriction enzymes and electrophoresis

The purification of plasmid DNA was performed using the Nucleospin® plasmid kit (Macherey-Nagel), which allows the quick isolation of supercoiled plasmid with high yields. Briefly: a single colony is inoculated in LB medium containing the antibiotic, and the cell culture is incubated at 37°C with constant shaking (200 rpm) overnight (> 16 h). Cells are harvested by centrifugation and the bacterial pellet is resuspended in a buffer solution containing RNAasiA 100 µg/ml. Then, an alkaline/SDS lysis is performed for few minutes at room temperature and the lysate is neutralized by adding a solution containing guanidinium hydrochloride and acetic acid. Precipitated protein, genomic DNA, and cell debris are then pelleted by a centrifugation step (10 min at 16000 g). The supernatant is loaded onto a NucleoSpin® Plasmid column and centrifuged for 1 min at 16000 g. The flow-through is discarded and the column is washed with a buffer containing guanidinium hydrochloride and isopropanol, followed by centrifugation for 1 min at 16000 g. An additional washing step is performed with a buffer containing ethanol. The centrifugation is repeated to remove residual ethanol and then plasmid DNA is eluted in µl 50 $H_2O$ or 10 mM Tris/HCl buffer, pH 8.5.

The DNA concentration was determined spectrophotometrically, using the conversion factor: $O.D._{260\ nm}$ 1.0 = 50 µg/ml.

Digestions with restriction enzymes were performed according to the manufacturer's instructions (Roche). The DNA fragments obtained were analysed on agarose gel and their sizes deduced by comparison with appropriate molecular weight standard (Fermentas).

The agarose gel (1% w/v) was prepared in 1X TAE buffer (0.04 M Tris;1 mM EDTA; 5 mM sodium acetate, adjusted to pH 7.5 with glacial acetic acid. Ethidium bromide (0.4 µg/ml), which intercalates into the DNA double helix, was added just before pouring the gel. Before loading, 0.2 volumes of dye (0.25% (w/v) bromophenol blue; 0.25% (w/v) xylene cyanol; 30% glycerol (v/v)) were added to each sample. Electrophoresis was performed at 70 V for a time ranging from 30 min to 1 h. After the run, the DNA in the gel was visualized by UV irradiation at 254 nm (transilluminator). The extraction of DNA from agarose gels was performed using Nucleospin® gel and PCR clean-up kit (Macherey-Nagel).

### 2.3.2 Competent cells: preparation and transformation

Competent cells of *E. coli* CC118, DH5α-$T1^R$, and BL21(DE3) were prepared by inoculating few colonies from an LB plate in 50 ml 2x XL. Cells were grown at 37°C to an $OD_{600}$ of 0.5 and then kept on ice for 90 minutes. Following centrifugation at 4000 rpm for 15 minutes, at 4°C, the cell pellet was resuspended in 20 ml of buffer containing 100 mM $CaCl_2$; 70 mM $MnCl_2$, 40 mM sodium acetate, pH 5.5 and kept in ice for 45 minutes. After a further centrifugation at 4000 rpm for 15 minutes, at 4°C, the cells were

resuspended in 3 ml of the same buffer containing 80% glycerol. The cells were stored at -80°C in aliquots of 220 µl.

For transformation, 100 µl of competent cells were added to 20-50 ng of DNA. The mixture was incubated for: 30 minutes on ice, 4 minutes at 37°C (thermal shock) and for 2 minutes on ice. SOC medium (1.05 ml) was added and the incubation prolonged for additional 15 minutes at room temperature. Cells were grown for 100 minutes at 37°C. An aliquot of the transformation (120 µl) was plated on LB agar containing the required antibiotic.

### 2.3.3 PCR

The polymerase chain reaction (PCR) was used for both amplification of specific DNA fragments to be cloned (preparative PCR; cfr. 2.4.1) and to verify for the presence of the desired DNA fragments after their cloning in different vectors (analytical PCR; cfr. 2.4.2 and 2.4.3). The oligonucleotides used in this work are listed in Table 2.2.

**Table 2.2.** *Oligonucleotides used in PCR.*

| **Oligo** | **Sequence** |
|---|---|
| Br_for2 * | 5'-GG*CATATG*ACTGGTTCAAACTATCCG-3' |
| Br_rev * | 5'-GG*GGATCC*TTATGTGTGGTGAAAGCCG-3' |
| TT3 ** | 5'-CCTCGAGGTCGACGGTA-3' |
| pET ** | 5'-GAAATTAATACGACTCACTATAGGG-3' |

* The italicized sequences indicate the *Nde*I (for) and *Bam*HI (rev) restriction sites.
** Oligonucleotides that anneal upstream of the cloning site of pSC-A and pET plasmid respectively.

## 2.4 Cloning of BmGadB

### 2.4.1 Preparative PCR

The *gadB* ORF (i.e. starting from the ATG codon identified by N-terminal sequencing) of *B. microti* was amplified by the FastStart High Fidelity PCR system using pBBR-*gadBC_Bm* (Table 2.1) as template. Oligonucleotides Br_for2 and Br_rev (Table 2.2) were designed to anneal over the start and the stop codons of the *gadB* gene respectively and comprise the *Nde*I and *Bam*HI restriction sites sequences, respectively, for subsequent directional cloning into the pET-3a expression vector (Novagen; cfr. 2.4.3).

Preparative PCR mixture (50 µl):

| | |
|---|---|
| - pBBR-*gadBC_Bm* | 1 µl (5 ng) |
| - Br_for2 (25 µM) | 0.8 µl (0.4 µM) |
| - Br_rev (25 µM) | 0.8 µl (0.4 µM) |
| - dNTPs (10 mM each) | 1 µl (0.2 mM) |
| - Buffer 10X High Fidelity (Roche) | 5 µl (1X, $MgCl_2$ 1.8 mM) |
| - Sterile $H_2O$ for PCR | 40.9 µl |
| - FastStart High Fidelity (Roche) | 0.5 µl (2.5 U) |

PCR reaction:

| | |
|---|---|
| 1) Hot Start: | 95° C for 2 min |
| 2) Cycle PCR (the cycle is repeated 25 times): | |
| Denaturation: | 95° C for 30 sec |
| Annealing: | 50° C for 30 sec |
| Extension: | 72° C for 1 min 30 sec |

3) Final extension: 72° C for 7 min

4) Cooling: 8° C for 5 min

### 2.4.2 Cloning with Strataclone PCR Cloning Kit

The PCR product obtained as described in 2.4.1 was analysed on agarose gel, extracted from gel (cfr. 2.3.1) and then directly cloned into the pSC-A vector of the StrataClone PCR Cloning Kit (cfr. 2.1) to generate the recombinant plasmids pSC-A_*Bm-gadB* (Table 2.1). Ligation and cloning were carried out following manufacture's protocol (Stratagene).

*E. coli* StrataClone SoloPack transformants were selected by blue/white screening. In order to verify if the selected white colonies resistant to ampicillin, contained the plasmid pSC-A_*Bm-gadBC*, transformants were screened for the presence of the insert by colony PCR. Since pSC-A plasmid contains a *Bam*HI restriction site, the orientation of the insert is important for the next step, i.e. cloning into pET-3a. Thus, colony PCR was performd using the following oligonucleotides: TT3, annealing upstream the insertion site of the PCR product, and Br_for2 which was used for *gadB* amplification (Table 2.2).

Mix for analytical PCR (30 µl):

A) 10 µl of sterile $H_2O$ for PCR in which the colony to be analyzed has been previously transferred.

B) Reaction Mix (20 µl)

- TT3 (25 µM) 0.6 µl (0.4 µM)
- Br_for2 (25 µM) 0.6 µl (0.4 µM)
- dNTPs (10 mM each) 0.6 µl (0.3 mM)

- Buffer 10X (GeneSpin) 3 µl (1X, $MgCl_2$ 1.5 mM)
- Taq Pol (GeneSpin) 0.3 µl (1.5 U)

PCR reaction:

1) Hot Start: 95° C for 2 min
2) Cycle PCR (the cycle is repeated 30 times):
   - Denaturation: 95° C for 30 sec
   - Annealing: 50° C for 30 sec
   - Extension: 72° C for 1 min 30 sec
3) Final extension: 72° C for 10 min
4) Cooling: 8° C for 5 min

Then, plasmid DNA was purified from two out of seven positive clones (cfr. 2.3.1). The obtained material was analysed using the restriction enzymes *Nde*I and *Bam*HI which were introduced into the PCR product with oligonucleotides Br_for2 and Br_rev, respectively (Table 2.2). Both plasmids produced the expected fragmentation pattern and were fully sequenced on both strands to check for any unwanted mutation. Only one plasmid was chosen for the next step of cloning.

### 2.4.3 Cloning into pET3a

Plasmid pSC-A_*Bm-gadB* was digested with *Nde*I and *Bam*HI and the resulting 1395-bp DNA fragment corresponding to the whole *Bm-gadB* ORF was subcloned into pET3a, previously digested with the same restriction enzymes and dephosphorylated at the 5' end using calf intestinal alkaline phosphatase (Roche).

The ligation reactions were carried out using the enzyme T4 DNA ligase (Roche). This enzyme promotes the joining of DNA strands which have 5'-phosphate and 3'-OH ends in a DNA molecule using ATP as a cofactor. The reactions were performed according to the manufacturer's instructions and using a vector/insert ratio 1:3.

The newly generated plasmid pET3a_*Bm-gadB* was used to transform *E. coli* DH5α competent cells prepared according to standard protocols (Sambrook *et al.*, 1989). Transformants were screened for the presence of the insert first by colony PCR using the following oligonucleotides: pET, which anneals upstream the polycloning site of pET3a, and Br_rev used, for *gadB* amplification (Table 2.2), and then by digestion with *Nde*I and *Bam*HI restriction enzymes.

Mixture for analytical PCR (30 µl):

A) 10 µl of sterile $H_2O$ for PCR in which the colony to be analyzed has been previously transferred.

B) Reaction Mix (20 µl)

- pET (25 µM) 0.6 µl (0.4 µM)
- Br_rev (25 µM) 0.6 µl (0.4 µM)
- dNTPs (10 mM each) 0.6 µl (0.3 mM)
- Buffer 10X (GeneSpin) 3 µl (1X, $MgCl_2$ 1.5 mM)
- Taq Pol (GeneSpin) 0.3 µl (1.5 U)

PCR reaction:

1) Hot Start: 95° C for 2 min
2) Cycle PCR (the cycle is repeated 30 times):
   Denaturation: 95° C for 30 sec

| | |
|---|---|
| Annealing: | 55° C for 30 sec |
| Extension: | 72° C for 1 min 30 sec |
| 3) Final extension: | 72° C for 10 min |
| 4) Cooling: | 8° C for 5 min |

Two clones were found to be positive by both PCR analysis and restriction analysis.

For protein purification, the plasmid construct pET3a_*Bm-gadB* was transferred into the expression strain *E. coli* strain BL21(DE3), a Gad-negative strain as based on the Rice test (cfr. 2.6.1) and the quantitative Gad activity assay (cfr.2.6.3).

## 2.5 Expression and purification of EcGadB and BmGadB

Protein purification of *EcGadB* (De Biase *et al.*, 1996) is described in this section.

The conditions used for expression and purification of *Bm*GadB from *E. coli* strain BL21(DE3)/pET3a_*Bm-gadB* were essentially as described for wild type *Ec*GadB, except that bacteria were grown in LB broth containing glucose 0.5% and chromatography was carried out on a smaller-sized column (2.1 cm x 20 cm).

Expression and purification of *Ec*GadB-D86NH465A from *E. coli* JM109/pREP4/*pQgadB-D86NH465A* was as described for wild type GadB except for the pH of the potassium phosphate buffer used during the DEAE-Sepharose chromatography, i.e. pH 6.0 instead of 6.5. Furthermore a second DEAE-Sepharose chromatography step was performed at pH 6.5, where the protein elutes during the washing step.

*Ec*GadB-H465A (Pennacchietti *et al.*, 2009) was purified for comparative analyses.

### 2.5.1 Growth and induction of the bacterial culture

*Ec*GadB was purified by adopting the protocol described by (De Biase *et al.*, 1996). Briefly, some colonies of the *E. coli* strain JM109/pREP4/pQ*gadB* from LB plate are inoculated into liquid medium LB containing ampicillin 100 mg/ml and kanamycin 25 mg/ml. Bacteria are grown overnight at 37° C under agitation (200 rpm). Subsequently, this pre-culture is inoculated (1:100) into 2 liters of SB , preheated to 37°C, containing:

- 50 mM potassium phosphate, pH 7.5;
- Ampicillin 200 mg/ml;
- Kanamycin 25 mg/ml;
- Pyridoxine (vitamin B6) 0.1 mg/ml.

The growth is carried out at 37° C under aeration. When the culture reaches $OD_{600}$ = 0.7, IPTG is added to a final concentration of 2 mM, to induce the expression of the gene inserted into pQE60 vector (or pET3a in the case of *Bm*GadB). Growth is carried out until the culture reaches an optical density not exceeding 2 (approximately 3 hours). It is important to not prolong the growth too much, in order to avoid the expression of endogenous GadA/B produced by JM109 in stationary phase. The choice of expressing GadB in this strain was also based on the experimental observation that although containing active *gadA/B* genes it does not express the enzyme at significant levels even when the culture reaches O.D.600 = 3 (De Biase *et al.*, 1996). At the end of growth, cells are collected by centrifugation at 5,000 rpm for 15 minutes at 4°C.

### 2.5.2 Bacterial lysis, precipitation of nucleic acids and ammonium sulphate fractionation

Bacteria, harvested by centrifugation, are resuspended in a solution containing 1 mM PLP and 1 mM DTT, and disrupted by sonication (16,000 Hz for 10 cycles of 30 seconds each alternating 1 minute in ice). After sonication, cell debris is removed by centrifugation at 10,000 rpm for 20 minutes at 4°C. In order to precipitate nucleic acids, 0.1 volume of a streptomycin sulfate 10% (w/v) solution is added to the supernatant after centrifugation. The solution is maintained under stirring for 10 minutes at room temperature and, then, centrifuged at 10,000 rpm for 20 minutes at 4°C. Solid ammonium sulfate was added to the supernatant at a concentration (390 mg/ml) which corresponds to 60% of saturation. At this percentage of saturation most of the proteins precipitate, including GadB. The precipitate, recovered by centrifugation at 10,000 rpm for 20 minutes at 4°C, is resuspended in few ml of 0.1 M potassium phosphate buffer, pH 6.5, containing 0.1 mM DTT. The material is dialyzed overnight at 4°C against 3 L of the same buffer to remove the ammonium sulfate.

### 2.5.3 DEAE-Sepharose chromatography

The dialyzed material is loaded on a DEAE-Sepharose anion exchange column of (30 cm x 2.5 cm diameter), pre-equilibrated with phosphate buffer. Chromatography is carried out by applying a gradient of potassium phosphate buffer, pH 6.5, containing 0.1 mM DTT, 0.1 M (300 ml ) to 0.5 M (300 ml), and collecting the eluate in fractions of about 12 ml. At pH 6.5 the absorption maximum of the chromophore at 340 nm and GadB is not visible, therefore its presence in each fraction is assayed by measuring the absorbance at 280

nm and by enzyme activity assay (cfr. 2.6.3). The purest fractions containing GadB are pooled and the protein material precipitated by ammonium sulfate at 60 % saturation (390 mg/ml). The precipitate is dissolved in few ml of 0.1 M sodium acetate/acetic acid buffer, pH 4.6, containing 0.1 mM DTT, and dialyzed overnight at 4°C against 3 L of the same buffer. The dialysate is centrifuged at 10,000 rpm for 15 minutes to remove conspicuous protein precipitate (contaminants, but not GadB) that occurs at acid pH.

Table 2.3 shows the trend of a typical purification of *E. coli* GadB from two liters of bacterial culture. The enzyme concentration and activity were assayed as described in 2.5.4 and 2.6.3.

The purity of the protein was judged by 12% SDS-PAGE (cfr. 2.6.6, Fig. 2.4)

**Table 2.3.** *Purification of wild type EcGadB.*

| Purification step | Total protein (mg) | Total Units (U) | Specific activity (U/mg) |
|---|---|---|---|
| Clarified lysate | 634 | 32130 | 50.7 |
| Streptomycin (Sn) | 567 | 34123 | 60.2 |
| 60% amm. Sulfate + dialysis | 426 | 32190 | 75.6 |
| # DEAE-Sepharose | 142 | 31247 | 220.0 |
| Dialysis at pH 4.6 | 130 | 29248 | 225.0 |

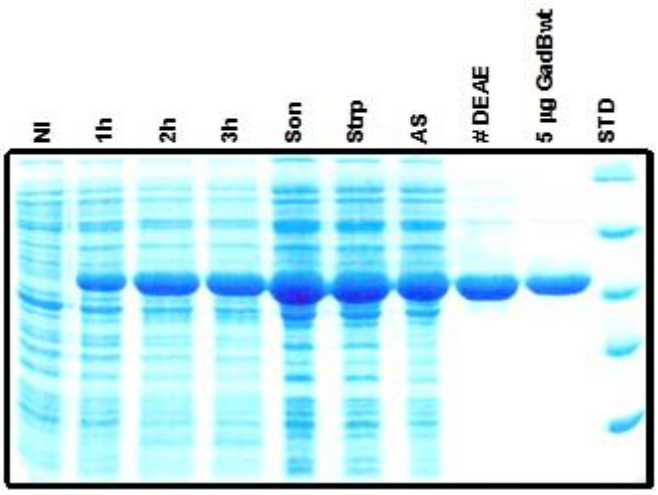


**Figure 2.4.** *Purification of wild type E. coli GadB(EcGadB).* 12% SDS-PAGE, stained with Coomassie Blue. Abbreviations used: **NI**, total cell extract from not induced cultures; **1h, 2h 3h**, total cell extract after 1 hour, 2 hours or 3 hours of induction with 2 mM IPTG respectively; **Son**, supernatant of clarified cell lysate; **Strp**, supernatant subjected to precipitation with streptomycin 1% (w/v) and centrifugation; **AS**, dialysate obtained after precipitation by ammonium sulphate at 60% saturation and resuspension in a buffer at pH 6.5; **# DEAE**, pooled fractions after anion exchange chromatography at pH 6.5; **STD**, molecular weight standard (from the top: 116 kDa, 66 kDa, 45 kDa, 35 kDa and 25 kDa).

### 2.5.4 Determination of Gad and cofactor concentration

The enzyme concentration was calculated by measuring the absorbance of the protein at 280 nm ($\varepsilon_{280}$ = 86 x $10^3$ $M^{-1}$ $cm^{-1}$; (Yang & Metzler, 1979)). The PLP content of the purified enzymes was determined spectrophotometrically after treating GadB or mutants with 0.1 M NaOH. In these conditions, the molar absorption coefficient (ε) at 388 nm of the released PLP is 6.55 x $10^3$ $M^{-1}$ $cm^{-1}$ (Peterson & Sober, 1954).

### 2.5.5 ApoGadB production

Recombinant *E. coli* GadB was purified in the *holo* form. The apoenzyme was prepared by mixing the enzyme (2.7 mg/ml) in 0.2 M pyridine/HCl buffer at pH 4.6, containing 0.1 mM DTT, with the substrate analogue α-methyl-Glu 0.1 M. In the presence of this substrate GadB catalyses an abortive transamination (cfr. 1.2.1), a slow side reaction, that leads to the formation of a ketoacid and pyridoxamine 5'-phosphate (PMP), with consequent inactivation of the enzyme. The reaction was performed o.n. at 4°C and followed spectrophotometrically (De Biase *et al.*, 1991).
In order to remove PMP and other contaminants, *apo*GadB was loaded onto a gel filtration PD10 column (GE Healthcare) and eluted in 50 mM HEPPS / 150 mM NaCl buffer, pH 8.0, containing 0.1 mM DTT.

## 2.6 Analytical techniques

### 2.6.1 Gad test (Rice test)

Glutamate decarboxylase activity was qualitatively detected as described by Rice *et al*. (Rice *et al.*, 1993). Gad test allows for rapid detection of Gad activity by the observation of the change in color from yellow to blue of the pH indicator bromocresol green following pH increase. In this rapid test, the hypertonicity of the reagent (9% NaCl) leads to release in the assay solution of the intracellular Gad enzyme. This allows the enzyme to react with the glutamic acid in the Gad reagent.
Briefly 2 ml of an overnight culture grown in LB broth are centrifuged (15 min at 4,000 rpm) and washed twice with an equal volume of physiological solution. The pellets are resuspended in 100 μl of Gad reagent (1 g glutamic

acid; 90 g NaCl; 3 ml of Triton X-100; 0.05 g of bromocresol green for 1 L of distilled water, pH 3.4), resuspended by vigorous vortexing and incubated at 37°C up to 1 hour. The test is judged positive if–the color of the supernatant from yellow turns blue, indicative of neutralization of the reaction solution.

### 2.6.2 GABA assay

The amount of GABA released in bacteria spent medium was measured using GABase (Sigma), a commercial preparation consisting of two enzymes, GABA-transaminase (GABA-T) and succinic semialdehyde deidrogenase (SSA-DH), which sequentially convert GABA into succinic semialdehyde (SSA) and succinic acid, with the concomitant reduction of $NADP^+$ into NADPH + $H^+$. The NADPH produced during the reaction is a direct measure of GABA present in the sample and it is calculated by reading the absorbance at 340 nm ($\varepsilon_{340}$ = 6,220 $cm^{-1}$ $M^{-1}$).

For *E. coli* MG1655 (or mutant derivatives), 25-50 µl of supernatant of a stationary phase overnight culture grown in LB broth + 0.4% glucose at pH 5.5 was added to 200 µl of assay solution. This solution consists of: 0.1 M HEPPS, pH 8.6; 1 mM $NADP^+$ pH 7.0; 1 mM α-ketoglutarate, pH 7.0; 3 mM β-mercaptoethanol and 0.03 U of GABase/assay.

For *E. coli* CC118, 50 µl of supernatant of a stationary phase overnight culture grown in LB broth pH 7.4 was added to 200 µl of assay solution.

### 2.6.3 Gad activity assay

Gad activity in both cell extracts and purified enzyme samples was assayed by measuring GABA production with Gabase as previously described (De Biase *et al.*, 1996).

To assay the decarboxylase activity two tubes are prepared, each containing:

1) 100 µl of sample (2-10 µl cell lysate/purified enzyme) in pyridine buffer;

2) 100 µl 100 mM monosodium glutamate in pyridine buffer.

The pyridine buffer consists in 0.2 M pyridine/HCl at pH 4.4-4.6 containing 0.1 mM DTT and 1 mM PLP. Both tubes are allowed to equilibrate at 37°C for 5 minutes and the content of tube 2 is transferred into tube 1 to start the reaction, which is allowed to proceed for 1 or 2 minutes. To halt the reaction 0.8 ml of 0.1 M HEPPS at pH 8.6 are added and the solution is vigorously vortexed. GABA is then quantified using Gabase (cfr. 2.6.2). The decarboxylase activity is expressed as U/mg, i.e. µmol of GABA produced per minute at 37°C per mg protein (total or purified).

The cells, harvested from overnight cultures grown in LBG at pH 5 (4,000 rpm for 15 min at 4°C), were resuspended in 1 ml of a solution containing 1 mM PLP, 1 mM DTT and protease inhibitors (Complete, Roche). The cells were sonicated for 7 cycles (15 seconds ON with 15 seconds OFF). Then the cell lysate was centrifuged at 12,000 rpm for 15 minutes at 4°C, to remove cells debris. The supernatant was immediately used to assay the protein concentration (Bradford assay) and the decarboxylase activity.

Gad activity of purified *Bm*GadB, *Ec*GadB wild type, H465A and D86NH465A mutants (0.2-0.4 µM, referred to the monomer concentration) was assayed in pyridine buffer, as described above. Alternatively, reactions were performed in 50 mM sodium acetate or potassium phosphate buffers at

different pH values, in the presence of 40 μM PLP and in the presence/absence of 50 mM NaCl. The protein concentration was 0.5-1.9 μM.

*GABA production* of purified *Ec*GadB wild type, H465A and D86NH465A mutants was assayed over a period of 3 hours, at 30°C, in 4 ml of 50 mM potassium phosphate buffer, pH 7, in the presence of 40 μM PLP and 50 mM sodium glutamate. The protein concentration was 2 μM. At time intervals, aliquots (100 μl) of the reaction mixture were withdrawn and analyzed for GABA content with the Gabase assay.

*Kinetic constants* of *Ec*GadB wild type, H465A and D86NH465A mutants (0.038 μM) were determined performing the reaction at 25°C in 500 μl of 50 mM sodium acetate pH 4.6, in the presence of 40 μM PLP, varying glutamate concentration (0.3-80 mM). At time intervals, aliquots (50 μl) of the reaction mixture were withdrawn and analyzed for GABA content with the Gabase assay.

### 2.6.4 Isotope effect

Analysis of isotope effect assumes that there are differences in kinetic or equilibrium properties of isotopically substituted molecules that can be measured (Cornish-Bowden, 1995). Two heavy isotopes of hydrogen, $^{2}H$ and $^{3}H$ (deuterium, D and tritium, T), are commonly used for studying isotope effect, due to their relative differences in atomic mass, which are at their greatest for the lightest elements. Isotope effect concerns both reacting bonds and solvent.

The *Ec*GadB D86NH465A were brought into 99.8% $D_2O$ by concentration and dilution. The enzyme (0.8 μM) was mixed with glutamate (30 mM). In

order to maintain constant pD to 4.6 (reading on pH meter = 4.2) DCl was added. The reaction rate was determined by recording the consumption of deuteron over time. The reaction was performed also in $H_2O$/HCl (pH 4.6). For comparison, *Ec*GadB wild type and H465A mutant were also analysed.

### 2.6.5 Protein assays

The *Bradford protein assay* method exploits the capacity of the dye Coomassie Brillant Blue (G-250) to bind to proteins in a solution and generate a colored compound which specifically absorbs at 595 nm in an acidic environment (Bradford, 1976).

A calibration curve is constructed by recording the reading at 595 nm of BSA (bovine serum albumin) at known concentration (10-100 μg/5 ml of Bradford reagent). The Bradford reagent contains: 0.01% Coomassie Brillant Blue, 4.7% ethanol, 8.5% phosphoric acid. The sample is assayed following the same procedure as used for BSA and its protein concentration interpolated on the calibration curve. For reliable measurements of protein concentration, the protein sample should always give a reading within the range of the calibration curve.

The *Bicinchoninic acid assay* (BCA) is a colorimetric assay for the quantitation of total protein in the presence of detergents, not compatible with Bradford assay. The system exploits the ability of BCA to detect the presence of $Cu^{+1}$, which results from reduction of $Cu^{+2}$ by protein, in an alkaline environment, according to the following scheme:

1) protein + $Cu^{+2}$ (colorless) → protein-$Cu^{+1}$

2) protein complex-$Cu^{+1}$ +2 BCA → complex BCA-$Cu^{+1}$ (violet)

The purple-colored reaction product is formed by the chelation of two molecules of BCA with one $Cu^{+1}$, exhibits absorption maximum at 562 nm. The color intensity is nearly linear with increasing protein concentrations. A calibration curve is constructed by recording the absorbance at 562 nm of BSA at known concentration (1-10 μg/0.5ml) diluted 1:2 with BCA reagent, incubated 1h at 60°C and cooled at room temperature. The BCA reagent (Thermo Scientific-Pierce) is composed of 25 parts of solution MA (sodium carbonate, sodium bicarbonate and sodium tartrate in 0.2 N NaOH), 24 parts of solution MB (bicinchoninic acid 4.0 % in water), 1 part of MC solution (copper sulfate 4.0 % in water). Protein samples are processed in the same manner and unknown protein concentrations are determined using the standard curve.

### 2.6.6 SDS-PAGE electrophoresis and immunoblot analysis

SDS-PAGE is a technique used to separate a mixture of proteins according to their molecular weight (Laemmli, 1970). The gel consists of an upper part (pH 6.8, stacking gel) in which the concentration of acrylamide is 5% (w/v), and a "separation" zone (pH 8.8, running gel) in which the percentage of acrylamide can be chosen depending on the MW of the protein(s) under analysis (typically 10% to 15%).

Electrophoresis is carried out at 200 V in a buffer containing 1 g/l SDS; 3 g/l Tris; 14.4 g/l glycine, pH 8.3. After the run, the gel is stained (0.25% (w/v) of Coomassie blue in 10% acetic acid/50% methanol) and then destained (7% acetic acid/25% methanol), to remove excess of stain and to visualize the proteins as blue bands on a clear background.

Samples were typically run on 12% SDS-PAGE and, when necessary, directly electroblotted onto polyvinylidene difluoride membranes (PVDF; Immobilon-P, Millipore). GadB was detected with a rabbit polyclonal antiserum directed against *E. coli* GadB (De Biase *et al.*, 1999) and horseradish peroxidase-labelled secondary antibody provided with the BM chemiluminescence western blotting kit (Roche), following manufacturer's instructions. Due to the significant degree of protein identity (73%), *Bm*GadB is recognized by the anti-Gad (*E. coli*).

### 2.6.7 Gel filtration chromatography

Gel filtration chromatography separates molecules according to differences in size as they pass through a gel filtration resin packed in a column. The resin is a porous matrix in the form of spherical particles chemically and physically stabile and inert, filled with buffer. Samples are eluted isocratically. Molecules that are larger than the pores, do not enter the matrix and are eluted in the void volume, $V_o$. Molecules with partial access to the pores of the matrix diffuse in and out of the pores (sample portioning between the mobile and stationary phase) and elute from the column in order of decreasing size. Small molecules such as salts that have full access to the pores do not separate from each other and usually elute just before one total column volume, $V_t$, of buffer has passed through the column. This technique can be applied to group separations (e.g. to remove high or low molecular weight contaminants) or high resolution fractionation of biomolecules (e.g. to determine molecular weight or separate one or more components).

*Determination of molecular mass of BmGadB.* A sample of *Bm*GAD (1 mg) was loaded onto a Superdex 200 10/300 GL column (GE Healthcare,

Life Sciences) on an Äkta Prime FPLC system at 4°C. The mobile phase (50 mM sodium acetate buffer, pH 4.5, containing 150 mM sodium chloride) for the equilibration and elution was pumped at a flow rate of 0.5 ml/min.

*Oligomerization state of EcGadB.* Samples of *apo*GadB (7-8 mg) or *apo*GadB reconstituted with PLP (5-fold the enzyme concentration) 1h at 4°C, were loaded onto a Superdex 200 10/300 GL column (GE Healthcare, Life Sciences) on an Äkta Prime FPLC system at 4°C. The mobile phase (flow rate of 0.5 ml/min) for the equilibration and elution consisted of 50 mM HEPPS / 150 mM NaCl buffer, pH 8, containing 0.1 mM DTT. The collected fractions (0.3 ml/fraction) were analysed spectrophotometrically.

The Gel Filtration HMW Calibration Kit (GE Healthcare, Life Sciences), with the exclusion of thyroglobulin (669 kDa and therefore outside the separation range of the column), was used for column calibration and molecular weight determination.

### 2.6.8 Spectroscopic analysis

#### 2.6.8.1 Steady-state spectroscopy

Enzyme absorption spectra and the absorbance changes in the presence of L-glutamate were recorded at the indicated temperatures on a Hewlett-Packard Agilent model 8452 diode array spectrophotometer.

Curve fitting and statistical analyses were carried out with Scientist (Micromath, Salt Lake City, UT) and GraphPad Prism 4.00 (GraphPad Software, San Diego, CA). The pH-dependent variations in 420-nm and 340-nm absorbance (Abs) were analyzed using Hill equation as in Prism, in which *pK* is the pH at the midpoint of the spectroscopic transition and *n* is the number of protons (i.e. Hill coefficient) participating in the transition.

*BmGadB kinetic constants*. Values for $k_{cat}$ and $K_m$ were determined in 100 mM sodium acetate buffer, pH 4.1, following the changes in absorbance at 420 nm and 340 nm occurring during the reaction of *Bm*GadB in the presence of different concentrations of L-glutamate, as previously reported (De Biase *et al.*, 1996, Tramonti *et al.*, 1998).

#### 2.6.8.2 Fluorescence

Many proteins and cofactors, absorbing light in the UV and visible, give rise to fluorescence emission spectra. Fluorescence is a type of luminescence: the property of some molecules, generally characterized by conjugated double bonds, to emit light of longer wavelength in response to electromagnetic waves absorption. The fluorescence phenomena occurs when the radiation is emitted at a rate of $10^{-8}$ seconds, while, if the emission is achieved at a speed in the order of milliseconds, it is called phosphorescence (Fig. 2.5; (Lakowicz, 1983)). Indeed, following excitation with monochromatic radiation of appropriate wavelength, the electrons of a luminescent molecule are brought from a fundamental electronic state $S_o$ to an excited states ($S_1$ or $S_2$; Fig. 2.5). During their stay in the excited state, the electrons can undergo internal and intersystem conversion processes, which result in the dissipation of the excitation energy through non-radiative processes (Stokes shift), resulting in a return to the lowest vibrational level of the excited electronic state. Therefore, the return to the fundamental electronic state $S_o$ is realized by the emission of a less energetic radiation, which correspond to a longer wavelength, than that absorbed.

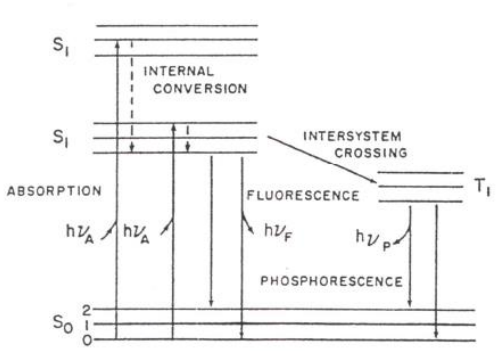


**Figure 2.5.** *Jablonski diagram.*

The fluorescence quantum yield (ϕ), i.e. the ratio of photons emitted and photons absorbed by a molecule, takes into account of the excitation energy dissipation factors and also includes two additional phenomena: *quenching* and the *energy transfer*. Quenching is the term that indicates the decrease in the intensity of fluorescence emission that can originate from different processes including collisions between the fluorophore and molecules such as molecular oxygen or acrylamide, excited-state reactions, complexes formation (Lakowicz, 1983). A particular phenomenon of fluorescence quenching is the *energy transfer*. This phenomenon takes place when the emission energy of a fluorophore, named donor, is not directly emitted, but is transferred to another fluorophore which acts as acceptor. A prerequisite for this phenomenon is a large overlap of the donor and acceptor emission spectra. Moreover it is necessary that the donor and acceptor are distanced less than 80Å and that oriented as electron transfers are allowed. The efficiency of energy transfer, which is maximum when the donor emission dipole and the acceptor absorption dipole are parallel and minimum when they are perpendicular, allows an estimation of the distance between the

acceptor and donor providing information about their spatial arrangement within a protein.

The quantum yield of a fluorophore and the centering of its emission peak depend on the surroundings in which the molecule is inserted, i.e. the polarity of the environment, the degree of solvation and the presence of groups able to act as energy transfer acceptors or donors. The amino acid tryptophan, excitable at 280 nm, is very sensitive to the environment in which it is located and for this reason its ability to emit light is exploited to analyze the conformational changes of proteins.

Fluorescence excitation and emission spectra were obtained with a FluoroMax-3 spectrofluorometer (Horiba Jobin-Yvon) equipped with a thermostatically controlled cell compartment at 20°C using 5 nm bandwidth on both slits (2 nm, when excited at 295 nm) and at a scan speed of 100 nm/min. The spectra were corrected by subtracting the corresponding buffer spectrum.

### 2.6.9 Cell fractionation

Cytoplasmic and membrane fractions from *E. coli* strain BL21(DE3)/pET3a_*Bm-gadB* were obtained by cell fractionation, essentially as described (Capitani *et al.*, 2003). After performing a growth as described in section 2.5.1, cell culture was centrifuged at 6000 rpm for 30 min at 4°C. The bacterial pellet was initially resuspended in 20 ml of 50 mM Tris/HCl, pH 7.0, containing 1 mM DTT and protease inhibitors (Complete, Roche). The suspension was then divided into two 10-ml aliquots, and brought to pH 7.2 and 5.1 by dropwise addition (few µl) of 6 N NaOH or HCl respectively. The two samples were then sonicated to disrupt cells and adjusted to the

desired pH values (respectively 5.1 and 7.2), where necessary. Cell debris and unbroken cells were removed by centrifugation at 5,000 rpm for 20 min at 20°C, thus generating the cell supernatants. The cytoplasmic and membrane fractions from each cell supernatant were separated via ultracentrifugation at 50,000 rpm for 1 h at 20°C. The pellet from ultracentrifugation, which represents the membrane fraction, was resuspended using 2 ml of 0.1 M Tris/HCl, pH 8.0, containing 150 mM NaCl, 5 mM EDTA and 0.5 % lauril sarcosine. Total protein content of each sample was determined using the detergent-compatible protein assay Micro BCA™ protein assay (Thermo Scientific-Pierce) (2.6.5). The presence of *Bm*GadB was analyzed by SDS-PAGE (2.6.6) and Gad activity assay (2.6.3).

## 2.7 Crystallization and structural analysis of the *apo* form of *Ec*GadB

Crystallization experiments and structural analysis were performed at the Paul Scherrer Institute (PSI) in Villigen (Switzerland) under the guidance of Dr. Guido Capitani and with the technical support of Dr. May Marsh and Dr. Florian Dworkowski.

### 2.7.1 Protein crystallization

Dimeric *apo*GadB at 8.9 mg/ml, in a solution containing 50 mM Hepes buffer, pH 8, 0.1 mM DTT, was crystallized at 293 K using the *vapor diffusion sitting drop method*. A drop composed of a mixture of protein and precipitant solutions is placed on a shelf in a sealed chamber, in vapor equilibration with a reservoir solution of higher precipitant concentration (e.g. salts and organic polyalcohols) (Rupp, 2009). The slow diffusion of

water vapor from the drop into the reservoir causes both precipitant and protein concentration to increase. The protein solution slowly reaches a supersaturation level, where nucleation and initial crystal growth occur. Afterwards, the solution depletes in protein and a few of the initial crystals continue to grow in the growth region of the crystallization diagram once the crystals are in equilibrium with the saturated protein solution. This method is easily automated: drops are set up once in 96 well plates using a robotic dispencer provided with syringe needles suitable for volumes down to about 100 nl. Plates are sealed with adhesive tape.

Several crystallization trials were set up in pre-prepared 96-well MRC2 plates (Hampton Research) using a Mosquito nanolitre pipetting robot (TTP Labtech): 100 or 200 nl of the protein solution was mixed with 100 nl of different reservoir solutions containing commonly used precipitants; the reservoir well contained 50 µl of the screen solution. The screening solutions used for the experiments were: Clear Strategy Screen I and Clear Strategy Screen II from Molecular Dimension; JCSG + Suite from Qiagen.

The 96-well plates were sealed, stored and automatically imaged at 20°C using a Rock Imager 1000 (Formulatrix, USA). Crystal growth was followed for several weeks using either optical microscopy (Leica MZ16 stereomicroscope) or a web interface that allows users to access and score digital images of their own experiments, collected at time intervals.

A *microseeding* experiment was also performed in order to obtain larger single crystals. In fact, ideal conditions for nucleation and growth differ, i.e. higher supersaturation for nucleation than for growth. Microseeding methods involve transferring a number of very small nuclei (crushed crystals) in a less supersaturated solution for continued growth.

Seed preparations were carried out using the 'seed-bead' method: crystals obtained from initial screens were placed in 50 µl of their respective reservoir solution, crushed manually using crystallisation microtools (Hampton Research) and then mechanically homogenized on a laboratory vortex (D'Arcy *et al.*, 2007). These seed stocks were stored at 193 K. Automated seeding was performed in a 96 well plate using the Mosquito robot: 200 nl of the protein solution of dimeric *apo*GadB (5.1 mg/ml) was mixed with 50 nl of the corresponding seeds stock and 150 nl of each crystallization solution (Clear Strategy Screen I).
Crystals grew to their full size within 40 days.

### 2.7.2 X-ray Diffraction Experiment

In a typical *X-ray diffraction experiment*, a single crystal of the molecule of interest is placed into a finely focused X-ray beam, and diffraction images are recorded. The electron density representing the atomic structure of the molecules in the crystal is reconstructed by Fourier methods from diffraction data and an atomic model of the structure is built into the electron density, and refined (Rupp, 2009). The Fourier reconstruction from reciprocal diffraction space back to direct molecular space requires two terms, as Fourier coefficients: the structural factor amplitudes (accessible in the form of square root of the measured and corrected spot intensities) and the phase angle. The absence of directly accessible phases constitutes the *phase problem*. To obtain the phases for each reflection, two different approaches exist: molecular replacement and experimental phasing (i.e. multiple isomorphous replacement and anomalous scattering). *Molecular replacement* method exploits a structurally similar available model to calculate initial

phases, which are applied in the initial reconstruction of the electron density. Specifically, the calculated Patterson function (the Fourier transform of the intensities) of the model molecule is oriented and translated over the Patterson function of the unknown structure, to find the correct position of the search molecule in the crystal.

In practice, crystals (10 to a few hundred μm) are harvested under a microscope and a single crystal is scooped out of the mother liquor (fishing) with a loop or other micro-device and mounted on the goniostat of a diffractometer for data collection (Blow, 2002). To prevent damage from exposure to X-ray radiation the crystals undergoes to cryocooling to liquid nitrogen temperature, sometimes increasing resolution (Pflugrath, 2004). To prevent crystalline ice formation during the rapid cooling, cryoprotectants (such as glycerol, ethylene glycol, MPD, sucrose and low molecular PEGs) are used. Once the data are collected all subsequent steps are conducted *in silico.*

Single crystals (25-30 μm) of dimeric *apo*GadB were fished and treated with cryo-protection solution containing a 4:1 (or 5:1) mixture of well-solution and ethylene glycol prior to freezing in a $N_2$ gas stream (flash cooling). Diffraction data to 3 Å were collected at 100 K at the PXII beamline of the Swiss Light Source using X-ray wavelength of 1 Å. Data were processed with XDS. For structure solution we employed molecular replacement using available GadB structures (Capitani *et al.*, 2003, Gut *et al.*, 2006) as a model.

## 2.8 Data Analysis

Sequence alignment was performed with Clustal Omega (http://www.ebi.ac.uk/Tools/msa/clustalo/). Secondary structure predictions were obtained using external resources accessible from Expasy (http://expasy.org/proteomics).

# *Results and Discussion*

## 3.1 PART I: Biochemical and spectroscopic properties of recombinant glutamate decarboxylase from *Brucella microti*

*Background:* Genome analysis indicated that the recently described *Brucella microti* CCM4915, an environment-borne pathogenic *Brucella* species isolated from common vole (Scholz *et al.*, 2008), red fox (Scholz *et al.*, 2009) and soil (Scholz *et al.*, 2008), contains intact *gadB* (BMI_II334) and *gadC* (BMI_II335) genes (Audic *et al.*, 2009). On the contrary, in the classical species of *Brucella*, i.e. *B. melitensis*, *B. abortus*, *B. suis B. canis*, *B. ovis*, and *B. neotomae*, *gadB* and/or *gadC* genes are inactivated by stop codons and/or frameshift mutations (Tab. 3.1, (Audic *et al.*, 2009)).

**Table 3.1.** *Differences in* gadB *and* gadC *genes between* B. microti *and other* Brucella *species*.

| *B. microti* ID | Status in *B. microti* | *B. suis* I330 ID | status in *B.suis* I330 | status in *B.ovis* ATCC 25840 | status in *B.suis* ATCC 23445 | status in *B . abortus* S19 | status in *B. melitensis* biovar Abortus 2308 | status in *B. abortus* biovar I str. 9-94I | status in *B.melitensis* I6M | status in *B. canis* ATCC 23365 | status in *O. anthropi* ATCC 49I88 | Annotation/comment |
|---|---|---|---|---|---|---|---|---|---|---|---|---|
| Glutamate metabolism | | | | | | | | | | | | |
| BMI_II334 | + | BRA0338 | * | + (diff. At the beg.) | + | *(2) | *(2) | *(2) | * | * | NF | glutamate decarboxylase |
| BMI_II335 | + | BRA0339 | fs | fs | fs | + | + | + | + | fs | NF | glutamate/ gamma-aminobutyrate antiporter |

BMi_II334 ortholog is pseudogene BRA0338, BMI_II335 ortholog is pseudogene BRA0339
Abbreviations include: *for internal stop, a number indicates multiple stops, fs for frameshift, + for an intact sequence, NF for not found.

(Adapted from (Audic *et al.*, 2009))

*Brucella* is a genus of Gram-negative facultative intracellular coccobacilli, belonging to the class α-Proteobacteria, that are highly pathogenic for a variety of mammals, not host specific but with different host preference. Humans, though not primary hosts, can become infected (human brucellosis is also known as Malta fever) essentially by the oral route, i.e. by ingestion of non-pasteurized milk and dairy products, and also *via* respiratory and conjunctival routes. Recently the World Health Organization (WHO) cited

brucellosis as the world's most widespread zoonosis (Franco *et al.*, 2007). Up to now, the potential pathogenicity of *B. microti* for livestock and humans remains unknown (Jimenez de Bagues *et al.*, 2010). Nevertheless, this new species is not only faster growing and more resistant to an acid stress respect to the classical *Brucella* species, but also lethal in the mouse model.

The involvement of *B. microti gadB* and *gadC* genes in GDAR was recently investigated in light of their possible involvement in acid survival within the host (Occhialini *et al.*, 2012): both genes were shown to play an essential role in GDAR *in vitro* and to contribute to survival of this microorganism in a murine model following oral infection. In addition, the acid sensitive strain *B. suis* 1330 became acid resistant in the presence of Glu when complemented with the *B. microti gadBC* operon carried by a low-copy-number plasmid (Occhialini *et al.*, 2012). This finding suggested that *gadB* and *gadC* are necessary and sufficient to complement for the missing GDAR phenotype in *B. suis*.

Unlike *E. coli*, the *B. microti* genome contains only one copy of the Gad encoding gene, namely *gadB*. Its protein product shares 73% sequence identity with *E. coli* GadB (henceforth *Ec*GadB), which is by no doubt the most extensively characterised bacterial Gad (De Biase & Pennacchietti, 2012). As mentioned in the Introduction (cfr. 1.2.3) the homologs of *Ec*GadB, including GadB from *B. microti* (henceforth *Bm*GadB), share a set of strictly conserved residues, which are known to occupy critical positions, i.e. near the active site or at sites where the conformational changes occur (De Biase & Pennacchietti, 2012). Amongst the conserved residues there is His465 which is responsible for the reversible inactivation of the enzyme, locking the active site at pH > 5.3 (or pH > 5.7 in the presence of chloride

ions) *via* formation of a substituted aldamine (Gut *et al.*, 2006, Pennacchietti *et al.*, 2009) (cfr. 1.1.3.2 and 1.2.2).

To date there are no reports on an in-depth functional, biochemical and spectroscopic characterization of Gad from bacterial species other than *E. coli*. One of the aims of the present work was to fill this lack of knowledge as well as to investigate whether the pH-dependent molecular mechanisms controlling the intracellular activation of *Ec*GadB are also conserved in other bacterial Gads, such as *Bm*GadB. Therefore, recombinant *Bm*GadB was overexpressed in the laboratory strain *E. coli* BL21 and the biochemical properties of the purified enzyme were compared with those of the thoroughly characterized *E. coli* counterpart.

### 3.1.1 Effect of the heterologous expression of *B. microti gadBC* in an *E. coli* acid-sensitive mutant strain

*Preliminary data*. A recent work, published by our group in collaboration with Dr. A. Occhialini in Montpellier (Occhialini *et al.*, 2012), showed that a 3.5 kb genomic region of *B. microti* encompassing the *gadBC* operon can be functionally expressed in two acid-sensitive mutant strains of *E. coli*, restoring the GDAR phenotype. Specifically, the low-copy-number plasmid (pBBR1MCS, hereafter pBBR) carrying the *gadBC* operon from *B. microti* (pBBR-*gadBC_Bm*) was introduced into the *E. coli* MG1655 Δ*gadA*/Δ*gadB* and Δ*gadC* strains, that are devoid of Gad activity and acid pH-dependent Glu/GABA antiport activity, respectively. In both mutants GDAR was restored by heterologous complementation, confirming that *gadB* and *gadC* of *B. microti* are functionally expressed in *E. coli* (Occhialini *et al.*, 2012). Furthermore, GABA was absent from the supernatant of the acid-sensitive *E.*

*coli* Δ*gadA*Δ*gadB* strain, whereas the wild-type strain and the mutant strains complemented with *gadBC_Ec* or *gadBC_Bm* exported comparable levels of GABA (Occhialini *et al.*, 2012). These findings provided the first strong evidence that the only source of GABA in *E. coli* is Gad.

When the Δ*gadC* mutant strain complemented with pBBR-*gadBC_Bm* was assayed for both GABA export and Gad activity, the relative levels were found to increase (i.e. almost doubled) respect to the mutant strain, though never attained those detected in the mutant strain transformed with the *gadBC* operon from *E. coli* (pBBR-*gadBC_Ec*; data reported in D. Bastianelli Ph.D. Thesis, 2012). Immunoblot analysis with crude lysates obtained from stationary phase cultures of *E. coli* grown under fermentative conditions, confirmed that expression of the GadB protein directed by the *gadBC_Bm* is much less abundant than that observed when GadB was expressed from plasmid pBBR-*gadBC_Ec*.

To further investigate on the effect of the expression of the *gadBC_Bm* in *E. coli*, it was necessary to construct the triple mutant MG1655Δ*gadA*Δ*gadBC* in which both the endogenous glutamate decarboxylase and antiporter activities were abolished. Therefore the triple mutant has the most suitable genetic background for assaying decarboxylase and Glu/GABA antiport activities of *B. microti* GadB and GadC, respectively, i.e. no interference from the *E. coli* gene products. In fact the double mutant MG1655Δ*gadA*Δ*gadB* and the single mutant MG1655Δ*gadC*, initially used for the functional analysis of *gadBC_Bm* (Occhialini *et al.*, 2012), still possessed functional *gadC* and *gadA/gadB* genes, respectively, and therefore still expressing the endogenous antiporter and decarboxylase activities.

Part of the following data were also reported in the PhD thesis (2012) of Daniela Bastianelli ,with whom I shared some of this preliminary work.

After construction of the triple mutant (described in D. Bastianelli Ph.D. thesis, 2012), pBBR-*gadBC_Ec* and pBBR-*gadBC_Bm* were used to transform it. In order to assess if *gadBC_Bm* complements the Gad negative phenotype of the *E. coli* triple mutant, a Gad test (i.e. Rice test) was initially performed on cell pellets from the relevant cultures (Fig. 3.1C). As controls, the wild type *E. coli* strain MG1655 (positive control) and its isogenic derivatives MG1655Δ*gadA*Δ*gadB* and MG1655Δ*gadA*Δ*gadBC* strain carrying the empty plasmid pBBR (negative control) were included. As expected the triple mutant strain carrying *gadBC_Bm* was found to be positive at the Gad test.

With the purpose of evaluating whether *gadBC_Bm* is capable to restore the GDAR phenotype of triple mutant *E. coli* strain, the same strains analysed by SDS-PAGE and immunoblot analysis were subjected to GDAR assay. Briefly, bacteria were grown for ≥ 22 hours in LB broth (pH 5) supplemented with 0.4% glucose and diluted 1:1000 in minimal medium EG either in the presence or in the absence of 1.5 mM glutamate. Following static incubation for 2 hours at 37°C, each sample is diluted and plated on LB plates and the percentage of survival determined, using as reference the culture immediately after dilution. Data in Fig. 3.1C show that the acid sensitive phenotype of MG1655Δ*gadA*Δ*gadBC* strain is fully reverted into acid resistant in the strain complemented with the *gadBC_Bm* indicating that *gadB* and *gadC* genes are indeed functionally expressed in *E. coli*. Despite the recovery of GDAR, the *gadBC_Bm* complemented strain exhibits low level of GABA in the spent medium as compared with both wild type and *gadBC_Ec* complemented strain (Fig. 3.1C).

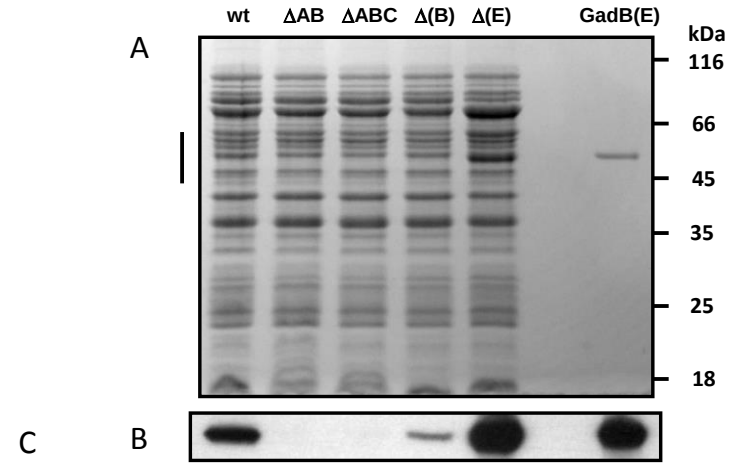


| Strain | Gad test | % Survival | GABA (mM) | Gad (U/mg) |
|---|---|---|---|---|
| wt/pBBR | + | 86 ± 14 | 0,74 ± 0,39 | 1,04 ± 0,04 |
| wtΔ*gadA* Δ*gadB* /pBBR | - | <1 | 0 | 0,07 ± 0,03 |
| wtΔ*gadA* Δ*gadBC* /pBBR | - | 0 | 0 | 0,062 ± 0,002 |
| wtΔ*gadA* Δ*gadBC* /pBBR-gadBC_*Bm* | + | 76 ± 27 | 0,28 ± 0,14 | 0,63 ± 0,04 |
| wtΔ*gadA* Δ*gadBC* /pBBR-*gadBC_Ec* | + | 70 ± 24 | 3,17 ± 0,21 | 5,47 ± 0,12 |

**Figure 3.1.** *Effects of* B. microti *gadBC in E. coli triple mutant.*The strains used are: MG1655/pBBR [wt]; MG1655Δ*gadA*Δ*gadB*/pBBR [ΔAB]; MG1655Δ*gadA*Δ*gadBC*/pBBR [ΔABC]; MG1655Δ*gadA*Δ*gadBC*/pBBR-*gadBC_Bm* [Δ(B)]; MG1655Δ*gadA*Δ*gadBC* /pBBR-*gadBC_Ec* [Δ(E)]. **(A)** SDS-PAGE of bacterial lysates (40 µg each) of the strains grown to the stationary phase in LBG, pH 5.0. Purified GadB from *E. co*li [GadB(E), 0.5 µg] is included as control (lane 6). **(B)** Western blot analysis with an anti-*Ec*GadB rabbit polyclonal antiserum. The region of the blot shown corresponds to the area indicated by the black bar in (A). The quantity of Δ(E) and GadB(E) samples were halved for blotting analysis. Molecular weights of protein standards are indicated on the right. **(C)** Properties of the strains in A in terms of *i*) % survival at pH 2.5 in minimal medium EG + 1.5 mM Glu (2 h); *ii*) Gad test (+, positive result, -, negative result); *iii*) Gad activity (U/mg) and *iv*) GABA export (mM). Abbreviations: *E. coli* MG1655 (wt).
The total protein content of each sample was assayed by the method of Bradford.

*Bm*GadB was assayed for activity (Fig 3.1C) and detected by immunoblot analysis with anti-*Ec*GadB polyclonal antiserum (Fig 3.1AB) using crude cell lysates obtained from the same cultures of the strains assayed for GDAR and GABA export (Fig. 3.1C). The levels of GadB activity (Fig 3.1C) in the complemented strain reflects the intensity of the signal observed in the

western blot (Fig 3.1B), i.e. the activity *gadBC_Bm* complemented strain is approximately 8 times lower than that assayed in the *gadBC_Ec* complemented strain.

Gad activity and GABA export were also assayed in crude lysates obtained from stationary-phase culture of MG1655Δ*gadA*Δ*gadBC*/pBBR*gadBC_Bm* grown at 37°C in two different media: LBG, i.e. LB pH 5.0 containing 0.4%, and LB, pH 7.4 (Tab. 3.2). For comparison, the same strain containing empty pBBR was tested. Notably, Gad activity from cells grown in LB is twice as high as those grown in LBG, whereas GABA in the spent medium is practically nil in spent LB medium but almost 2 mM in the spent LBG medium. The basal level of Gad activity detected in the triple mutant strain carrying the empty plasmid is not unexpected. In fact the assay we use consists in the measurement of GABA production (rather than $CO_2$ release), but this compound can also be present in the cell extract, though at very low levels, because it can originate from the reverse reaction carried out by the endogenous activities of GABA-transaminase and succinic semyaldehyde dehydrogenase.

**Table 3.2.** *Gad activity and GABA export under different growth conditions.*

| **Strain / condition** | **GABA (mM)** | **Gad (U/O.D.$_{600}$)** |
|---|---|---|
| **LB pH 7.4** | | |
| wtΔ*gadA* Δ*gadBC* /pBBR | 0,016 ± 0,001 | 1,07 ± 0,05 |
| wtΔ*gadA* Δ*gadBC* /pBBR-gadBC_*Bm* | 0 | 32,87 ± 1,04 |
| **LBG pH 5.0** | | |
| wtΔ*gadA* Δ*gadBC* /pBBR | 0,050 ± 0,004 | 0,98 ± 0,71 |
| wtΔ*gadA* Δ*gadBC* /pBBR-gadBC_*Bm* | 1,97 ± 0,06 | 15,36 ± 2,45 |

The results provided in this section indicate that the *gadBC* operon of *B. microti* is capable of restoring GDAR in an acid sensitive *E. coli* strain which

was constructed to be devoid of Gad and Glu/GABA activities, required to fully develop GDAR. Moreover the protein product of the *gadB* and *gadC* genes were shown to be functional because GAD activity and GABA export, undetectable in the *E. coli* triple mutant strain, were indeed detected in the strain complemented with *gadBC_Bm.* Interestingly, although there is a total recovery of GDAR, both the concentration of exported GABA during overnight growth in LBG and the Gad activity of the lysates never attain the values obtained when the triple mutant was complemented with the *E. coli gadBC* operon (Fig. 3.1).

### 3.1.2 Expression and purification of recombinant *Bm*GadB

The amino acid sequences of *Bm*GadB provided in different databases, i.e. NCBI and Patric (Gillespie *et al.*, 2011), differ in the N-terminal region (Fig. 3.3). In the NCBI Reference Sequence (YP_003105130.1) *Bm*GadB is reported to have 6 extra amino acids at the N-terminal end respect to *Ec*GadB, whereas in the Patric database the sequence is 2 residues shorter than *Ec*GadB. In order to validate experimentally the correct translation initiation site among those reported in the different databases, the N-terminal amino acid sequence was determined on a partially purified *Bm*GadB overproduced in the *E. coli* CC118 strain transformed with plasmid pBBR-*gadBC_Bm*, i.e. carrying the whole *B. microti gadBC* operon under its indigenous promoter (Occhialini *et al.*, 2012). CC118 strain is suitable for *Bm*GadB expression because it displays very low level of Gad, as assayed by Rice test. Furthermore, Gad activity performed on crude lysates of CC118 from an overnight culture grown at 37°C in LB medium (1.2 ± 1.2 U/O.D.$_{600}$) was more than 15 folds lower than that detected in a common *E.*

*coli* strain used for cloning and plasmid propagation, i.e. *E. coli* DH5α (17 ± 2.8 U/O.D.$_{600}$).

The expression and functionality of *Bm*GadB were assessed as described in Material and Methods (cfr. 2.2). Gad activity in cell lysate obtained from a 50 ml stationary-phase culture was 21.2 ± 2.7 U/O.D.$_{600}$ (at least 10 folds higher than in *E. coli* CC118 strain carrying the empty plasmid pBBR), and Gad protein was detected by immunoblot analysis only in CC118 carrying pBBR-*gadBC_Bm* (data not shown). Using the same protocol described for *Ec*GadB (cfr. 2.5), *Bm*GadB was purified from *E. coli* CC118/pBBR-*gadBC_Bm* to approx. 50% purity, as estimated by SDS-PAGE (Fig. 3.2).

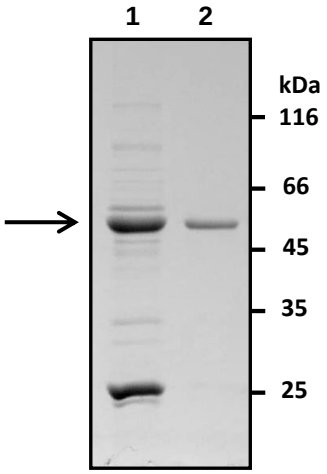


**Figure 3.2.** *SDS-PAGE of partially purified* Bm*GadB, used for electroblotting.* Lane 1, partially purified *Bm*GadB (10 μg); lane 2, *Ec*GadB (1 μg). The molecular mass of protein standards is indicated on the right.

Following electroblotting onto PVDF membrane, the protein band corresponding to 5 μg (94 pmoles) of *Bm*GadB was subjected to N-terminal sequencing by Edman degradation (Proteome Factory, Germany). The resulting sequence, Met-Thr-Gly-Ser-Asn, confirmed that the correct N-terminal sequence is that provided in the Patric database. Thus the sequence

of *Bm*GadB consists of 464 amino acids, i.e. it is two amino acids shorter at the N-terminal end respect to the *Ec*GadB, with a calculated molecular weight of 52,184 Da (Fig. 3.3).

```
E. coli     ------MDKKQVTDLRSELLDSRFGAKSISTIAESKRFPLHEMRDDVAFQIINDELYLDG   54
B. microti  MKITLEVIMTGSNYPARDLIASVFGTEALQEIAASRGFPEKEMQANAVYQIIHDELFLDG   52
                  :  .  .    :*: * **::::. ** *: ** :**: :..:***.***:***

E. coli     NARQNLATFCQTWDDENVHKLMDLSINKNWIDKEEYPQSAAIDLRCVNMVADLWHAPAPK  114
B. microti  NARQNLATFCQTWDDDYVHKLMDLSINKNWIDKEEYPQSAAIDLRCVNMVADLWNAPKFA  112
            ***************: ************************************.**

E. coli     NGQAVGTNTIGSSEACMLGGMAMKWRWRKRMEAAGKPTDKPNLVCGPVQICWHKFARYWD  174
B. microti  -DNATGTNTIGSSEACMLGGMAMKWRWRKKMQEMGKPTDKPNFVCGPVQVCWHKFARYWD  171
              :*.************************:*:  ********:******:**********

E. coli     VELREIPMRPGQLFMDPKRMIEACDENTIGVVPTFGVTYTGNYEFPQPLHDALDKFQADT  234
B. microti  VEIREIPMEPGRLFMGPEQMLEAVDENTIGVVPTFGVTYTGNYEFPEPLQDALDKLQKTK  231
            **:*****.**:*** *::*:** **********************:**:*****:*  .

E. coli     GIDIDMHIDAASGGFLAPFVAPDIVWDFRLPRVKSISASGHKFGLAPLGCGWVIWRDEEA  294
B. microti  GLDIDIHVDAASGGFLAPFCAPDIPWDFRLPRVKSISASGHKYGLAPLGCGWVVWRDKEA  291
            *:***:*:*********** **** *****************:**********:***:**

E. coli     LPQELVFNVDYLGGQIGTFAINFSRPAGQVIAQYYEFLRLGREGYTKVQNASYQVAAYLA  354
B. microti  LPEELIFNVDYLGGQVGTFAINFSRPAGQVISQYYEFMRLGREGYTKVQQAAYRVAQYIA  351
            **:**:*********:***************:*****:***********:*:*:** *:*

E. coli     DEIAKLGPYEFICTGRPDEGIPAVCFKLKDGEDPGYTLYDLSERLRLRGWQVPAFTLGGE  414
B. microti  REIEPLGPYEFICAGEEKGGIPAVCFRIREGEDPGYSLYDLSERLRLTGWQVPAFALSGK  411
             **  ********:*. . *******::::******:********** *******:*.*:

E. coli     ATDIVVMRIMCRRGFEMDFAELLLEDYKASLKYLSDHPKLQGIAQ-QNSFKHT         466
B. microt   ASDITVMRVMCRRGFEMDLAALFIRDFKAGIEFFKSHPSPKITPSMGTGFHHT         464
            *:**.***:*********:* *::.*:**.::::..**. :   .  ..*:**
```

**Figure 3.3.** *Clustal Omega (version 1.2.0) alignment of* Ec*GadB and* Bm*GadB*. The residues in bold in *Bm*GadB correspond to the N-terminal sequence experimentally determined by Edman degradation and which the indicated numbering is based on. The first 8 amino acids (with waved underlining) in *Bm*GadB are those present in the NCBI Reference Sequence (YP_003105130.1). The amino acid residues corresponding to the regions undergoing the most prominent conformational changes in *Ec*GadB are underlined. The residues participating in chloride binding are in a gray background.

Following the identification of the correct ORF in *Bm*GadB, plasmid pET3a_*Bm-gadB* was constructed using the cloning strategy described in

(cfr. 2.4). The choice of *E. coli* BL21(DE3) as host strain for GadB expression was based on the consideration that it is a commonly employed pET system expression host and, more importantly, exhibits undetectable levels of endogenous Gad activity. In fact BL21(DE3) was negative to the qualitative Gad test (cfr 2.6.1). Furthermore, from bacteria grown, harvested and sonicated as described for *Bm*GadB purification (cfr. 2.5), Gad activity assay gave a 2.8 ± 0.4 U/Liter of culture, i.e. 0.15% of the minimum activity assayed in BL21(DE3)/pET3a_*Bm-gadB* lysates which yielded approx. 1900 U/Liter of culture. The Gad-negative phenotype of BL21(DE3) might arise from mutations in the promoter regions of the *gadA* and *gadB* genes or the transcriptional regulators of GDAR, as the publicly available genome sequence of *E. coli* BL21(DE3) indicates that both *gad* genes are present and intact.

Purification of *Bm*GadB was carried out following the protocol used for *Ec*GadB (De Biase *et al.*, 1996), with minor modifications (cfr. 2.5), and yielded approximately 10 mg from a 2-Liter bacterial culture. The purity of the protein was judged to be 95%, as based on SDS-PAGE analysis (Fig. 3.4), in agreement with the holoenzyme content (i.e. > 95% of total protein concentration) assessed by calculating the PLP concentration. Based on these data we conclude that *Bm*GadB is purified with the full complement of PLP.

Under the standard assay conditions used for *Ec*GadB (50 mM sodium glutamate in 0.2 M pyridine/HCl buffer, pH 4.4, containing 0.1 mM PLP, at 37°C), the specific activity of *Bm*GadB was 190 units/mg, a value close to that of the *E. coli* counterpart.

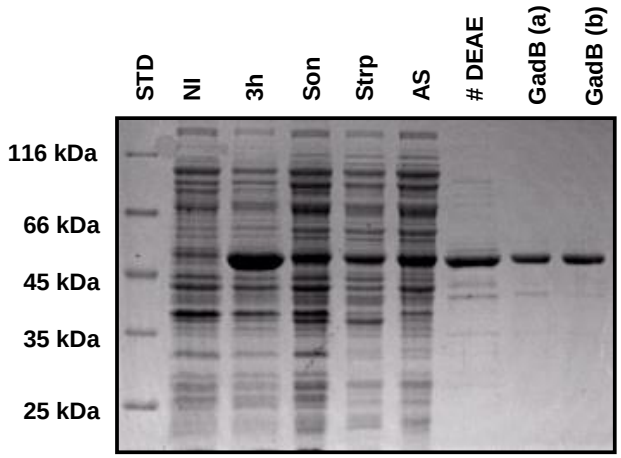


**Figure 3.4.** *Purification of recombinant* Bm*GadB.* 12% SDS-PAGE, stained with Coomassie Blue. Abbreviations used: **NI**, total cell extract from uninduced cultures; **3h**, total cell extract after 3 hours of induction with 2 mM IPTG; **Son**, supernatant of cell lysate clarified by low-speed centrifugation; **Strp**, supernatant after precipitation with streptomycin 1% (w/v) and centrifugation; **AS**, dialysate obtained after precipitation with ammonium sulphate at 60% saturation and resuspension in a buffer at pH 6.5; **# DEAE**, pooled fractions after anion exchange chromatography at pH 6.5; purified **GadB** is boiled for 5 min (a) or not (b) before loading; STD, molecular mass standard.

The $k_{cat}$ and $K_m$ values calculated for *Bm*GadB are provided in Table 3.3. Compared to that of wild type *E. coli* GadB, the $K_m$ of *Bm*GadB is comparable, while $k_{cat}$ is twice as high, thus resulting in an enzyme with a higher specificity constant ($k_{cat}/K_m$).

**Table 3.3.** *Kinetic parameters of* Bm*GadB compared to* E. coli *GadB.*

| GadB | $k_{cat}$ ($s^{-1}$) | $K_m$ (mM) | $k_{cat}$ / $K_m$ ($s^{-1}mM^{-1}$) |
|---|---|---|---|
| *Bm*GadB | 43.63 ± 0.39 | 1.72 ± 0.07 | 25.44 ± 1.30 |
| *Ec*GadB* | 24.85 ± 0.13 | 2.32 ± 0.05 | 10.71 ± 0.02 |

The values reported were calculated using the integrated Michaelis-Menten equation to fit the curves of the disappearance of the enzyme-substrate complex as a function of time as described by (Tramonti *et al.*, 1998). * Data from (Pennacchietti *et al.*, 2009)

The purified recombinant *Bm*GadB has an apparent molecular mass of 52 kDa (based on SDS-PAGE) and migrates as a 307.4-kDa species in FPLC gel filtration on a Superdex 200 10/300 GL column (Fig. 3.5). These results indicate that at acidic pH, i.e. when the enzyme is maximally active (cfr. 3.1.3), *Bm*GadB exists as a hexamer like *Ec*GadB.

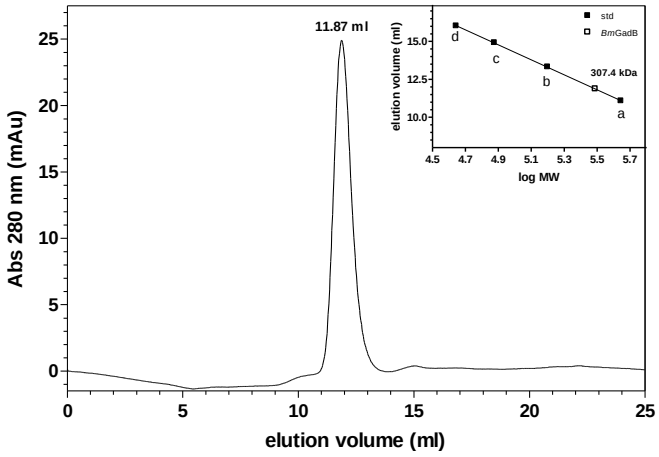


**Figure 3.5.** *Determination of molecular mass of* Bm*GadB*. Gel filtration chromatography of *Bm*GadB on a Superdex 200 10/300 GL (GE Healthcare) column was carried out in 50 mM sodium acetate buffer, pH 4.5, containing 150 mM NaCl, at a flow rate of 0.5 ml/min. HMW Calibration Kit (GE Healthcare) included ferritin (440 kDa; a), aldolase (158 kDa; b), conalbumin (75 kDa; c), ovalbumin (44 kDa; d). 1 mg of *Bm*GadB was loaded on the column immediately after calibration.

### 3.1.3 pH-dependent absorbance and activity changes

*Bm*GadB undergoes distinct pH-dependent spectroscopic changes in the absorption spectrum of the cofactor (Fig. 3.6A), just like the *E. coli* counterpart (Pennacchietti *et al.*, 2009) (cfr. 1.2.2). The buffer systems used were the followings: 50 mM acetate buffer, in the pH range 3.8-5.8, and phosphate buffer in the pH range 6.0-7.0. The absorption spectra of *Bm*GadB indicate that the shift of cofactor absorbance from 420 nm to 340 nm occurs

upon changing the pH from 4.4 to 5.2, with a clear isosbestic point at 361 nm. The change in the absorption spectrum corresponds to the conversion from the active form of the internal aldimine (i.e. the ketoenamine), which absorbs maximally at 420 nm, to the inactive form (i.e. substituted aldamine, as confirmed by fluorescence spectra, see Fig. 3.8), which absorbs maximally at 340 nm (O'Leary & Brummund, 1974, Gut *et al.*, 2006, Pennacchietti *et al.*, 2009).

The titration curve (Fig. 3.6B) generated by plotting the 420-nm absorbance (or the 340-nm absorbance; data not shown) versus pH exhibits a sigmoidal dependence and fits well to the Hill equation. The best-fit values returned for *n* (number of protons) and *pK* (midpoint) of the spectroscopic transition are given in Table 3.4. Compared to *Ec*GadB (Pennacchietti *et al.*, 2009), the pH-dependent spectroscopic transition occurs in a more acidic range ($pK = 4.9$) and is complete at pH 5.2 (Fig. 3.6B). In other words, the 420-nm absorbing species is practically undetectable at pH > 5.4 (Fig. 3.6). This latter observation point out to an efficient locking of the active site in *Bm*GadB, a finding that is also substantiated by the activity assays at pH > 5.4 (see below).

Chloride ions were reported to bind to *Ec*GadB underneath the triple helical bundles formed at acidic pH by the N-terminal region encompassing residues 3-15 (Gut *et al.*, 2006). The triple helical bundles are structural elements that were shown to be involved in recruiting *Ec*GadB to the cytosolic side of the inner membrane, in a pH-dependent manner. To date the nature of the interaction with the membrane, i.e. protein-protein or protein-lipid, has not been conclusively established. In *Ec*GadB chloride ions (as well as other halides) were shown to act as positive allosteric activators by delaying the spectroscopic transition (and the decrease in the activity) to less

acidic pH values. In other words chloride ions stabilize the active form, absorbing at 420-nm, of *Ec*GadB (O'Leary & Brummund, 1974, Gut *et al.*, 2006). Also in *Bm*GadB the pH-dependent spectroscopic transition is significantly affected by the addition of 50 mM sodium chloride in the buffers used to record the absorption spectra (Fig. 3.6B): the 420-nm species persists up to pH 5.2 and the *pK* of the spectroscopic transition is increased by 0.4 pH units (Tab. 3.4). These results are consistent with the conservation in the *Bm*GadB sequence of the residues that in *Ec*GadB were shown to be involved in halides binding (Fig. 3.3 and (Gut *et al.*, 2006)). However, the allosteric effect of chloride ions on *Bm*GadB is apparently unlinked to the formation of the triple helical bundles (cfr. 3.1.5).

**Table 3.4.** *Hill parameters from curve fitting of the 420 nm absorbance readings as a function of pH*

| | ***n*** | ***pK*** |
|---|---|---|
| *Bm*GadB | 3,52 ± 0,67 | 4,97 ± 0,03 |
| *Bm*GadB + NaCl | 7,52 ± 1,58 | 5,414 ± 0,008 |
| *Ec*GadB* | 12,07 ± 1,82 | 5,308 ± 0,006 |
| *Ec*GadB + NaCl* | 6,74 ± 0,66 | 5,690 ± 0,007 |

The values reported were calculated using the integrated Hill equation.
* Data from (Pennacchietti *et al.*, 2009)

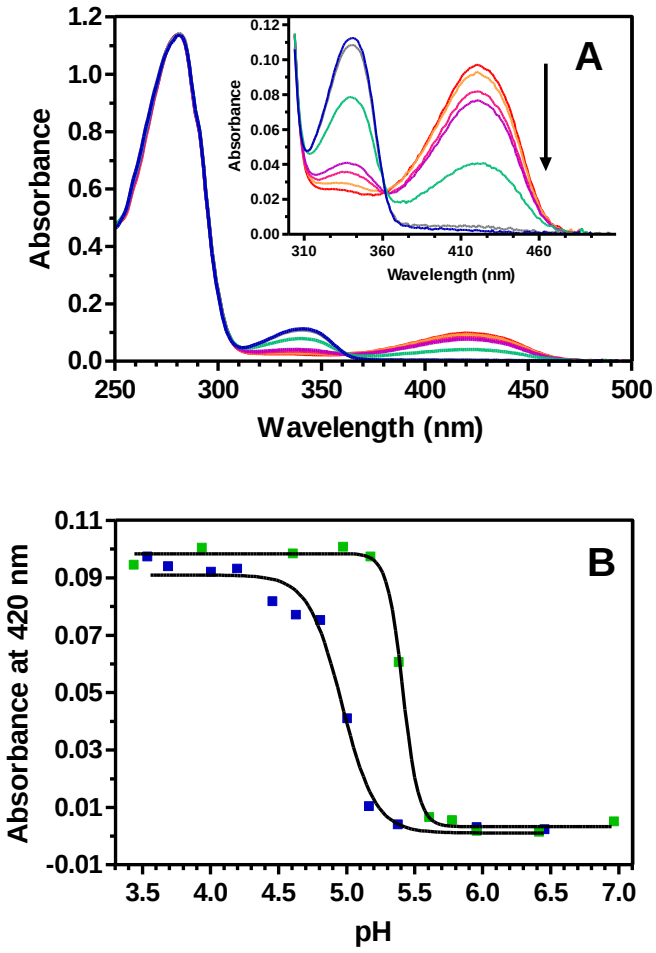


**Figure 3.6.** *pH-Dependent absorbance changes*. **(A)** Absorption spectra of *Bm*GadB were recorded in 50 mM sodium acetate buffer at pH values of 3.5, 4.2, 4.46, 4.6, 5.0, 5.4 and 6.5. Spectra were normalized taking into account the full PLP content (11.6 µM). The arrow indicates the change in absorbance at 420 nm upon increasing pH. **(B)** pH-dependent change in absorbance at 420 nm in the absence (blue squares) and presence (green squares) of 50 mM NaCl. The solid lines through the experimental points show the theoretical curves obtained using the Hill equation.

To assess whether the pH dependency of the activity of *Bm*GadB follows the same trend of the UV-visible spectroscopic changes, Gad activity was assayed both in the absence and in the presence of sodium chloride in the pH

range 3.8-6.5. Similarly to the *E. coli* counterpart (Gut *et al.*, 2006), *Bm*GadB displays its maximal activity at low pH, but only up to pH 4.5 (Fig. 3.7).

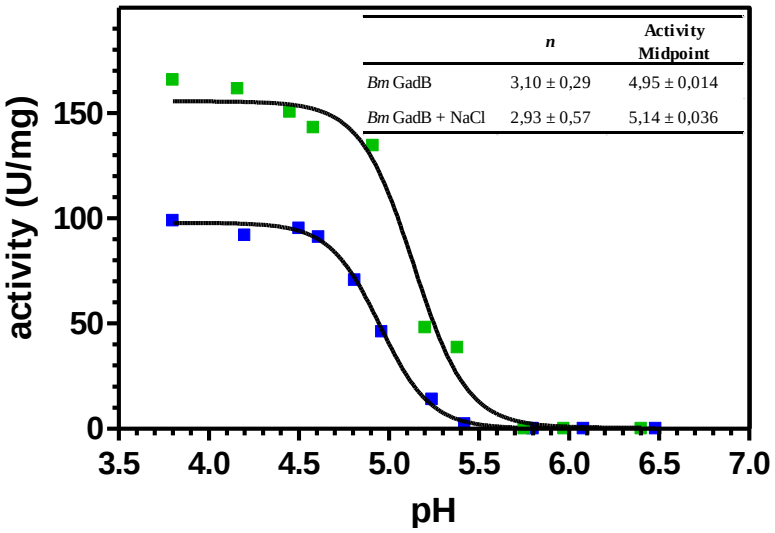


**Figure 3.7.** *Effect of pH on the activity of* Bm*GadB.* Glutamate decarboxylase activity (units mg) was measured at 37°C in 50 mM sodium acetate (pH 3.8 - 5.8) or phosphate (pH 6.0 - 6.5) buffer containing 40 µM PLP, 50 mM glutamate and in the absence (blue squares) or presence (green squares) of 50 mM NaCl. The protein concentration is 0.5-2 µM. The solid lines through the experimental points represent the theoretical curves obtained using Hill equation. Hill parameters from curve fitting of the specific activities as a function of pH are provided in the inset.

At pH ~ 5 the enzyme exhibits 50% of the specific activity measured in the pH range 3.8-4.5 and becomes inactive at pH values higher than 5.6. The data of activity *versus* pH fit well to the Hill equation suggesting that cooperativity ($n$ = 3) in the activity occurs. Notably, in the pH range 3.8-5.3 *Bm*GadB is 1.5-3 times more active when chloride ions are present. Notably, the shift of 0.4 pH units observed in the spectroscopic transition (Fig. 3.6B) does not lead to a similar shift in the pH range of activity of the enzyme.

The finding that the enzyme activity is still measurable at pH 5.4, i.e. where the 420-nm active form is undetectable, suggests that during the activity

assays the presence of glutamate delays the conversion between the active and the inactive forms, as proposed for *Ec*GadB (Pennacchietti *et al.*, 2009).

### 3.1.4 Fluorescence properties

Fluorescence analysis provides useful insights into the nature of the cofactor species embedded in the active site at different pHs. When *Bm*GadB in a buffer at pH 4.0 was excited at 430 nm, the emission spectrum (with a maximum at 500 nm) was typical of the ketoenamine, which on the contrary is barely detectable when the enzyme is excited at the same wavelength but at neutral pH (Fig 3.8A). These data are similar to those reported for *E. coli* GadB (Pennacchietti *et al.*, 2009) and, in combination with the UV-visible spectra, confirm that the active form of *Bm*GadB has the internal aldimine protonated on the imine nitrogen, a pre-requisite for being catalytically competent.

In order to discriminate on the chemical nature of the 340-nm absorbing species (Fig. 3.6A), i.e. substituted aldamine or enolimine, the emission spectrum of *Bm*GadB, following excitation at 345 nm, was recorded both at acidic and near-to-neutral pH. In *Ec*GadB at pH > 5.5 the residue His465 is responsible for the formation of a substituted aldamine (Gut *et al.*, 2006), which emits with a maximum at 390 nm when excited at 345 nm, whereas the corresponding His465Ala mutant exhibits, in addition to an emission at 390 nm, a second emission band at 510 nm (Fig. 3.8C). This latter emission spectrum is characteristic of the enolimine tautomer of the internal aldimine, i.e. with the hydrogen on the phenolic oxygen typical of internal aldimines in a less polar environment ((Pennacchietti *et al.*, 2009) and references therein). Similar results were obtained with *Ec*GadB by exciting at 295 nm and

recording the fluorescence emission spectrum in the range 300-540 nm, though in this case the emission maxima were detected at 355 and 520 nm (Pennacchietti *et al.*, 2009).

In the *Bm*GadB sequence His462 and His463 occupy the last but two and penultimate position, respectively (Fig. 3.3). Therefore the possibility exists that also in *Bm*GadB the 340-nm species, corresponding to the inactive form of the enzyme, arises from the formation of a substituted aldamine. Indeed fluorescence emission spectra obtained by exciting either at 295 nm (Fig. 3.8B) or at 345 nm (Fig. 3.8C) provide a strong indication that in *Bm*GadB aldamine is formed; in fact only one maximum is detected at 350 nm and 390 nm, respectively (Fig. 3.8B and C). At present we cannot unequivocally assign aldamine formation to any of the two histidine residues, though based on the sequence alignment we propose His463 in *Bm*GadB as the most likely candidate.

Overall the UV-visible and fluorescence emission spectra provide a clear indication that PLP in the active site of *Bm*GadB at neutral pH is in the form of a substituted aldamine, strongly suggesting that the reversible inactivation mechanism which was shown to be operative in *Ec*GadB is conserved in *Bm*GadB.

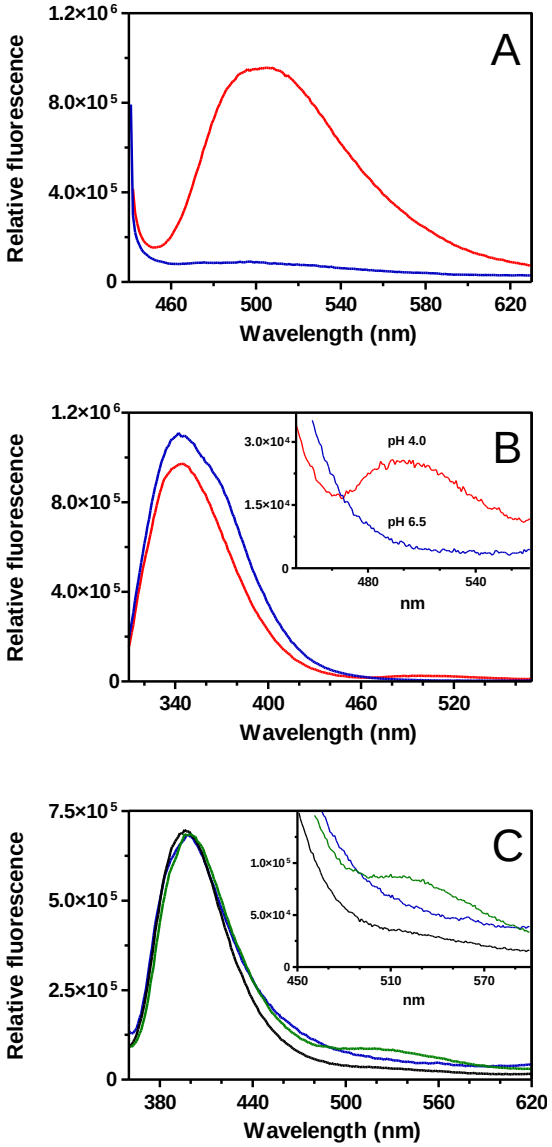


**Figure 3.8**. *Fluorescence emission spectra at different pHs*. *Bm*GadB emission spectra were recorded at pH 4.0 (red line) and at pH 6.5 (blue lines) following excitation at 430 nm **(A)** and 295 nm **(B)**. **(C)** Emission spectra of *Bm*GadB (blue line), *Ec*GadB (black line) and *Ec*GadB-H465A (green line) were recorded following excitation at 345 nm at pH 6.5. The protein concentration of *Bm*GadB was 13 µM. The protein concentration of wild type *Ec*GadB and GadB-H465A mutant was 3 µM. The buffers used were 50 mM sodium acetate at pH 4.0 and 50 mM potassium phosphate at pH 6.5.

### 3.1.5 pH-dependent cellular partition

In *E. coli* the acid-induced formation of two triple helical bundles, provided by the N-terminal regions of each subunit in the GadB hexamer, participates in the recruitment of the protein to the inner membrane (cfr. 1.1.3.2). The relocalization of *Ec*GadB in the cell, i.e. at the cytosolic side of the inner membrane, was proposed to be beneficial because this district is that mostly affected by incoming protons (Capitani *et al.*, 2003, Pennacchietti *et al.*, 2009).

Secondary structure predictions tools confirm that the N-terminal sequence of *Bm*GadB (which includes a Pro residue in the $7^{th}$ position) does not support formation of α-helical bundles, which on the contrary are predicted to be formed in the N-terminal region of *Ec*GadB (Fig. 3.9), in agreement with the crystal structure. Although *Bm*GadB and *Ec*GadB share 73 % amino acid sequence identity, the sequence alignment reveals that the two sequences mostly diverge in the N-terminal and C-terminal regions, with the notable exceptions of residues Ser14, Phe16, Gly17 and residues Pro459, Phe461, His463 and Thr464, the equivalent positions of which were shown to be instrumental in *Ec*GadB for chloride binding and active site plugging, respectively (Fig. 3.3). The N-terminal triple helical bundles in *E. coli* possess a hydrophobic core formed through one and a half heptad repeats (**V**TD**L**RSE**L**) and are polar/charged on the outside. The N-terminal region of *Bm*GadB does not possess any of these features and in addition it lacks the residues corresponding to Asp2, Asp8 and Asp15 of *Ec*GadB (Fig. 3.9A), the protonation of which is a likely requirement in driving triple helices formation.

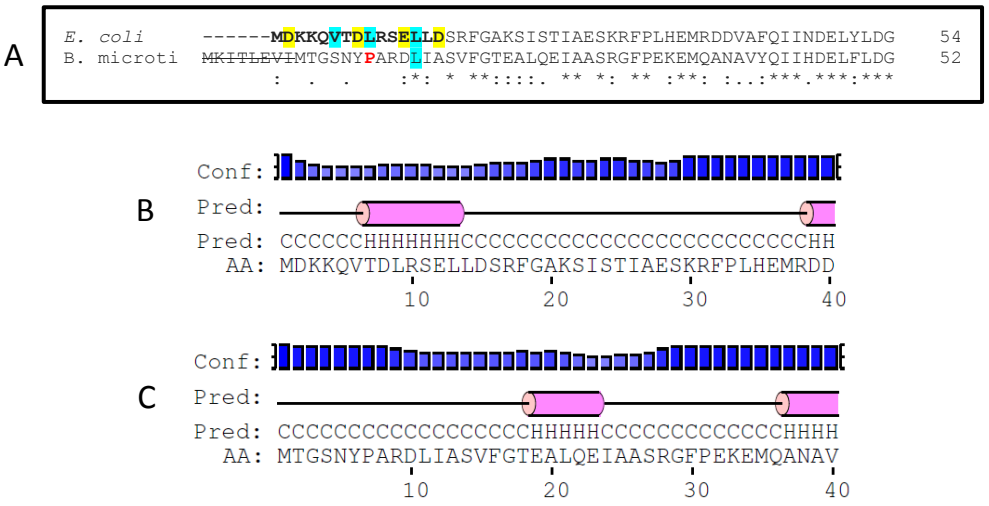


**Figure 3.9.** *Secondary structure prediction of* Bm*GadB N-terminal region.* **(A)** Clustal Omega (version 1.2.0) alignment of *Ec*GadB and *Bm*GadB (only N-terminal portion is shown). In *Ec*GadB: the residues in bold correspond to residues involved in α-helix formation; blue shaded residues contribute to the hydrophobic core of the bundle ; yellow shaded residues are the charged residues. In *Bm*GadB: the first 8 amino acids (barred) are not part of GadB protein, as determined experimentally; the red residue is the proline. Secondary structure prediction of *Ec*GadB **(B)** and *Bm*GadB **(C)** N-terminal regions, performed with PSIPRED. Conf: confidence of prediction. Pred: predicted secondary structure (violet cylinders represent α-helices, H, and black lines random coil regions, C).

Despite the apparent inability to form an α-helix in the N-terminal region of each subunit of the hexamer, *Bm*GadB might still possess the ability to partition between the cytosol and the membrane following a decrease in cytoplasmic pH. In order to answer to this issue, cell fractionation of the *E. coli* strain BL21(DE3) overexpressing *Bm*GadB was performed by ultracentrifugation. Cytoplasmic and membrane fractions at neutral and mildly acidic pH were assayed for enzyme activity (Fig. 3.10A) and analysed by SDS-PAGE (Fig. 3.10B). As hypothesized on the basis of the secondary structure predictions, the cellular localization of *Bm*GadB is not influenced by pH: a significant fraction of the protein (approximately 30%) is already

associated to the membrane at neutral pH and its levels do not increase further upon decreasing the pH of the cell extract.

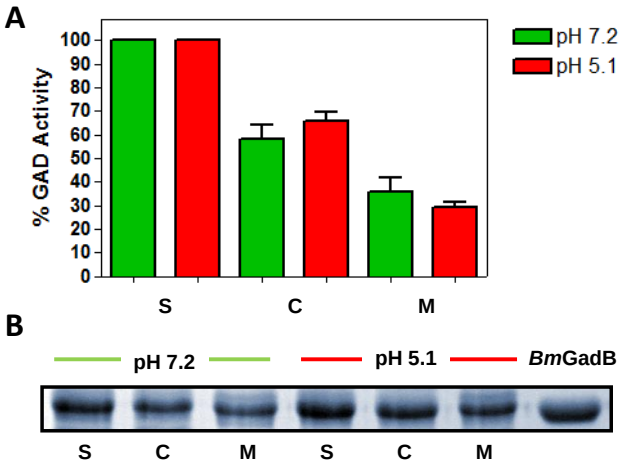


**Figure 3.10.** *Effect of pH on the cellular localization of* Bm*GadB*. Cell supernatants (S), obtained after cell lysis and centrifugation to remove cell debris; the cytoplasmic (C) and membrane (M) fractions were obtained as described in previously (Capitani *et al.*, 2003). **A)** The decarboxylase activity is provided as percentage with respect to the starting activity in S. **B)** The relative abundance of *Bm*GadB in each sample at the specified pH was compared by 12% SDS-PAGE of 30 µg-samples. For comparison *Bm*GadB (52 kDa, 2 µg) on the right.

### 3.1.6 Discussion

In the present work overexpression, purification, biochemical and spectroscopic characterization of recombinant GadB from *B. microti* (*Bm*GadB) is reported. To our knowledge, this is the first report of a Gad from an Gram-negative α-Proteobacterium and from the genus *Brucella* which is regarded as highly pathogenic (Franco *et al.*, 2007). The purity of *Bm*GadB was over 95%, which allowed to perform a comparative characterization with the biochemical and spectroscopic properties of the intensively investigated *Ec*GadB (De Biase & Pennacchietti, 2012).

The finding that *Bm*GadB undergoes spectroscopic (UV-visible and fluorescence) and activity changes and is affected by chloride ions just like *Ec*GadB provides a strong evidence that also in *Bm*GadB occur the conformational changes in the C-terminal region that were reported to affect the intracellular activity of the *E. coli* enzyme.

The role of chloride ions as positive effectors of the enzyme activity in the acidic pH range is even more evident in *Bm*GadB than in *E. coli* GadB. However, *Bm*GadB is also peculiar in that it is maximally active up to pH 4.5 and the allosteric effect of chloride ions is apparently unlinked to the formation of triple helical bundles in the N-terminal region, which in *E. coli* GadB were shown to contribute to the cooperativity of the system as well as to the recruitment of the enzyme to the cytosolic side of the inner membrane.

The experiments of cellular partition of *Bm*GadB suggest that the interaction of this protein with some components of the inner membrane is not significantly affected by acidification of the intracellular compartment. However we cannot exclude that in the inner membrane of *E. coli* some components, present in *B. microti* and responsible for driving *Bm*GadB intracellular re-localization in response to acidic stimuli, are actually missing.

Although the physiological function of *Bm*GadB has been elucidated, i.e. it plays a pivotal role in *B. microti* extreme acid resistance (Occhialini *et al.*, 2012), it is possible that protection is also contributed by the protein products of other genes besides *gadB* and *gadC,* as for *E. coli*. In this respect it should be recalled that in *B. microti*, as well as in other *Brucella* species, the *gadBC* genes is located immediately upstream of the *ybaS* (BMI_II336) and the *hdeA* (BMI_II337) genes with which they constitute an operon (Occhialini *et al.*, 2012). The *hdeA* gene codes for a periplasmic protein that functions at low pH and contributes to acid resistance in *B. abortus* and is regulated by the

RNA chaperone and post-transcriptional regulator Hfq (Valderas *et al.*, 2005). The role of acid-induced periplasmic chaperones has been investigated in *E. coli* because they are part of the AFI (cfr. 1.1.2. and Fig. 1.3) and because of their peculiar mode of action. Periplasmic chaperone HdeA contributes to acid resistance in a range of different species, including *E. coli*, *S. flexneri* and *B. abortus* (recently reviewed by (Hong *et al.*, 2012)). In all these species (which infect with a low ID), loss of one or both of the periplasmic chaperons impairs growth at low pH. The molecular details of their mode of action are beginning to be elucidated (Tapley *et al.*, 2010, Zhang *et al.*, 2011, Foit *et al.*, 2013). Moreover the role of *ybaS*, coding for a glutaminase, in *B. microti* is likely to be the same as that described recently for the *E. coli* counterpart (cfr. 1.1.1 and Fig. 1.1A).

With the present work we aimed at obtaining detailed information on a novel prokaryotic GadB. This work not only contributes to our understanding of the GadB-mediated mechanism protecting bacteria from acid stress (together with the urease system it is in fact the most potent AR system known in neutrophilic bacteria), but also has allowed to discriminate between biochemical differences which might reflect not only the differences in the physiology and metabolism of the two specific microorganism but also in the niches they occupy.

## 3.2 PART II: The Asp86-His465 mutant of *Escherichia coli* glutamate decarboxylase exhibits improved GABA synthesis at alkaline pH

As described in the introduction, *E. coli* GadB was extensively characterized at the biochemical and structural level (Capitani *et al.*, 2003, Gut *et al.*, 2006). Its pH-dependent activation relies on important local structural reorganizations (Capitani *et al.*, 2003, Gut *et al.*, 2006) and can be easily monitored by the change in the absorption spectrum of PLP, which probes it. At neutral pH, the C-tail (the last 15 residues) was found to plug the active site and reversibly inactivate the enzyme *via* formation of the substituted aldamine.

Spectroscopic analyses of His465 mutants demonstrated that this residue is indispensable for the reversible inactivation of the enzyme at neutral pH, but does not contribute to the cooperative change of GadB activity (Pennacchietti *et al.*, 2009). Even though the GadB-His465 mutant enzymes display a pH-range of activity broader than that of the wild type enzyme, their catalytic activity falls at pH 6.0, i.e. much before the spectroscopic transition midpoint (pH ≈ 7.5) occurs. The decrease of the catalytic activity as a function of increasing pH was thus attributed to the deprotonation of substrate-binding or catalytic residues, with an expected *pK* of 6.0 (Pennacchietti *et al.*, 2009). One such candidate could be Asp86, which is involved in the binding of the distal γ-carboxylate of glutamate and of which the ionizable side chain takes up different conformations at neutral and acidic pH (Capitani *et al.*, 2003, Pennacchietti *et al.*, 2009) (Fig. 3.11). Notably the role of Asp86, strictly conserved in the pH-dependent prokaryotic and plant

GADs, is replaced by a non-ionizable glutamine residue and a positively charged arginine residue in both human GADs, which indeed display maximal activity at neutral pH (Fenalti *et al.*, 2007).

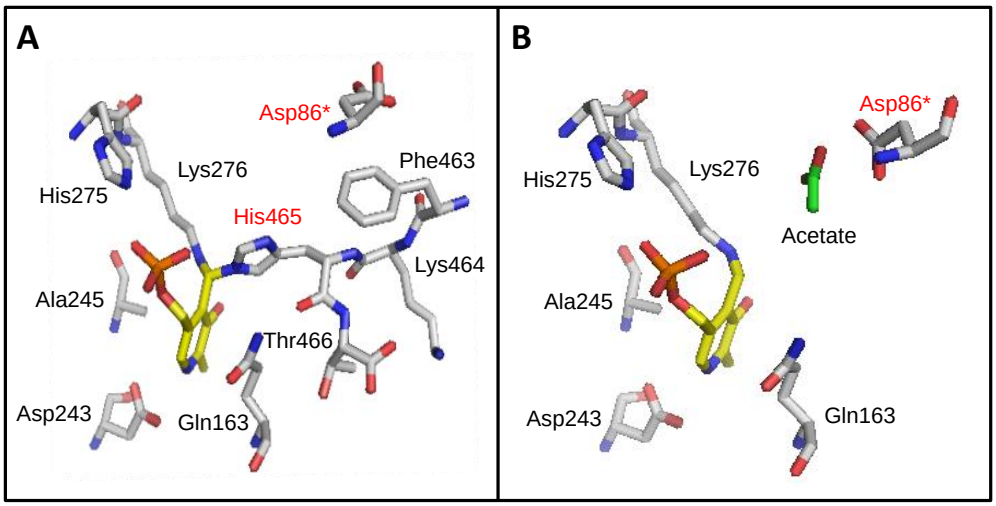


**Figure 3.11**. *Active site of wild-type* Ec*GadB at neutral and acidic pH.* **(A)** At neutral pH, the C-tail is directed into the active site precluding the access of the substrate. Residue His465 is involved in the formation of the substituted aldamine with PLP-Lys276 Schiff base Asp 86* side chain points away from the active site. **(B)** At acidic pH the C-tail no longer blocks the active site and the residue Asp86* changes orientation, moving in the direction of the acetate molecule (present in the crystallization buffer), which mimics the γ-carboxyl group of the substrate glutamate.

In order to elucidate the role of Asp86, a biochemical and structural characterization of the GadB_Asp86Asn-His465Ala mutant (hereafter named GadB-D86NH465A), which incorporates the mutation Asp86Asn in the already characterized GadB-His465Ala mutant (Pennacchietti *et al.*, 2009), was performed.

The production of GadB-D86NH465A mutant, its purification and spectroscopic analysis was the subject of my MSc thesis. During my Ph.D. I continued to work with this mutant with the aim to improve the purification

protocol, perform a more detailed analysis of the catalytic properties and interpret the structural data obtained in the meanwhile on crystals of highly pure protein which was provided to Dr. Guido Capitani (Paul Scherrer Institute, PSI Villigen, Switzerland).

### 3.2.1 *Preliminary data*: purification and spectroscopic properties of GadB-D86NH465A

The double mutant, GadB-D86NH465A, was generated by incorporating the Asp86Asn mutation into the single mutant protein GadB-His465Ala already available in our laboratory (Pennacchietti *et al.*, 2009). GadB-D86NH465A was overexpressed in *E. coli* and purified as previously described (De Biase *et al.*, 1996) except that the DEAE-Sepharose chromatography was carried out at pH 6.0 instead than at pH 6.5, because at the latter pH GadB-D86NH465A did not bind the resin. The initial purification protocol has been further improved by a second DEAE chromatography step, where the collected fractions obtained from the first run at pH 6.0 were reconstituted with PLP (5-fold of the protein concentration) for 1h at room temperature to increase the *holo/apo* form ratio. In fact, in the absence of added PLP during purification, the holoenzyme content is approx. 70 %. The reconstituted enzyme was re-loaded on DEAE column at pH 6.5. Under these conditions the protein does not bind the column resin and is recovered in the flow-through during the washing step, while other protein contaminants remain bound to the resin (Fig. 3.12).
Following the optimized purification GadB-D86NH465A is ≥ 95 % pure (as judged by SDS-PAGE) and is stable for several months at 4°C (Fig. 3.12). The PLP content is 90-95%. The yield of the purified enzyme from a

standard purification (2 L bacterial culture) is 30 mg. The specific activity towards L-glutamate (assayed at 37°C in 0.2 M pyridine/HCl buffer, pH 4.6, containing 0.1 mM PLP) is 140 U/mg, corresponding to 64 % and 80 % of the specific activity of wild type GadB and GadB-H465A, respectively (Pennacchietti *et al.*, 2009). When assayed in the presence of aspartate and glutamine, GadB-D86NH465A does not show any detectable activity, thus confirming that Asp86Asn mutation in the active site does not affect substrate specificity.

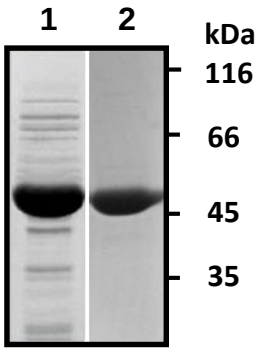


**Figure 3.12.** *Purification of GadB-D86NH465A.* 12% SDS-PAGE, stained with Coomassie Blue. Lane 1, GadB-D86NH465A, after a standard purification (7 μg). Lane 2, GadB-D86NH465A, after the optimized purification (6.5 μg). Molecular mass of protein standards are indicated on the left.

As shown in Figure 3.13, the pH-dependent UV-visible spectroscopic changes of GadB-D86NH465A differ significantly from those reported for wild type GadB (Shukuya & Schwert, 1960, Tramonti *et al.*, 2002), while resembling those of GadB-H465A (Pennacchietti *et al.*, 2009). In fact the absorption spectra, recorded in the pH range 4.5 - 9.1, show that the 420 nm → 332 nm spectroscopic transition does not undergo completion, and in fact 42 % of the ketoenamine is still detectable at pH ≥ 9 (Fig. 3.13A).

The incomplete spectroscopic transition has a midpoint at pH 7.23, two units higher than that of wild type GadB, and cooperativity is abolished (Fig. 3.13B, Table 3.5.). An isosbestic point is present at 360 nm as in wild type GadB, whereas in GadB-H465A it is blue-shifted (348 nm) (Pennacchietti *et al.*, 2009).

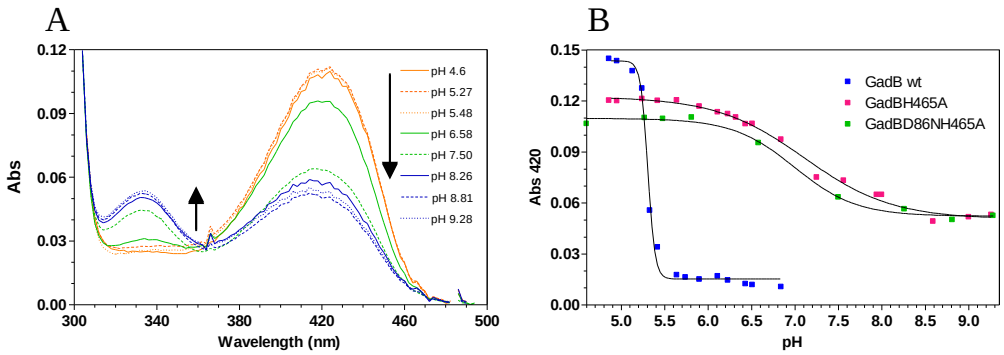


**Figure 3.13.** *pH-Dependent absorbance changes.* **(A)** Spectra of GadB-D86NH465A are recorded in 50 mM sodium acetate buffer at pH values of 4.6, 5.27, 5.48 and in 50 mM potassium phosphate buffer at pH 6.58, 7.5, 8.26, 8.81, 9.1. The protein concentration is 15.4 μM and the arrows indicate the change in absorbance at 420 nm and at 332 nm upon increasing pH. **(B)** The pH-dependent readings at 420 nm are reported for GadB-D86NH465A (green), for GadBH465A (magenta) and wild type GadB (blue). The solid lines through the experimental points represent the theoretical curves obtained using Hill equation.

**Table 3.5.** *Midpoint (pK) and Hill coefficient (n) of spectroscopic transition in wild type and mutants forms of GadB*

| **GadB** | ***pK*** | ***n*** |
|---|---|---|
| wild type | 5,31 ± 0,001 | 10,52 ± 1,48 |
| H465A | 7,11 ± 0,06 | 0,86 ± 0,08 |
| D86N-H465A | 7,23 ± 0,09 | 0,86 ± 0,17 |

Chloride ions, which are known to act as positive allosteric activators of GadB (Gut *et al.*, 2006), do not affect further the spectroscopic transition (data not shown).

### 3.2.2 Catalytic Properties

#### 3.2.2.1 Effect of pH on specific activity

All the above findings suggest that Asp86 does not contribute to the pH-dependent spectroscopic properties of *E. coli* GadB and that these properties in GadB-D86NH465A can be ascribed to the H465A mutation, which is shared by GadB-H465A and GadB-D86NH465A.

To further investigate on the role of Asp86 in *E. coli* GadB, decarboxylation of L-Glu was assayed both at different pH values and at time intervals at a specific pH. As shown in Figure 3.13, spectroscopic data indicate that in GadB-D86NH465A at neutral pH still a significant fraction the coenzyme is present in the 420 nm-absorbing form (ketoenamine), typical of a hydrated active site. Assuming that the active site is still accessible to the substrate, the possibility exists that the introduction of D86N mutation might allow GadB-D86NH465A to bind L-Glu and catalyse its decarboxylation at higher pH values than both wild type enzyme and GadB-H465A. In fact, as previously mentioned, the midpoint of the partial spectroscopic transition in GadB-H465A occurs at pH 7.1 (Table 3.5), which is one pH unit above the pH at which 50% of the change in the catalytic activity is detected (Pennacchietti *et al.,* 2009). This observation suggested that the catalytic activity of GadB, is influenced by an ionisable group with *pK* 6.0 besides being heavily influenced by His465 which is primarily responsible to control the access to active site (Pennacchietti *et al.,* 2009).

The activity profile of GadB-D86NH465A in the pH range 4.6-8.3 was compared with that of wild-type GadB and GadB-H465A (Fig. 3.14A).

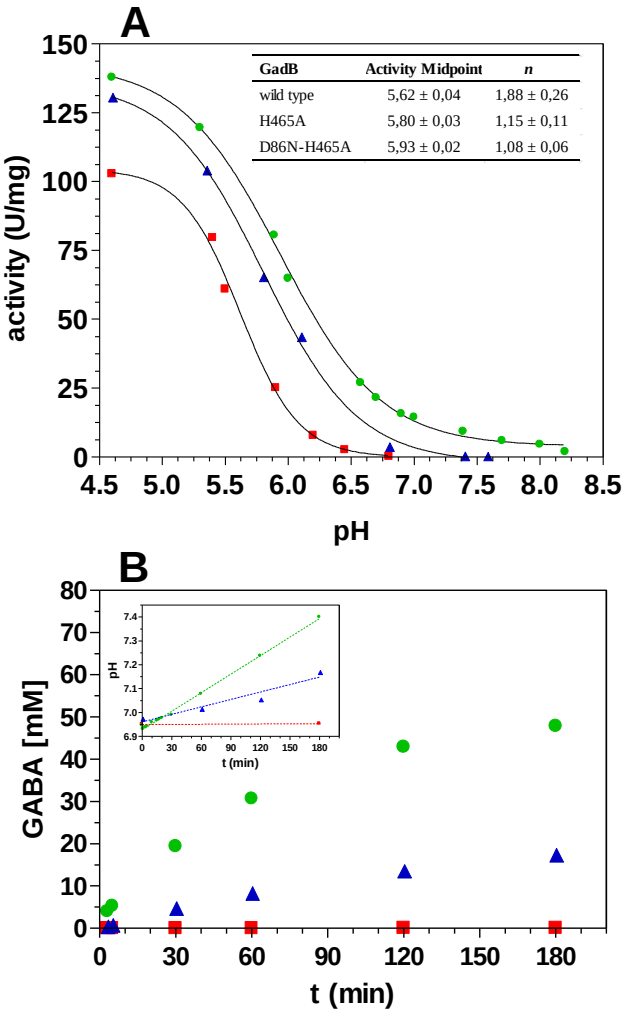


**Figure 3.14.** *Effect of pH on the specific activity and time course of GABA production***.** Red squares, wt GadB; blue triangles, GadB-H465A; green circles, GadB-D86NH465A. **(A)** Activity assays were carried out at 37°C in 50 mM acetate (pH 4.5 - 5.8) or phosphate (pH 5.9 – 8.3) buffer in presence of 40 µM PLP, 50 mM NaCl and 50 mM L-Glu. Protein concentration was 0.9-2 µM. The solid lines through the experimental points represent the theoretical curves obtained using the Hill equation. The reported data are the means of three independent experiments, with a standard deviation <10 % of the given value. The *n* and Activity Midpoint values retrieved from curve fitting are given in the inset Table. **(B)** GABA production was analysed over a period of 3 hours. The reaction was carried out at 30°C in 4 ml of 50 mM potassium phosphate buffer, pH 7.0, containing 40 µM PLP and 50 mM L-Glu. The protein concentration was 2 µM. At each time point aliquots (100 µl) were withdrawn and analyzed for GABA content with the Gabase assay. The pH changes during the reaction were also recorded (inset).

The data in the above Figure show that GadB-D86NH465A displays an enhanced activity in a broader pH range. In particular 6 % of the starting activity is still present at pH 8.0. This is noteworthy if one considers that in the spectroscopically similar GadB-H465A mutant catalytic activity is undetectable above pH 7.2 (Fig. 3.14 and (Pennacchietti *et al.*, 2009)) and that in wild type GadB the activity drastically falls at pH > 5.3, corresponding to the *pK* of the spectroscopic transition which leads to aldamine formation and therefore autoinactivation.

Differently from previous work, in which the reactions were carried out in phosphate buffer (Pennacchietti *et al.*, 2009) or in water (Lammens *et al.*, 2009), in the present work the assays were performed using two different buffer to cover such a wide pH range: acetate buffer (4.5 - 5.8) and phosphate buffer (pH 5.9-8.3). Under these experimental conditions, in GadB-H465A mutant the pH-triggered transition from the active to the inactive form of the enzyme is not a cooperative process ($n \approx 1$) (Fig. 3.14). The double mutant GadB-D86NH465A exhibits a similar behavior. The pH-dependent activity profile of wild type enzyme confirms that the transition is still cooperative ($n \approx 2$), as reported in previous works.

Given that GadB-D86NH465A is still active at pH close to 8.0, it was decided to assay GABA production in potassium phosphate buffer at pH 7.0 over a period of 3 hours (Fig. 3.14B). For comparative purposes the time course of GABA production was analysed in the presence of 50 mM L-Glu for the three enzymes, GadB-D86NH465A, GadB-H465A and wild type GadB. As shown in Figure 3.14B, GadB-D86NH465A converts approx. 86 % and 96 % of L-Glu into GABA after 2 and 3 hours of reaction, respectively. Following the first hour of reaction, the rate at which it occurs gradually decreases due to L-Glu consumption which after 3 hours is only 2 mM. These

results are remarkable when compared with those obtained with GadB-H465A, which converts only 35 % of L-Glu into GABA after 3 hours. As expected, wild-type GadB decarboxylates only 0.2 % of glutamate after 3 hours. During reaction, the pH of the solutions was monitored: after 3 h the pH was increased by 0.2 and 0.4 pH units in GadB-H465A and GadB-D86NH465A reaction mixtures respectively, coherently with $H^+$ consumption due to the decarboxylation reaction. In the GadB wild type sample no pH changes was recorded.

#### 3.2.2.2 Kinetic constants and solvent isotopic effect

The kinetic constants of the reaction catalyzed by GadB-D86NH465A were obtained at 25°C in 50 mM acetic acid/sodium acetate buffer at pH 4.6, varying the substrate concentration from 0.3 to 80 mM. Since it was not possible to follow the reaction spectrophotometrically (De Biase *et al.*, 1996), the reaction rate was determined by measuring the accumulation of GABA at 1 min time intervals by Gabase assay (cfr 2.6.3). This was possible since the decarboxylation reaction is irreversible.

The $k_{cat}$ and $K_m$ values calculated for GadB-D86NH465A are provided in Table 3.6 and compared with those of GadB wild type and H465A mutant. $K_m$ of GadB-D86NH465A is significantly higher than that calculated or the other two enzymes, while $k_{cat}$ is only slightly increased. This results in an overall reduction of the specificity constant ($k_{cat}/K_m$).

The decarboxylation reaction was also conducted both in water and in deuterium oxide under saturating conditions, and by keeping the pH (or pD) of the reaction constant at 4.6 (cfr 2.6.4).

**Table 3.6.** *Kinetic parameters of GadB-D86NH465A compared to GadB wild type and GadB-H465A.*

| GadB | $k_{cat}$ $s^{-1}$ | $K_m$ (mM) | $k_{cat}/K_m$ ($s^{-1}$ $mM^{-1}$) |
|---|---|---|---|
| wild type | 18,1 ± 1,2 | 0,68 ± 0,09 | 26,4 ± 5,3 |
| H465A | 16,1 ± 0,4 | 0,82 ± 0,05 | 19,6 ± 1,7 |
| D86N-H465A | 27,1 ± 2,1 | 2,60 ± 0,32 | 10,45 ± 2,1 |

The values reported were calculated from the experimental data using the *Lineweaver-Burk* equation.

The $k_{cat}$ of the reactions carried out by GadB-D86NH465A, GadB-H465A and wild type enzyme, were determined in both conditions and compared, to determine the solvent isotope effect (Table 3.7). In fact, it is known that *E. coli* glutamate decarboxylase undergoes a marked solvent isotope effect on $k_{cat}$ (O'Leary *et al.*, 1981, Tramonti *et al.*, 1998).While H465A mutant displayed an isotope effect similar to that of wild type enzyme, in GadB-D86NH465A the isotope effect is still present but reduced more than 5 fold respect to wild type GadB (Table 3.7). Given that the decrease in isotope effect is observed only in the double mutant and not in the single H465A mutant, and that the residue Asp68 binds the distal carboxylate of L-Glu (i.e. stabilizing the interaction with the substrate, which must be properly oriented in the active site in order to be decarboxylated at C-α), the present finding suggests that the D86N mutation probably affects a stage that involves proton transfer before the formation of the substrate-enzyme complex.

**Table 3.7.** *Isotope effect on GadB-D86NH465A $k_{cat}$ compared to GadB wild type and GadB-H465A*

| GadB | $k_{cat}$ $s^{-1}$ in $H_2O$ | $k_{cat}$ $s^{-1}$ in $D_2O$ | Isotope effect |
|---|---|---|---|
| wild type | 21,3 ± 0,27 | 1,48 ± 0,06 | 14,4 |
| H465A | 32,70 ± 0,87 | 2,58 ± 0,16 | 12,7 |
| D86N-H465A | 56,8 ± 0,89 | 20,7 ± 0,16 | 2,7 |

### 3.2.3 Structural analysis

Highly purified GadB-D86NH465A was provided to the collaborating laboratory of Dr. Guido Capitani (PSI, Villigen, Switzerland) which solved, from a pseudomerohedrally twinned monoclinic crystal form, the structure of GadB-D86NH465A at pH close to neutrality and at 3.1 Å resolution. The crystals possessed two GadB-D86NH465A molecules per asymmetric unit mimicking an orthorhombic space group. In spite of the twinning, the structure could be refined by taking the twin law into account (G. Capitani personal communication).

The two GadB-D86NH465A molecules in the asymmetric unit display a hybrid conformation with the N-terminal regions of each chain being disordered, typical of the neutral-pH inactive form of GadB (1PMO), and no visible C-tail in the active site, typical of the low-pH active form (1PMM) (Capitani *et al.*, 2003, Gut *et al.*, 2006). Also, the β-hairpin formed by residues 300-313 is partly disordered, with variations from subunit to subunit. Taking one subunit as reference, the conformation resembles more that of the low pH form of GadB (1PMM) than that of the neutral pH forms. This latter finding suggests that at alkaline pH His465 is instrumental to stabilize the C-tail in its position and that when this residue is missing not only the C-tail has more freedom, but also the 300-313 β-hairpin cannot adopt the same conformation as in the inactive wild-type GadB, in which it contacts residues 461-463 in the C-tail (in 1PMO).

The active site of GadB-D86NH465A (Fig. 3.15) exhibits a conformation very similar to that of the wild type enzyme at both low-pH (1PMM) and neutral-pH (2DGK, 1PMO), with the following distinctive points: the side chain of Asn86 is free from ligands in 10 subunits out of 12, while in the

remaining two it is close to additional density corresponding to a ligand in the active site (interpreted as acetate, which was present at 150 mM in the crystallization solution). In 3 GadB-D86NH465A subunits out of 12 the conformation of Asn86 is similar to that observed for Asp86 in the low pH form of GadB (1PMM) and points towards the acetate binding site, while in the other 9 it is very similar to that of Asp86 in the neutral-pH forms (1PMO and 2DGK). These observations suggest that GadB-D86NH465A has a low affinity for acetate and are in accord with the finding that GadB-D86NH465A is probably affected by acetate ions to a lesser extent respect to the wild type enzyme (Fig. 3.14).

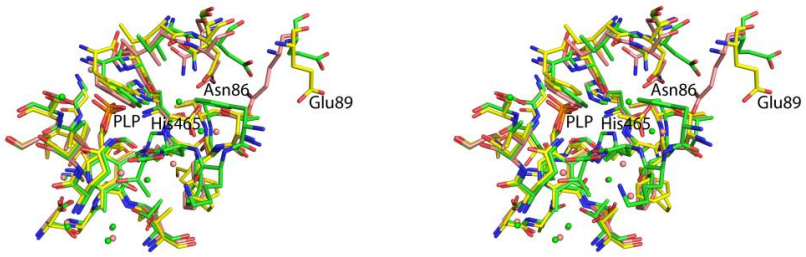


**Figure 3.15.** *Conformation and environment of Asn86 of GadB-D86NH465A and Asp86 of GadB at low and neutral pH.* Stereo ball-and-stick depiction of the active site of GadB-D86NH465A (yellow and atom colors) with the active sites of 1PMM (GadB at low pH, salmon) and 2DGK (GadB -1-14 at neutral pH, green) superimposed. The aldamine-bound C-terminal tail of 2DGK, green, is not seen in the active site of GadB-D86NH465A. An acetate ion is present is the depicted active site (chain A) but it absent in the majority of the 12 active sites in the asymmetric unit.

### 3.2.4 Discussion

In this chapter the analysis of the contribution of Asp86, the residue involved in the binding of the γ-carboxyl group of L-Glu , to the catalytic properties of *E. coli* GadB is presented. The GadB-D86NH465A mutant was also characterized at the structural level by collaborators, to provide a more

complete picture of the structural/functional consequences of the double mutation Asp86Asn-His465Ala in *E. coli* GadB.

Based on the analysis of His465 mutants it was proposed that in the absence of His465 GadB remains in the open conformation at pH values well above pH 6.0, even though the activity significantly decreases at this pH (Pennacchietti *et al.*, 2009). This latter finding was attributed to the effect of one or more residue(s) directly involved in substrate binding or catalysis. Asp86, a residue provided by the neighbouring subunit of the functional dimer, is a likely candidate because it undergoes a significant side chain reorientation during the pH-dependent conformational changes (Capitani *et al.*, 2003) and the *pK* of the its β-carboxylate might directly correlate with the pH-dependency in the enzyme activity. At acidic pH the side-chain of Asp86 is tilted towards the active site and its β-carboxylate interacts with an acetate ion, mimicking the γ-carboxylate of the substrate glutamate (Fig. 3.11). For this interaction to occur clearly at least one (if not both) of the two carboxylate groups must be protonated (Capitani *et al.*, 2003).

To assess the role of Asp86 in *E. coli* GadB, GadB-D86NH465A double mutant was produced. This was necessary to appreciate the contribution of Asp86 in substrate binding, an interaction otherwise undetectable because of the presence of His465 in the active site at pH > 5.5. Asp86 was replaced with a similarly sized, but neutral Asn residue. This mutation was expected not to affect polarity in the GadB active site. The intention was to abolish the charge repulsion with the γ-carboxylate of glutamate at non permissive pH (> 5.5) thus allowing substrate binding at pH values well above 6.

Preliminary data confirmed that Asp86Asn mutation in the double mutant GadB-D86NH465A does not affect the spectroscopic properties (cfr. 3.2.1) with respect to the single mutant GadB-H465A, i.e. mutating His465 is

sufficient to unlock the active site. However the data obtained in this thesis show that GadB-D86NH465A has an expanded pH-range of activity, i.e. GadB-D86NH465A is able to catalyze the decarboxylation reaction at a significant rate at pH 7.0, where the activity of both GadB-H465A and wild type GadB is greatly reduced or practically nil.

The Asp→Asn substitution might have altered the non-covalent interactions system (e.g. hydrogen bond) involved in substrate anchoring. A non-optimal initial interaction with glutamate might explain the worsened substrate affinity (higher $K_m$) at acidic pH. However, following substrate binding, L-Glu might be in a more favourable location for the subsequent reaction steps (higher $k_{cat}$). The kinetic constants and isotope effect discrepancies between GadB-D86NH465A and both GadB wild type or H465A mutant suggest that the above are likely possibilities.

Structurally, GadB-D86NH465A, present in two copies in the asymmetric unit, exhibits features of both the low-pH (1PMM) and the neutral-pH (2DGK, 1PMO) forms of the enzyme: its C-terminal tail is disordered and the active site is accessible to bulk solvent, like in 1PMM, while the N-terminal helical bundle is absent like in 1PMO. Even though, the lattice of the GadB-D86NH465A crystals does not provide enough space to accommodate all N-terminal bundles, if they formed, it is reasonable to assume that at pH ~7.0 (the pH of the crystallization drop) the N-terminal bundles are not present, as suggested by previous experiments (Pennacchietti *et al.*, 2009). In the active site, Asn86 is found in a conformationally mixed situation with respect to the two canonical wild-type structures (i.e. low pH and neutral pH) and no ligands are found only in a fraction of the active sites. The full accessibility of the active site at a pH around 7 is in accord with the biochemical data. In spite of the presence of 0.3 M sodium acetate in the reservoir solution of the

crystallization setup, an acetate ion is found only in two active sites out of 12 at the site observed in 1PMM, where Asp86 is involved in the binding.

The availability of a GadB-D86NH465A mutant, which is active in a broad pH range, could have important implications in the biotechnological field, where wild type GadB has already been proposed to be used. In fact, GadB may be immobilized in bioreactors for industrial production of GABA, to be used as an intermediate for the synthesis of precursors of biopolymers (Introduction 1.3.2). The enzymatic conversion of L-Glu to GABA via *E. coli* GadB, carried out in bioreactors at the industrial level, was proposed as a strategy to decrease the dependence on fossil fuels, allowing the production of chemicals from renewable resources, such as biomass (Lammens *et al.*, 2009). However, during L-Glu decarboxylation GadB activity is slowed down by the pH rise caused by the consumption of protons (Lammens *et al.*, 2009, Pennacchietti *et al.*, 2009). To circumvent this problem, Lammens et al. showed that the optimal pH for the decarboxylation reaction could be kept constant by the addition of L-Glu (acid) in an unbuffered fed-batch reaction which uses immobilized *E. coli* GadB (Lammens *et al.*, 2009). Working in a buffer-free system had also the advantage of making the downstream separation steps easier. However, at acidic pH glutamic acid displays a very low solubility (Amend & Helgeson, 1997), a limiting factor for GABA production in a batch mode.

The GadB-D86NH465A mutant characterized in this thesis is expected to be useful because, unlike wild-type GadB, it is able to catalyze the decarboxylation reaction across a wider pH range that extends toward pH > 8.0, thereby rendering the pH of the reaction not a limiting parameter. Beyond the results presented in this thesis, many other studies in recent years

have focused on enhancing GABA production and improving the catalytic properties of bacterial GAD. Thus engineered *E. coli* GadB, such as a C-terminal truncated mutant (Yu *et al.*, 2012), His465 mutants (Pennacchietti *et al.*, 2009) Glu89/His465 mutants (Ho *et al.*, 2013) and GadB mutants extended or reduced in length by just one residue at the C-terminus (Kang *et al.*, 2013) were designed with the aim of improving and enhancing the enzymatic properties of GAD and the reaction conditions for potential industrial applications.

## 3.3 PART III: Preliminary structural analysis of *Escherichia coli* glutamate decarboxylase *apo* form

Although the biochemical properties of *E. coli* glutamate decarboxylase have been extensively investigated (cfr. 1.1.3.2 and 1.2.2), the structural role of PLP in protein folding, oligomeric assembly and stability, has not been completely elucidated and represents an interesting topical of research.

Recently, the structure of the *apo* form of another member of group II decarboxylase family, i.e. the human L-DOPA decarboxylase (DDC), was solved (Giardina *et al.*, 2011). As other mammalian decarboxylases, DDC is a homodimer. Comparing available structure of the homolog pig kidney enzyme in the *holo* form with that of the human apoenzyme, it was clear that PLP binding triggers a dramatic conformational rearrangement consisting of a rigid body displacement of the dimer subunit large domains, that move by 20 Å assuming a totally open conformation (Giardina *et al.*, 2011). In the *apo* form the dimer interface is reduced and active sites are completely exposed to solvent. In this condition, the global enzyme shape changes, key structural elements are mobile or unfolded, and regions that were buried inside the closed *holo*-structure become solvent exposed, giving a reasonable explanation for the instability and preferential degradation of the *apo* form *in vivo* (Matsuda et al., 2004). Furthermore, a combination of structural and kinetic analysis allowed to unveil the mechanism of cofactor binding to the open structure (that exist as a dynamic system of alternative conformations). The entry of PLP into the active site activates an initial conformational change, where the rearrangement of loop1 is likely transmitted from the

active site region to other structural elements leading to the transition into the closed-state (Giardina *et al.*, 2011).

The unexpected structural reorganization observed in human *apo*DDC may also occur in other members of group II decarboxylases, such as GadB.
The active form of the bacterial *E. coli* GadB consists in a homoexamer of 320 kDa (53 kDa per subunit), composed of three functional dimers (Capitani *et al.*, 2003). Dissociation of PLP in certain conditions, i.e. cooling of the purified enzyme in diluted solution, was hypothesized to be related to structural rearrangements (Shukuya & Schwert, 1960). As described in the introduction (1.2.2), electron microscopy investigations of *E. coli* glutamate decarboxylase indicated that the oligomeric state of the enzyme depends on several factors, including temperature, protein concentration, PLP and pH. The hexameric apoenzyme dissociate into the dimers upon increasing of pH above 6, and the dissociation is totally reversible through the addition of the cofactor to the solution (Tikhonenko *et al.*, 1968). The structural features of the apodimers however have not been further investigated.
The goal of this preliminary study was to separate the different oligomeric species. This consisted in isolating dimeric *apo*GadB by gel filtration chromatography at a sufficient level of purity, i.e. no contamination from hexamer or other intermediate oligomers, and to use the apodimers for crystallization experiments and structural-functional analysis.

### 3.3.1 Gel filtration chromatography

Recombinant *E. coli* GadB was purified in the *holo* form, as described by (De Biase *et al.*, 1996) (cfr. 2.5). The *apo* form was prepared from *holo*GadB performing the abortive decarboxylation-transamination (cfr. 1.2.1) of the

substrate analogue α-methyl-glutamate (more prone to the side reaction compared to L-Glu), that leads to the formation of 4-oxo-valerate and pyridoxamine 5'-phosphate (PMP), with consequent inactivation of the enzyme. The reaction was followed spectrophotometrically (De Biase *et al.*, 1991) and PMP was removed by a gel filtration step, in which the protein was eluted in a buffer with an alkaline pH (50 mM HEPPS / 150 mM NaCl pH 8, containing 0.1 mM DTT) (Fig. 3.16). In these conditions (pH > 6) *apo*GadB is expected to dissociate into dimers (cfr. 1.2.2; (Tikhonenko *et al.*, 1968)). In order to separate the dimer from the other oligomeric forms, likely to be present in solution in equilibrium with the dimer, the protein was loaded onto a gel filtration Superdex G200 column and eluted in the same HEPPS buffer at pH 8 (cfr. 2.6.7).

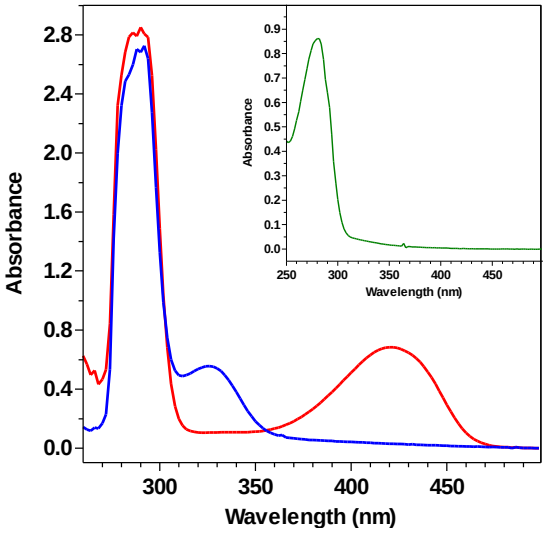


**Figure 3.16.** apo*GadB preparation***.** Absorption spectra of *Ec*GadB (3.6 mg/ml) in 0.2M pyridine/HCl buffer pH 4.6 containing 0.1 mM DTT: before (red, *holo*GadB) and after (blue) incubation with α-methyl-Glu. The 420 nm-absorbing species (ketoenamine) is replaced by the 325 nm-absorbing species, which corresponds to PMP. In the inset, the spectrum of *apo*GadB (10 µM) after gel filtration (PD10) in 50 mM HEPPS buffer / 150 mM NaCl buffer pH 8, containing 0.1 mM DTT.

The chromatogram showed two sharp peaks at 12,9 ml and 14,6 ml (Fig. 3.17): the fastest eluting corresponding to a putative tetramer (229 kDa) and the slowest consistent with a dimer (108 kDa). The dimeric form is prevailing over the putative tetramer (the peak is 1.75 times higher). The minor peak at 9,4 ml is likely the product of protein aggregates. The fractions were analysed spectrophotometrically (no absorbance was recorded in the 300-500 nm region) and those corresponding to the dimer were collected with the aim of analysing this species by crystallography.

To confirm that in these conditions the equilibrium between the dimer and the hexamer depends on PLP-binding, *apo*GadB was reconstituted with an excess of PLP (five times the enzyme concentration) and loaded onto the gel filtration column. The chromatogram was composed of four peaks (Fig. 3.17): the first ($V_e$ = 8.6 ml) can be attributed to protein aggregates, the second corresponds to the hexamer or a combination of hexameric and tetrameric forms (275 kDa), the third corresponds to the dimer (110 kDa), while the last peak corresponds to PLP (that was present in excess in the sample solution). Preliminary data confirmed that at pH > 6 the *holo*GadB eluted as a single peak corresponding to the hexamer (312 kDa, data not shown). The absorption spectra of the fractions showed that PLP was indeed bound to the protein (data not shown). The addition of PLP shifted the equilibrium toward the hexamer formation and the relative ratio between the two peaks was inverted, with the peak corresponding to the 275 kDa species 1.74 times higher than that of the 110 kDa species. The overall result is a relative decrease of the dimeric form of 3 times.

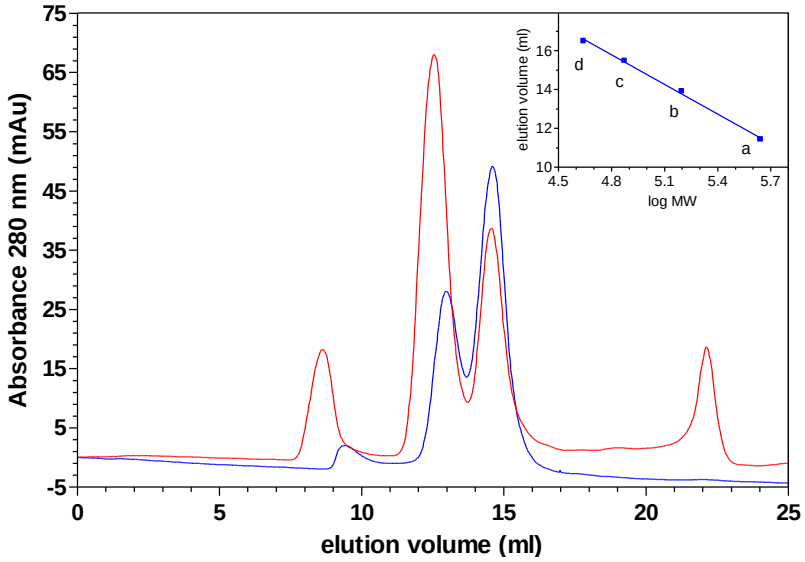


**Figure 3.17.** *Gel filtration cromatography of* apo*GadB at pH 8.0.* Gel filtration analysis was performed in 50 mM HEPPS/ 150 mM NaCl buffer containing 0.1 mM DTT, at a flow rate of 0.5 ml/min, at 4°C. In blue, *apo*GadB (approx. 7 mg). In red *apo*GadB (approx. 7.8 mg) reconstituted 1h 4°C with an excess of PLP. Peaks with $V_e$ = 8-10 ml can be attributed to protein aggregates, while the last peak ($V_e$ = 22.1 ml) corresponds to PLP. Inset: calibration curve. HMW Calibration Kit (GE Healthcare) included ferritin (440 kDa; a), aldolase (158 kDa; b), conalbumin (75 kDa; c), ovalbumin (44 kDa; d).

### 3.3.2 Crystallization and structural analysis

With the aim of analysing the dimeric *apo*GadB by X-ray crystallography, I visited Dr. Guido Capitani's team for two months at the Biomolecular Research Laboratory (BMR) at Paul Scherrer Institut (PSI, Villigen, Switzerland).

Dimeric *apo*GadB isolated by gel filtration chromatography was crystallized using the vapour diffusion sitting drop method (cfr. 2.7.1) at 20°C. Several crystallization trials were set up in order to find the best conditions for crystallization. In parallel, a microseeding experiment was also performed with the purpose of obtaining larger single crystals (cfr. 2.7.1).

Single crystals grew in several conditions within weeks and some of them achieved a sufficient size (25-30 μm; Fig. 3.18) to be tested with X-rays, using the Swiss Light Source at PSI (cfr. 2.7.2). Diffraction data were collected to 3 Å resolution from a crystal obtained in 0.1 M Tris pH 8.5 buffer / 0.3 M sodium acetate, containing 25% w/v PEG 2K MME.

**Figure 3.18.** *Crystal of dimeric apoGad.*

Since several crystallographic structures of *E. coli* GadB are available (Capitani *et al.*, 2003, Gut *et al.*, 2006) we tried to solve the structure employing the molecular replacement method. The neutral-pH form of GadB (1PMO) with the first 56 residues removed (start at Arg57) was used as a model. Although the large domain of *apo*GadB was superimposable with our model, it was not possible to derive an electron density map of the protein. Most likely we have incurred in a difficult case of twinning, a condition that occurs when the crystal is composed of distinct domains whose orientations differ but are related in a particular, precise way (twin law).

### 3.3.3 Discussion

The preliminary study described in this chapter lays the foundation for an in-depth study on the quaternary structure rearrangement and conformational changes within the subunits induced by cofactor dissociation in *E. coli* GadB and more in general on the structural role of PLP in protein folding. Interestingly, the apoenzymatic forms of several decarboxylases (and other

PLP enzymes) are associated with a lower stability (Chen *et al.*, 1998) and preferential degradation of the protein *in vivo* (Matsuda et al., 2004), and might be involved in autoimmunity in humans.

The experimental hypothesis of this work consisted in the assumption that the structure of *E. coli* GadB apodimer may experience a wide conformational rearrangement, similar to that observed in human *apo*DDC (Giardina *et al.*, 2011), leading to a different positioning of entire domains and a global change of the entire protein structure with respect to the simple structure of dimers composing the hexameric holoenzyme.

Gel filtration chromatography turned out to be a suitable method to both discriminate between the multiple oligomeric states of GadB (i.e. hexamer, tetramer and dimer) and to isolate for preparative purpose the dimeric apoenzyme (by performing the separation of the apoform at alkaline pH). The optimization of this part of the work constitutes a prerequisite to perform structural studies on an extra pure sample.

Initial crystallization trials have defined the conditions for a successful protein crystallization. In fact, several diffracting crystals were obtained and diffraction data were collected at a reasonable resolution for detecting large conformational changes. Unfortunately, it was not possible to solve the structure by the molecular replacement method.

The structural analysis of dimeric *apo*GadB will be tackled also using other analytical techniques such as analytical ultracentrifugation, SAXS and multiangled light scattering, which might help if X-ray crystallography will not be successful or to implement the structural information from X-ray analysis.

## 3.4 Conclusions and perspectives

In the present thesis, I performed a detailed biochemical and spectroscopic characterization of a new bacterial Gad (GadB from *B. microti*, namely *Bm*GadB), the first from the genus *Brucella*, and I gave a contribution to the understanding of catalytic and structural aspects of the most investigated *E. coli* GadB.

The first part of this thesis focused on the expression, purification and biochemical characterization of *Bm*GadB, which turned out to share with the *E. coli* homolog the autoinhibition mechanism that involves the formation of a substituted aldamine and the allosteric activation triggered by chloride ions (Gut *et al.*, 2006, Pennacchietti *et al.*, 2009). On the other hand, *Bm*GadB exhibits peculiar features concerning the pH range of activity (more acidic) and the cellular localization (not influenced by pH), that in *E. coli* involves pH-dependent conformational changes of the N-terminal regions (Capitani *et al.*, 2003).

Besides representing the first detailed biochemical study on a bacterial Gad, other than *E. coli* GadB, this work is part of a wider project in collaboration with A. Occhialini (CPBS, CNRS, Montpellier, France) which includes the characterization of the *gadBC* operon in *B. microti* (Occhialini *et al.*, 2012) and in other new *Brucella* species possessing potentially functional GDAR system (i.e. *B. inopinata* BO1, *B. inopinata-like* BO2 and *Brucella sp.* strains isolated from Australian rodents), to determine its relevance in the pathogenesis.

One of the aims of this thesis consisted in the completion of the characterization of a site-directed *Ec*GadB mutant regarding residues His465,

responsible for the reversible inactivation of the enzyme, and Asp86, required for substrate binding. In addition to gain more insight on the role of specific residues in catalysis, this study revealed that GadB-D86NH465A mutant is active in a wider range of pH (up to pH 8), a feature that makes it a good candidate for biotechnological applications. In fact, the Gad enzyme has been proposed to be applicable in industrial production of GABA, an intermediate in the synthesis of various bulk chemicals, by immobilizing *E. coli* GadB in bioreactors (Lammens *et al.*, 2009). The availability of a mutant capable of catalyzing the reaction at pH 7 would allow the Gad-mediated production of GABA also at neutral pH. Further work will concern the stabilization of this and other mutants, since the enzyme tends to lose the cofactor during the catalysis.

Finally, the preliminary structural study on *E. coli apo*GadB, started in this thesis work, has interesting implications in the open issue of PLP-dependent enzymes folding and in the possible involvement of proteins in the *apo* form in autoimmune diseases etiology. Supplementary work is required to optimize the experimental conditions and perform analytical and structural studies on an extra pure sample.

# 4 References


Abe Y, Umemura S, Sugimoto K-i, Hirawa N, Kato Y, Yokoyama N, Yokoyama T, Iwai J & Ishii M (1995) Effect of green tea rich in γ-aminobutyric acid on blood pressure of Dahl salt-sensitive rats. *American Journal of Hypertension* **8**: 74-79.

Accardi A & Miller C (2004) Secondary active transport mediated by a prokaryotic homologue of ClC Cl- channels. *Nature* **427**: 803-807.

Adeghate E & Ponery AS (2002) GABA in the endocrine pancreas: cellular localization and function in normal and diabetic rats. *Tissue and Cell* **34**: 1-6.

Aiso T, Murata M & Gamou S (2011) Transcription of an antisense RNA of a gadE mRNA is regulated by GadE, the central activator of the acid resistance system in Escherichia coli. *Genes Cells* **16**: 670-680.

Akbarian S & Huang H-S (2006) Molecular and cellular mechanisms of altered GAD1/GAD67 expression in schizophrenia and related disorders. *Brain Research Reviews* **52**: 293-304.

Amend JP & Helgeson HC (1997) Solubilities of the common L-a-amino acids as a function of temperature and solution pH. *Pure and Applied Chemistry* **69**: 935-942.

Antoine R & Locht C (1992) Isolation and molecular characterization of a novel broad-host-range plasmid from Bordetella bronchiseptica with sequence similarities to plasmids from gram-positive organisms. *Molecular microbiology* **6**: 1785-1799.

Arafat Y, Fenalti G, Whisstock JC, Mackay IR, Garcia de la Banda M, Rowley MJ & Buckle AM (2009) Structural determinants of GAD antigenicity. *Molecular immunology* **47**: 493-505.

Asada H, Kawamura Y, Maruyama K, Kume H, Ding RG, Kanbara N, Kuzume H, Sanbo M, Yagi T & Obata K (1997) Cleft palate and decreased brain gamma-aminobutyric acid in mice lacking the 67-kDa isoform of glutamic acid decarboxylase. *Proceedings of the National Academy of Sciences of the United States of America* **94**: 6496-6499.

Asada H, Kawamura Y, Maruyama K, *et al.* (1996) Mice lacking the 65 kDa isoform of glutamic acid decarboxylase (GAD65) maintain normal levels of GAD67 and GABA in their brains but are susceptible to seizures. *Biochemical and biophysical research communications* **229**: 891-895.

Audic S, Lescot M, Claverie JM & Scholz HC (2009) Brucella microti: the genome sequence of an emerging pathogen. *BMC genomics* **10**: 352.

Ausubel FM, Brent R, Kingston RE, Moore DD, Seidman JG, Smith JA & Struhl K (1987) *Current Protocols in Molecular Biology* John Wiley & Sons, New York.

Battaglioli G, Liu H & Martin DL (2003) Kinetic differences between the isoforms of glutamate decarboxylase: implications for the regulation of GABA synthesis. *Journal of Neurochemistry* **86**: 879-887.

Baum G, Lev-Yadun S, Fridmann Y, Arazi T, Katsnelson H, Zik M & Fromm H (1996) Calmodulin binding to glutamate decarboxylase is required for regulation of glutamate and GABA metabolism and normal development in plants. *The EMBO journal* **15**: 2988-2996.

Bertoldi M, Gonsalvi M, Contestabile R & Voltattorni CB (2002) Mutation of tyrosine 332 to phenylalanine converts dopa decarboxylase into a decarboxylation-dependent oxidative deaminase. *The Journal of biological chemistry* **277**: 36357-36362.

Bhagwat AA & Bhagwat M (2004) Comparative analysis of transcriptional regulatory elements of glutamate-dependent acid-resistance systems of Shigella flexneri and Escherichia coli O157:H7. *FEMS microbiology letters* **234**: 139-147.

Blindermann JM, Maitre M, Ossola L & Mandel P (1978) Purification and some properties of L-glutamate decarboxylase from human brain. *European journal of biochemistry / FEBS* **86**: 143-152.

Blow D (2002) *Outline of Crystallography for Biologist*. Oxford University Press.

Bordi C, Theraulaz L, Mejean V & Jourlin-Castelli C (2003) Anticipating an alkaline stress through the Tor phosphorelay system in Escherichia coli. *Molecular microbiology* **48**: 211-223.

Bouche N & Fromm H (2004) GABA in plants: just a metabolite? *Trends in plant science* **9**: 110-115.

Bouche N, Fait A, Zik M & Fromm H (2004) The root-specific glutamate decarboxylase (GAD1) is essential for sustaining GABA levels in Arabidopsis. *Plant molecular biology* **55**: 315-325.

Bown AW, Macgregor KB & Shelp BJ (2006) Gamma-aminobutyrate: defense against invertebrate pests? *Trends in plant science* **11**: 424-427.

Bradford MM (1976) A rapid and sensitive method for the quantitation of microgram quantities of protein utilizing the principle of protein-dye binding. *Analytical Biochemistry* **72**: 248-254.

Burton NA, Johnson MD, Antczak P, Robinson A & Lund PA (2010) Novel aspects of the acid response network of E. coli K-12 are revealed by a study of transcriptional dynamics. *Journal of molecular biology* **401**: 726-742.

Capitani G, De Biase D, Aurizi C, Gut H, Bossa F & Grutter MG (2003) Crystal structure and functional analysis of Escherichia coli glutamate decarboxylase. *The EMBO journal* **22**: 4027-4037.

Castanie-Cornet MP & Foster JW (2001) Escherichia coli acid resistance: cAMP receptor protein and a 20 bp cis-acting sequence control pH and stationary phase expression of the gadA and gadBC glutamate decarboxylase genes. *Microbiology (Reading, England)* **147**: 709-715.

Castanie-Cornet MP, Penfound TA, Smith D, Elliott JF & Foster JW (1999) Control of acid resistance in Escherichia coli. *Journal of bacteriology* **181**: 3525-3535.

Castanie-Cornet MP, Treffandier H, Francez-Charlot A, Gutierrez C & Cam K (2007) The glutamate-dependent acid resistance system in Escherichia coli: essential and dual role of the His-Asp phosphorelay RcsCDB/AF. *Microbiology (Reading, England)* **153**: 238-246.

Castanie-Cornet MP, Cam K, Bastiat B, Cros A, Bordes P & Gutierrez C (2010) Acid stress response in Escherichia coli: mechanism of regulation of gadA transcription by RcsB and GadE. *Nucleic acids research* **38**: 3546-3554.

Chen C-H, Wu SJ & Martin DL (1998) Structural Characteristics of Brain Glutamate Decarboxylase in Relation to Its Interaction and Activation. *Archives of Biochemistry and Biophysics* **349**: 175-182.

Cho HH, Jeon JW, Lee MH, Lee SH & Kwon ST (2011) Structure and physical properties of variously drawn nylon 6- ran-nylon 4 copolymer fibers. . *Text Sci Eng* **48**: 150-155.

Christgau S, Aanstoot HJ, Schierbeck H, Begley K, Tullin S, Hejnaes K & Baekkeskov S (1992) Membrane anchoring of the autoantigen GAD65 to microvesicles in pancreatic beta-cells by palmitoylation in the NH2-terminal domain. *The Journal of Cell Biology* **118**: 309-320.

Chu WC & Metzler DE (1994) Enzymatically active truncated cat brain glutamate decarboxylase: expression, purification, and absorption spectrum. *Archives of biochemistry and biophysics* **313**: 287-295.

Coleman ST, Fang TK, Rovinsky SA, Turano FJ & Moye-Rowley WS (2001) Expression of a glutamate decarboxylase homologue is required for normal oxidative stress tolerance in Saccharomyces cerevisiae. *The Journal of biological chemistry* **276**: 244-250.

Cornish-Bowden A (1995) Fundamentals of Enzyme Kinetics. p.^pp. Portland Press Ltd, London.

Cotter PD, Gahan CG & Hill C (2001) A glutamate decarboxylase system protects Listeria monocytogenes in gastric fluid. *Molecular microbiology* **40**: 465-475.

Cozzani I, Misuri A & Santoni C (1970) Purification and general properties of glutamate decarboxylase from Clostridium perfringens. *The Biochemical journal* **118**: 135-141.

D'Arcy A, Villard F & Marsh M (2007) An automated microseed matrix-screening method for protein crystallization. *Acta crystallographica Section D, Biological crystallography* **63**: 550-554.

De Biase D & Pennacchietti E (2012) Glutamate decarboxylase-dependent acid resistance in orally acquired bacteria: function, distribution and biomedical implications of the gadBC operon. *Molecular microbiology* **86**: 770-768.

De Biase D & Pennacchietti E (2012) Glutamate decarboxylase-dependent acid resistance in orally acquired bacteria: function, distribution and biomedical implications of the gadBC operon. *Molecular microbiology*.

De Biase D, Maras B & John RA (1991) A chromophore in glutamate decarboxylase has been wrongly identified as PQQ. *FEBS letters* **278**: 120-122.

De Biase D, Tramonti A, John RA & Bossa F (1996) Isolation, overexpression, and biochemical characterization of the two isoforms of glutamic acid decarboxylase from Escherichia coli. *Protein expression and purification* **8**: 430-438.

De Biase D, Tramonti A, Bossa F & Visca P (1999) The response to stationary-phase stress conditions in Escherichia coli: role and regulation of the glutamic acid decarboxylase system. *Molecular microbiology* **32**: 1198-1211.

Denner LA, Wei SC, Lin HS, Lin CT & Wu JY (1987) Brain L-glutamate decarboxylase: purification and subunit structure. *Proceedings of the National Academy of Sciences of the United States of America* **84**: 668-672.

Di Cagno R, Mazzacane F, Rizzello CG, De Angelis M, Giuliani G, Meloni M, De Servi B & Gobbetti M (2010) Synthesis of gamma-aminobutyric acid (GABA) by Lactobacillus plantarum DSM19463: functional grape must beverage and dermatological applications. *Applied microbiology and biotechnology* **86**: 731-741.

Dirkx R, Jr., Thomas A, Li L, Lernmark A, Sherwin RS, De Camilli P & Solimena M (1995) Targeting of the 67-kDa isoform of glutamic acid decarboxylase to intracellular organelles is mediated by its interaction with the NH2-terminal region of the 65-kDa isoform of glutamic acid decarboxylase. *The Journal of biological chemistry* **270**: 2241-2246.

Dutyshev DI, Darii EL, Fomenkova NP, Pechik IV, Polyakov KM, Nikonov SV, Andreeva NS & Sukhareva BS (2005) Structure of Escherichia coli glutamate decarboxylase (GADalpha) in complex with glutarate at 2.05 angstroms resolution. *Acta crystallographica* **61**: 230-235.

Elzer PH, Kovach ME, Phillips RW, Robertson GT, Peterson KM & Roop Ii RM (1995) In Vivo and in Vitro Stability of the Broad-Host-Range Cloning Vector pBBR1MCS in Six Brucella Species. *Plasmid* **33**: 51-57.

Esclapez M, Tillakaratne NJ, Kaufman DL, Tobin AJ & Houser CR (1994) Comparative localization of two forms of glutamic acid decarboxylase and their mRNAs in rat brain supports the concept of functional differences between the forms. *The Journal of neuroscience : the official journal of the Society for Neuroscience* **14**: 1834-1855.

Fagiolini M, Fritschy JM, Low K, Mohler H, Rudolph U & Hensch TK (2004) Specific GABAA circuits for visual cortical plasticity. *Science* **303**: 1681-1683.

Fang Y, Kolmakova-Partensky L & Miller C (2007) A bacterial arginine-agmatine exchange transporter involved in extreme acid resistance. *The Journal of biological chemistry* **282**: 176-182.

Fang Y, Jayaram H, Shane T, Kolmakova-Partensky L, Wu F, Williams C, Xiong Y & Miller C (2009) Structure of a prokaryotic virtual proton pump at 3.2 A resolution. *Nature* **460**: 1040-1043.

Fenalti G & Buckle AM (2010) Structural biology of the GAD autoantigen. *Autoimmunity reviews* **9**: 148-152.

Fenalti G, Law RH, Buckle AM, *et al.* (2007) GABA production by glutamic acid decarboxylase is regulated by a dynamic catalytic loop. *Nature structural & molecular biology* **14**: 280-286.

Flint HJ, Bayer EA, Rincon MT, Lamed R & White BA (2008) Polysaccharide utilization by gut bacteria: potential for new insights from genomic analysis. *Nature reviews* **6**: 121-131.

Foit L, George JS, Zhang BW, Brooks CL, 3rd & Bardwell JC (2013) Chaperone activation by unfolding. *Proceedings of the National Academy of Sciences of the United States of America* **110**: E1254-1262.

Fonda M (1972) Glutamate decarboxylase. Substrate specificity and inhibition by carboxylic acids. *Biochemistry* **11**: 1304-1309.

Fonda ML (1972) Glutamate decarboxylase. Substrate specificity and inhibition by carboxylic acids. *Biochemistry* **11**: 1304-1309.

Foster JW (2001) Acid stress responses of Salmonella and E. coli: survival mechanisms, regulation, and implications for pathogenesis. *JOURNAL OF MICROBIOLOGY-SEOUL-* **39**: 89-94.

Foster JW (2004) Escherichia coli acid resistance: tales of an amateur acidophile. *Nature reviews* **2**: 898-907.

Franco MP, Mulder M, Gilman RH & Smits HL (2007) Human brucellosis. *The Lancet infectious diseases* **7**: 775-786.

Gao X, Lu F, Zhou L, Dang S, Sun L, Li X, Wang J & Shi Y (2009) Structure and Mechanism of an Amino Acid Antiporter. *Science* **324**: 1565-1568.

Ge S, Goh ELK, Sailor KA, Kitabatake Y, Ming G-l & Song H (2006) GABA regulates synaptic integration of newly generated neurons in the adult brain. *Nature* **439**: 589-593.

Giangrossi M, Zattoni S, Tramonti A, De Biase D & Falconi M (2005) Antagonistic role of H-NS and GadX in the regulation of the glutamate decarboxylase-dependent acid resistance system in Escherichia coli. *The Journal of biological chemistry* **280**: 21498-21505.

Giannella RA, Broitman SA & Zamcheck N (1972) Gastric acid barrier to ingested microorganisms in man: studies in vivo and in vitro. *Gut* **13**: 251-256.

Giardina G, Montioli R, Gianni S, Cellini B, Paiardini A, Voltattorni CB & Cutruzzola F (2011) Open conformation of human DOPA decarboxylase reveals the mechanism of PLP addition to Group II decarboxylases. *Proceedings of the National Academy of Sciences of the United States of America* **108**: 20514-20519.

Gillespie JJ, Wattam AR, Cammer SA, *et al.* (2011) PATRIC: the comprehensive bacterial bioinformatics resource with a focus on human pathogenic species. *Infection and immunity* **79**: 4286-4298.

Gobbetti M, Cagno RD & De Angelis M (2010) Functional microorganisms for functional food quality. *Critical reviews in food science and nutrition* **50**: 716-727.

Gong S, Richard H & Foster JW (2003) YjdE (AdiC) is the arginine:agmatine antiporter essential for arginine-dependent acid resistance in Escherichia coli. *Journal of bacteriology* **185**: 4402-4409.

Gong S, Ma Z & Foster JW (2004) The Era-like GTPase TrmE conditionally activates gadE and glutamate-dependent acid resistance in Escherichia coli. *Molecular microbiology* **54**: 948-961.

Gottlieb DI, Chang YC & Schwob JE (1986) Monoclonal antibodies to glutamic acid decarboxylase. *Proceedings of the National Academy of Sciences of the United States of America* **83**: 8808-8812.

Gut H, Pennacchietti E, John RA, Bossa F, Capitani G, De Biase D & Grutter MG (2006) Escherichia coli acid resistance: pH-sensing, activation by chloride and autoinhibition in GadB. *The EMBO journal* **25**: 2643-2651.

Gut H, Dominici P, Pilati S, Astegno A, Petoukhov MV, Svergun DI, Grutter MG & Capitani G (2009) A common structural basis for pH- and calmodulin-mediated regulation in plant glutamate decarboxylase. *Journal of molecular biology* **392**: 334-351.

Han D, Kim HY, Lee HJ, Shim I & Hahm DH (2007) Wound healing activity of gamma-aminobutyric Acid (GABA) in rats. *Journal of microbiology and biotechnology* **17**: 1661-1669.

Hao R & Schmit JC (1993) Cloning of the gene for glutamate decarboxylase and its expression during conidiation in Neurospora crassa. *The Biochemical journal* **293 ( Pt 3)**: 735-738.

Hayakawa K, Kimura M, Kasaha K, Matsumoto K, Sansawa H & Yamori Y (2004) Effect of a gamma-aminobutyric acid-enriched dairy product on the blood pressure of spontaneously hypertensive and normotensive Wistar-Kyoto rats. *The British journal of nutrition* **92**: 411-417.

Hayes ET, Wilks JC, Sanfilippo P, Yohannes E, Tate DP, Jones BD, Radmacher MD, BonDurant SS & Slonczewski JL (2006) Oxygen limitation modulates pH

regulation of catabolism and hydrogenases, multidrug transporters, and envelope composition in Escherichia coli K-12. *BMC microbiology* **6**: 89.

Hiraga K, Ueno Y & Oda K (2008) Glutamate decarboxylase from Lactobacillus brevis: activation by ammonium sulfate. *Biosci Biotechnol Biochem* **72**: 1299-1306.

Ho NAT, Hou CY, Kim WH & Kang TJ (2013) Expanding the active pH range of Escherichia coli glutamate decarboxylase by breaking the cooperativeness. *J Biosci Bioeng* **115**: 154-158.

Hommais F, Krin E, Coppee JY, Lacroix C, Yeramian E, Danchin A & Bertin P (2004) GadE (YhiE): a novel activator involved in the response to acid environment in Escherichia coli. *Microbiology (Reading, England)* **150**: 61-72.

Hommais F, Krin E, Laurent-Winter C, Soutourina O, Malpertuy A, Le Caer JP, Danchin A & Bertin P (2001) Large-scale monitoring of pleiotropic regulation of gene expression by the prokaryotic nucleoid-associated protein, H-NS. *Molecular microbiology* **40**: 20-36.

Hong W, Wu YE, Fu X & Chang Z (2012) Chaperone-dependent mechanisms for acid resistance in enteric bacteria. *Trends in microbiology* **20**: 328-335.

Hong W, Jiao W, Hu J, Zhang J, Liu C, Fu X, Shen D, Xia B & Chang Z (2005) Periplasmic protein HdeA exhibits chaperone-like activity exclusively within stomach pH range by transforming into disordered conformation. *The Journal of biological chemistry* **280**: 27029-27034.

Honnorat J, Saiz A, Giometto B & et al. (2001) Cerebellar ataxia with anti–glutamic acid decarboxylase antibodies: Study of 14 patients. *Archives of Neurology* **58**: 225-230.

Inoue Y, Ishii K, Miyazaki M & Ueno H (2008) Purification of L-glutamate decarboxylase from monkey brain. *Bioscience, biotechnology, and biochemistry* **72**: 2269-2276.

Ito K, Tanaka K, Nishibe Y, Hasegawa J & Ueno H (2007) GABA-synthesizing enzyme, GAD67, from dermal fibroblasts: Evidence for a new skin function. *Biochimica et Biophysica Acta (BBA) - General Subjects* **1770**: 291-296.

Itou J, Eguchi Y & Utsumi R (2009) Molecular mechanism of transcriptional cascade initiated by the EvgS/EvgA system in Escherichia coli K-12. *Bioscience, biotechnology, and biochemistry* **73**: 870-878.

Jansonius JN (1998) Structure, evolution and action of vitamin B6-dependent enzymes. *Current opinion in structural biology* **8**: 759-769.

Jimenez de Bagues MP, Ouahrani-Bettache S, Quintana JF, *et al.* (2010) The new species Brucella microti replicates in macrophages and causes death in murine models of infection. *The Journal of infectious diseases* **202**: 3-10.

Kang TJ, Ho NA & Pack SP (2013) Buffer-free production of gamma-aminobutyric acid using an engineered glutamate decarboxylase from Escherichia coli. *Enzyme and microbial technology* **53**: 200-205.

Kanjee U & Houry WA (2013) Mechanisms of acid resistance in Escherichia coli. *Annual review of microbiology* **67**: 65-81.

Kanjee U & Houry WA (2013) Mechanisms of Acid Resistance in Escherichia coli. *Annual review of microbiology*.

Kash SF, Tecott LH, Hodge C & Baekkeskov S (1999) Increased anxiety and altered responses to anxiolytics in mice deficient in the 65-kDa isoform of glutamic acid decarboxylase. *Proceedings of the National Academy of Sciences* **96**: 1698-1703.

Kash SF, Johnson RS, Tecott LH, Noebels JL, Mayfield RD, Hanahan D & Baekkeskov S (1997) Epilepsy in mice deficient in the 65-kDa isoform of glutamic acid decarboxylase. *Proceedings of the National Academy of Sciences* **94**: 14060-14065.

Kern R, Malki A, Abdallah J, Tagourti J & Richarme G (2007) Escherichia coli HdeB is an acid stress chaperone. *Journal of bacteriology* **189**: 603-610.

Kim HW, Kashima Y, Ishikawa K & Yamano N (2009) Purification and characterization of the first archaeal glutamate decarboxylase from Pyrococcus horikoshii. *Bioscience, biotechnology, and biochemistry* **73**: 224-227.

Kobayashi A, Hirakawa H, Hirata T, Nishino K & Yamaguchi A (2006) Growth phase-dependent expression of drug exporters in Escherichia coli and its contribution to drug tolerance. *Journal of bacteriology* **188**: 5693-5703.

Komatsuzaki N, Nakamura T, Kimura T & Shima J (2008) Characterization of glutamate decarboxylase from a high gamma-aminobutyric acid (GABA)-producer, Lactobacillus paracasei. *Bioscience, biotechnology, and biochemistry* **72**: 278-285.

Kovach ME, Phillips RW, Elzer PH, Roop RM, 2nd & Peterson KM (1994) pBBR1MCS: a broad-host-range cloning vector. *BioTechniques* **16**: 800-802.

Kowalczyk L, Ratera M, Paladino A, *et al.* (2011) Molecular basis of substrate-induced permeation by an amino acid antiporter. *Proceedings of the National Academy of Sciences* **108**: 3935-3940.

Krulwich TA, Sachs G & Padan E (2011) Molecular aspects of bacterial pH sensing and homeostasis. *Nature reviews* **9**: 330-343.

Laemmli UK (1970) Cleavage of structural proteins during the assembly of the head of bacteriophage T4. *Nature* **227**: 680-685.

Lakowicz JR (1983) *Principles of fluorescence spectroscopy*. Plenum Press, NY.

Lammens TM, Franssen MCR, Scott EL & Sanders JPM (2010) Synthesis of biobased N-methylpyrrolidone by one-pot cyclization and methylation of [gamma]-aminobutyric acid. *Green Chemistry* **12**: 1430-1436.

Lammens TM, Potting J, Sanders JP & De Boer IJ (2011) Environmental comparison of biobased chemicals from glutamic acid with their petrochemical equivalents. *Environmental science & technology* **45**: 8521-8528.

Lammens TM, Franssen MCR, Scott EL & Sanders JPM (2012) Availability of protein-derived amino acids as feedstock for the production of bio-based chemicals. *Biomass and Bioenergy* **44**: 168-181.

Lammens TM, De Biase D, Franssen MCR, Scott EL & Sanders JPM (2009) The application of glutamic acid alpha-decarboxylase for the valorization of glutamic acid. *Green Chemistry* **11**: 1562-1567.

Langendorf CG, Tuck KL, Key TL, Fenalti G, Pike RN, Rosado CJ, Wong AS, Buckle AM, Law RH & Whisstock JC (2013) Structural characterization of the mechanism through which human glutamic acid decarboxylase auto-activates. *Bioscience reports* **33**: 137-144.

Lanoue AC, Dumitriu A, Myers RH & Soghomonian J-J (2010) Decreased glutamic acid decarboxylase mRNA expression in prefrontal cortex in Parkinson's disease. *Experimental Neurology* **226**: 207-217.

Le Vo TD, Kim TW & Hong SH (2011) Effects of glutamate decarboxylase and gamma-aminobutyric acid (GABA) transporter on the bioconversion of GABA in engineered Escherichia coli. *Bioprocess Biosyst Eng.*

Lee E-S, Kim H-W, Kim D-E, Kim Y-H, Nam S-W, Kim B-W & Jeon S-J (2013) Gene expression and characterization of thermostable glutamate decarboxylase from Pyrococcus furiosus. *Biotechnology and Bioprocess Engineering* **18**: 375-381.

Lee S, Ahn J, Kim YG, Jung JK, Lee H & Lee EG (2013) Gamma-aminobutyric Acid production using immobilized glutamate decarboxylase followed by downstream processing with cation exchange chromatography. *Int J Mol Sci* **14**: 1728-1739.

Lernmark Å (1996) Glutamic Acid Decarboxylase – Gene to Antigen to Disease. *Journal of Internal Medicine* **240**: 259-277.

Lin J, Lee IS, Frey J, Slonczewski JL & Foster JW (1995) Comparative analysis of extreme acid survival in Salmonella typhimurium, Shigella flexneri, and Escherichia coli. *Journal of bacteriology* **177**: 4097-4104.

Lin J, Smith MP, Chapin KC, Baik HS, Bennett GN & Foster JW (1996) Mechanisms of acid resistance in enterohemorrhagic Escherichia coli. *Appl Environ Microbiol* **62**: 3094-3100.

Lu P, Ma D, Chen Y, Guo Y, Chen GQ, Deng H & Shi Y (2013) L-glutamine provides acid resistance for Escherichia coli through enzymatic release of ammonia. *Cell research* **23**: 635-644.

Ma D, Lu P & Shi Y (2013) Substrate selectivity of the acid-activated glutamate/gamma-aminobutyric acid (GABA) antiporter GadC from Escherichia coli. *The Journal of biological chemistry* **288**: 15148-15153.

Ma D, Lu P, Yan C, Fan C, Yin P, Wang J & Shi Y (2012) Structure and mechanism of a glutamate-GABA antiporter. *Nature* **483**: 632-636.

Ma Z, Masuda N & Foster JW (2004) Characterization of EvgAS-YdeO-GadE branched regulatory circuit governing glutamate-dependent acid resistance in Escherichia coli. *Journal of bacteriology* **186**: 7378-7389.

Ma Z, Gong S, Richard H, Tucker DL, Conway T & Foster JW (2003) GadE (YhiE) activates glutamate decarboxylase-dependent acid resistance in Escherichia coli K-12. *Molecular microbiology* **49**: 1309-1320.

Manoil C & Beckwith J (1985) TnphoA: a transposon probe for protein export signals. *Proceedings of the National Academy of Sciences* **82**: 8129-8133.

Masuda N & Church GM (2002) Escherichia coli gene expression responsive to levels of the response regulator EvgA. *Journal of bacteriology* **184**: 6225-6234.

Mates AK, Sayed AK & Foster JW (2007) Products of the Escherichia coli acid fitness island attenuate metabolite stress at extremely low pH and mediate a cell density-dependent acid resistance. *Journal of bacteriology* **189**: 2759-2768.

Matsuda N, Hayashi H, Miyatake S, Kuroiwa T & Kagamiyama H (2004) Instability of the apo form of aromatic L-amino acid decarboxylase in vivo and in vitro: implications for the involvement of the flexible loop that covers the active site. *Journal of biochemistry* **135**: 33-42.

Matsumoto T, Yamaura I & Funatsu M (1986) Purification and Properties of Glutamate Decarboxylase from Squash(Biological Chemistry). *Agricultural and biological chemistry* **50**: 1413-1417.

Merrell DS & Camilli A (2002) Acid tolerance of gastrointestinal pathogens. *Current opinion in microbiology* **5**: 51-55.

Momany C, Ghosh R & Hackert ML (1995) Structural motifs for pyridoxal-5'-phosphate binding in decarboxylases: an analysis based on the crystal structure of the Lactobacillus 30a ornithine decarboxylase. *Protein Sci* **4**: 849-854.

Nakatsu Y, Tyndale RF, DeLorey TM, *et al.* (1993) A cluster of three GABAA receptor subunit genes is deleted in a neurological mutant of the mouse p locus. *Nature* **364**: 448-450.

Nishino K, Senda Y & Yamaguchi A (2008) The AraC-family regulator GadX enhances multidrug resistance in Escherichia coli by activating expression of mdtEF multidrug efflux genes. *Journal of infection and chemotherapy : official journal of the Japan Society of Chemotherapy* **14**: 23-29.

Nomura M, Kimoto H, Someya Y, Furukawa S & Suzuki I (1998) Production of γ-Aminobutyric Acid By Cheese Starters During Cheese Ripening. *Journal of Dairy Science* **81**: 1486-1491.

Nomura M, Nakajima I, Fujita Y, Kobayashi M, Kimoto H, Suzuki I & Aso H (1999) Lactococcus lactis contains only one glutamate decarboxylase gene. *Microbiology (Reading, England)* **145 ( Pt 6)**: 1375-1380.

O'Leary MH & Brummund W, Jr. (1974) pH jump studies of glutamate decarboxylase. Evidence for a pH-dependent conformation change. *The Journal of biological chemistry* **249**: 3737-3745.

O'Leary MH, Yamada H & Yapp CJ (1981) Multiple isotope effect probes of glutamate decarboxylase. *Biochemistry* **20**: 1476-1481.

Occhialini A, Jimenez de Bagues MP, Saadeh B, Bastianelli D, Hanna N, De Biase D & Kohler S (2012) The glutamic acid decarboxylase system of the new species Brucella microti contributes to its acid resistance and to oral infection of mice. *The Journal of infectious diseases* **206**: 1424-1432.

Oh SH & Oh CH (2003) Brown rice extract with enhanced levels of GABA stimulate immune cells. *Food Sci Biotechnol* **12**: 248-252.

Oh SH, Soh JR & Cha YS (2003) Germinated brown rice extract shows a nutraceutical effect in the recovery of chronic alcohol-related symptoms. *Journal of medicinal food* **6**: 115-121.

Okada T, Sugishita T, Murakami T & Murai H (2000) Effect of the defatted rice germ enriched with GABA for sleeplessness, depression, autonomic disorder by oral administration *Nippon Shokuhin Kagaku Kaishi* **47**: 596-603.

Opdyke JA, Kang JG & Storz G (2004) GadY, a small-RNA regulator of acid response genes in Escherichia coli. *Journal of bacteriology* **186**: 6698-6705.

Park H, Ahn J, Lee J, Lee H, Kim C, Jung JK & Lee EG (2012) Expression, immobilization and enzymatic properties of glutamate decarboxylase fused to a cellulose-binding domain. *Int J Mol Sci* **13**: 358-368.

Park K-B & Oh S-H (2007) Production of yogurt with enhanced levels of gamma-aminobutyric acid and valuable nutrients using lactic acid bacteria and germinated soybean extract. *Bioresource technology* **98**: 1675-1679.

Park KB & Oh SH (2006) Enhancement of gamma-aminobutyric acid production in Chungkukjang by applying a Bacillus subtilis strain expressing glutamate decarboxylase from Lactobacillus brevis. *Biotechnol Lett* **28**: 1459-1463.

Park KB & Oh SH (2007) Cloning, sequencing and expression of a novel glutamate decarboxylase gene from a newly isolated lactic acid bacterium, Lactobacillus brevis OPK-3. *Bioresource technology* **98**: 312-319.

Park KB, Ji GE, Park MS & Oh SH (2005) Expression of rice glutamate decarboxylase in Bifidobacterium longum enhances gamma-aminobutyric acid production. *Biotechnol Lett* **27**: 1681-1684.

Park SJ, Kim EY, Noh W, Oh YH, Kim HY, Song BK, Cho KM, Hong SH, Lee SH & Jegal J (2013) Synthesis of nylon 4 from gamma-aminobutyrate (GABA) produced by recombinant Escherichia coli. *Bioprocess Biosyst Eng* **36**: 885-892.

Peltola J, Kulmala P, Isojarvi J, Saiz A, Latvala K, Palmio J, Savola K, Knip M, Keranen T & Graus F (2000) Autoantibodies to glutamic acid decarboxylase in patients with therapy-resistant epilepsy. *Neurology* **55**: 46-50.

Pennacchietti E, Lammens TM, Capitani G, Franssen MC, John RA, Bossa F & De Biase D (2009) Mutation of His465 alters the pH-dependent spectroscopic properties of Escherichia coli glutamate decarboxylase and broadens the range of its activity toward more alkaline pH. *The Journal of biological chemistry* **284**: 31587-31596.

Peterson EA & Sober HA (1954) Preparation of crystaline phosphorilated derivatives of vitamin B6. *Journal of American Chemical Society* **76**: 169-175.

Pflugrath JW (2004) Macromolecular cryocrystallography--methods for cooling and mounting protein crystals at cryogenic temperatures. *Methods (San Diego, Calif)* **34**: 415-423.

Porter TG, Spink DC, Martin SB & Martin DL (1985) Transaminations catalysed by brain glutamate decarboxylase. *Biochem J* **231**: 705-712.

Ramirez-Montealegre D, Chattopadhyay S, Curran TM, *et al.* (2005) Autoimmunity to glutamic acid decarboxylase in the neurodegenerative disorder Batten disease. *Neurology* **64**: 743-745.

Rice EW, Johnson CH, Dunnigan ME & Reasoner DJ (1993) Rapid glutamate decarboxylase assay for detection of Escherichia coli. *Applied and environmental microbiology* **59**: 4347-4349.

Richard H & Foster JW (2004) Escherichia coli glutamate- and arginine-dependent acid resistance systems increase internal pH and reverse transmembrane potential. *Journal of bacteriology* **186**: 6032-6041.

Roberfroid MB (1999) What is beneficial for health? The concept of functional food. *Food and chemical toxicology : an international journal published for the British Industrial Biological Research Association* **37**: 1039-1041.

Rorsman P, Berggren P-O, Bokvist K, Ericson H, Mohler H, Ostenson C-G & Smith PA (1989) Glucose-inhibition of glucagon secretion involves activation of GABAA-receptor chloride channels. *Nature* **341**: 233-236.

Rupp B (2009) *Biomolecular Crystallography: Principles Practice and Application to Structural*. Garland Science.

Sambrook J, Fritsch EF & Maniatis T (1989) *Molecular Cloning: A Laboratory Manual*. Cold Spring Harbor Laboratory Press, Cold Spring Harbor, NY.

Sanders JW, Leenhouts K, Burghoorn J, Brands JR, Venema G & Kok J (1998) A chloride-inducible acid resistance mechanism in Lactococcus lactis and its regulation. *Molecular microbiology* **27**: 299-310.

Sandmeier E, Hale TI & Christen P (1994) Multiple evolutionary origin of pyridoxal-5'-phosphate-dependent amino acid decarboxylases. *European journal of biochemistry / FEBS* **221**: 997-1002.

Sayed AK, Odom C & Foster JW (2007) The Escherichia coli AraC-family regulators GadX and GadW activate gadE, the central activator of glutamate-dependent acid resistance. *Microbiology (Reading, England)* **153**: 2584-2592.

Scholz HC, Hofer E, Vergnaud G, Le Fleche P, Whatmore AM, Al Dahouk S, Pfeffer M, Kruger M, Cloeckaert A & Tomaso H (2009) Isolation of Brucella microti from mandibular lymph nodes of red foxes, Vulpes vulpes, in lower Austria. *Vector borne and zoonotic diseases* **9**: 153-156.

Scholz HC, Hubalek Z, Nesvadbova J, *et al.* (2008) Isolation of Brucella microti from soil. *Emerging infectious diseases* **14**: 1316-1317.

Scholz HC, Hubalek Z, Sedlacek I, *et al.* (2008) Brucella microti sp. nov., isolated from the common vole Microtus arvalis. *International journal of systematic and evolutionary microbiology* **58**: 375-382.

Scott E, Peter F & Sanders J (2007) Biomass in the manufacture of industrial products—the use of proteins and amino acids. *Applied microbiology and biotechnology* **75**: 751-762.

Se-Hee Kim B-HS, Yeon-Hee Kim, Soo-Wan Nam and Sung-Jong Jeon (2007) Cloning and Expression of a full-lenght Glutamate decarboxylase Gene from *Lactobicillus brevis* BH12. *Biotechnology and Bioprocess Engineering* **12**: 707-712.

Shah MS, Siddique IH & Dalvi RR (1981) Studies on glutamic acid decarboxylase from Listeria monocytogenes. *Canadian journal of comparative medicine Revue canadienne de medecine comparee* **45**: 196-198.

Shukuya R & Schwert GW (1960) Glutamic acid decarboxylase. III. The inactivation of the enzyme at low temperatures. *The Journal of biological chemistry* **235**: 1658-1661.

Shukuya R & Schwert GW (1960) Glutamic acid decarboxylase. I. Isolation procedures and properties of the enzyme. *The Journal of biological chemistry* **235**: 1649-1652.

Shukuya R & Schwert GW (1960) Glutamic acid decarboxylase. II. The spectrum of the enzyme. *The Journal of biological chemistry* **235**: 1653-1657.

Siragusa S, De Angelis M, Di Cagno R, Rizzello CG, Coda R & Gobbetti M (2007) Synthesis of gamma-aminobutyric acid by lactic acid bacteria isolated from a variety of Italian cheeses. *Applied and environmental microbiology* **73**: 7283-7290.

Slonczewski JL, Rosen BP, Alger JR & Macnab RM (1981) pH homeostasis in Escherichia coli: measurement by 31P nuclear magnetic resonance of

methylphosphonate and phosphate. *Proceedings of the National Academy of Sciences of the United States of America* **78**: 6271-6275.

Slonczewski JL, Fujisawa M, Dopson M & Krulwich TA (2009) Cytoplasmic pH measurement and homeostasis in bacteria and archaea. *Advances in microbial physiology* **55**: 1-79, 317.

Snedden WA, Arazi T, Fromm H & Shelp BJ (1995) Calcium/Calmodulin Activation of Soybean Glutamate Decarboxylase. *Plant physiology* **108**: 543-549.

Snedden WA, Koutsia N, Baum G & Fromm H (1996) Activation of a recombinant petunia glutamate decarboxylase by calcium/calmodulin or by a monoclonal antibody which recognizes the calmodulin binding domain. *The Journal of biological chemistry* **271**: 4148-4153.

Soghomonian JJ & Martin DL (1998) Two isoforms of glutamate decarboxylase: why? *Trends in pharmacological sciences* **19**: 500-505.

Solimena M, Folli F, Aparisi R, Pozza G & De Camilli P (1990) Autoantibodies to GABA-ergic neurons and pancreatic beta cells in stiff-man syndrome. *The New England journal of medicine* **322**: 1555-1560.

Solimena M, Folli F, Denis-Donini S, Comi GC, Pozza G, De Camilli P & Vicari AM (1988) Autoantibodies to glutamic acid decarboxylase in a patient with stiff-man syndrome, epilepsy, and type I diabetes mellitus. *The New England journal of medicine* **318**: 1012-1020.

Spink DC, Porter TG, Wu SJ & Martin DL (1985) Characterization of three kinetically distinct forms of glutamate decarboxylase from pig brain. *Biochem J* **231**: 695-703.

Stanton C, Ross RP, Fitzgerald GF & Van Sinderen D (2005) Fermented functional foods based on probiotics and their biogenic metabolites. *Current opinion in biotechnology* **16**: 198-203.

Stapleton A, Tyrer NM, Goosey MW & Cooper ME (1989) A Rapid Purification of L-Glutamic Acid Decarboxylase from the Brain of the Locust Schistocerca gregaria. *Journal of Neurochemistry* **53**: 1126-1133.

Stincone A, Daudi N, Rahman AS, Antczak P, Henderson I, Cole J, Johnson MD, Lund P & Falciani F (2011) A systems biology approach sheds new light on Escherichia coli acid resistance. *Nucleic acids research* **39**: 7512-7528.

Strausbauch PH & Fischer EH (1970) Chemical and physical properties of Escherichia coli glutamate decarboxylase. *Biochemistry* **9**: 226-233.

Studier FW, Rosenberg AH, Dunn JJ & Dubendorff JW (1990) Use of T7 RNA polymerase to direct expression of cloned genes. *Methods in enzymology* **185**: 60-89.

Sukhareva BS (1986) Amino acid decarboxylases. *Pyridoxal phosphate: chemical, Biochemical and medical aspects* **1B**: 325-353.

Tapley TL, Franzmann TM, Chakraborty S, Jakob U & Bardwell JC (2010) Protein refolding by pH-triggered chaperone binding and release. *Proceedings of the National Academy of Sciences of the United States of America* **107**: 1071-1076.

Thompson M, Weickert CS, Wyatt E & Webster MJ (2009) Decreased glutamic acid decarboxylase(67) mRNA expression in multiple brain areas of patients with schizophrenia and mood disorders. *Journal of psychiatric research* **43**: 970-977.

Tikhonenko AS, Sukhareva BS & Braunstein AE (1968) Electron-microscopic investigation of Escherichia coli glutamate decarboxylase. *Biochimica et biophysica acta* **167**: 476-479.

Tillakaratne NJK, Medina-Kauwe L & Gibson KM (1995) Gamma-aminobutyric acid (GABA) metabolism in mammalian neural and nonneural tissues. *Comparative Biochemistry and Physiology Part A: Physiology* **112**: 247-263.

To CM (1971) Quaternary structure of glutamate decarboxylase of Escherichia coli as revealed by electron microscopy. *Journal of molecular biology* **59**: 215-217.

Tokiwa Y, Calabia BP, Ugwu CU & Aiba S (2009) Biodegradability of plastics. *Int J Mol Sci* **10**: 3722-3742.

Tramonti A, De Canio M & De Biase D (2008) GadX/GadW-dependent regulation of the Escherichia coli acid fitness island: transcriptional control at the gadY-gadW divergent promoters and identification of four novel 42 bp GadX/GadW-specific binding sites. *Molecular microbiology* **70**: 965-982.

Tramonti A, John RA, Bossa F & De Biase D (2002) Contribution of Lys276 to the conformational flexibility of the active site of glutamate decarboxylase from Escherichia coli. *European journal of biochemistry / FEBS* **269**: 4913-4920.

Tramonti A, De Biase D, Giartosio A, Bossa F & John RA (1998) The roles of His-167 and His-275 in the reaction catalyzed by glutamate decarboxylase from Escherichia coli. *Journal of Biological Chemistry* **273**: 1939-1945.

Tramonti A, De Biase D, Giartosio A, Bossa F & John RA (1998) The roles of His-167 and His-275 in the reaction catalyzed by glutamate decarboxylase from Escherichia coli. *The Journal of biological chemistry* **273**: 1939-1945.

Tramonti A, Visca P, De Canio M, Falconi M & De Biase D (2002) Functional characterization and regulation of gadX, a gene encoding an AraC/XylS-like transcriptional activator of the Escherichia coli glutamic acid decarboxylase system. *Journal of bacteriology* **184**: 2603-2613.

Tramonti A, De Canio M, Delany I, Scarlato V & De Biase D (2006) Mechanisms of transcription activation exerted by GadX and GadW at the gadA and gadBC gene promoters of the glutamate-based acid resistance system in Escherichia coli. *Journal of bacteriology* **188**: 8118-8127.

Treiman DM (2001) GABAergic Mechanisms in Epilepsy. *Epilepsia* **42**: 8-12.

Tsai MF & Miller C (2013) Substrate selectivity in arginine-dependent acid resistance in enteric bacteria. *Proceedings of the National Academy of Sciences of the United States of America* **110**: 5893-5897.

Tsai MF, McCarthy P & Miller C (2013) Substrate selectivity in glutamate-dependent acid resistance in enteric bacteria. *Proceedings of the National Academy of Sciences of the United States of America* **110**: 5898-5902.

Tsuchiya K, Nishimura K & Iwahara M (2003) Purification and Characterization of Glutamate Decarboxylase from Aspergillus oryzae. *Food Science and Technology Research* **9**: 283-287.

Tucker DL, Tucker N, Ma Z, Foster JW, Miranda RL, Cohen PS & Conway T (2003) Genes of the GadX-GadW regulon in Escherichia coli. *Journal of bacteriology* **185**: 3190-3201.

Ueno H (2000) Enzymatic and structural aspects on glutamate decarboxylase. *Journal of Molecular Catalysis B: Enzymatic* **72**: 2269-2276.

Ueno Y, Hayakawa K, Takahashi S & Oda K (1997) Purification and characterization of glutamate decarboxylase from Lactobacillus brevis IFO 12005. *Bioscience, biotechnology, and biochemistry* **61**: 1168-1171.

Valderas MW, Alcantara RB, Baumgartner JE, Bellaire BH, Robertson GT, Ng W-L, Richardson JM, Winkler ME & Roop Ii RM (2005) Role of HdeA in acid resistance and virulence in Brucella abortus 2308. *Veterinary Microbiology* **107**: 307-312.

Veatch F, Callahan JL, Idol JD & Milberger EC (1960) New route to acrylonitrile. *Chem Eng Prog* **56**: 65-67.

Weber H, Polen T, Heuveling J, Wendisch VF & Hengge R (2005) Genome-wide analysis of the general stress response network in Escherichia coli: sigmaS-

dependent genes, promoters, and sigma factor selectivity. *Journal of bacteriology* **187**: 1591-1603.

Wong CG, Bottiglieri T & Snead OC, 3rd (2003) GABA, gamma-hydroxybutyric acid, and neurological disease. *Annals of neurology* **54 Suppl 6**: S3-12.

Wu J-Y, Matsuda T & Roberts E (1973) Purification and Characterization of Glutamate Decarboxylase from Mouse Brain. *Journal of Biological Chemistry* **248**: 3029-3034.

Yang BI & Metzler DE (1979) Pyridoxal 5'-phosphate and analogs as probes of coenzyme-protein interaction. *Methods in enzymology* **62**: 528-551.

Yu K, Lin L, Hu S, Huang J & Mei L (2012) C-terminal truncation of glutamate decarboxylase from Lactobacillus brevis CGMCC 1306 extends its activity toward near-neutral pH. *Enzyme Microb Technol* **50**: 263-269.

Zhang H, Yao H-y & Chen F (2006) Accumulation of γ-Aminobutyric Acid in Rice Germ Using Protease. *Bioscience, biotechnology, and biochemistry* **70**: 1160-1165.

Zhang M, Lin S, Song X, Liu J, Fu Y, Ge X, Fu X, Chang Z & Chen PR (2011) A genetically incorporated crosslinker reveals chaperone cooperation in acid resistance. *Nature chemical biology* **7**: 671-677.

Zhao B & Houry WA (2010) Acid stress response in enteropathogenic gammaproteobacteria: an aptitude for survival. *Biochemistry and cell biology = Biochimie et biologie cellulaire* **88**: 301-314.

Zik M, Arazi T, Snedden WA & Fromm H (1998) Two isoforms of glutamate decarboxylase in Arabidopsis are regulated by calcium/calmodulin and differ in organ distribution. *Plant molecular biology* **37**: 967-975.

# 5 Publications

1. Pennacchietti E., **Grassini G.**, Dworkowski F., Capitani G. and De Biase D. "The Asp86-His465 mutant of *Escherichia coli* glutamate decarboxylase (GAD) exhibits improved GABA synthesis at alkaline pH". Manuscript submitted to FEBS (revision 1).

2. **Grassini G.**, Pennacchietti E., Occhialini A. and De Biase D. "Biochemical and spectroscopic properties of *Brucella microti* glutamate decarboxylase, a major component of the glutamate-dependent acid resistance system". Manuscript to be submitted.